UNIVERSITÉ DE LORRAINE | BIBLIOTHÈQUES UNIVERSITAIRES

AVERTISSEMENT
DROIT D'AUTEUR

Ce document est le fruit d'un long travail approuvé par le jury de soutenance et mis à disposition de l'ensemble de la communauté universitaire élargie.

Il est soumis à la propriété intellectuelle de l'auteur. Ceci implique une obligation de citation et de référencement lors de l'utilisation de ce document. Toute contrefaçon, plagiat ou reproduction illicite encourt une poursuite pénale.

Contact bibliothèque : ddoc-theses-contact@univ-lorraine.fr
(Cette adresse ne permet pas de contacter les auteurs)

Code de la Propriété Intellectuelle. articles L 122. 4
Code de la Propriété Intellectuelle. articles L 335.2- L 335.10

UNIVERSITÉ DE LORRAINE
34 COURS LÉOPOLD — CS 25233
54052 NANCY CEDEX
TÉL : 03 54 50 54 00
CONTACT@UNIV-LORRAINE.FR
WWW.UNIV-LORRAINE.FR

UNIVERSITÉ DE LORRAINE

École doctorale IAEM Lorraine

A harmonic framework for identification and robust control of linear time-periodic systems

THÈSE

présentée et soutenue publiquement le 10 mars 2026

pour l'obtention du

Doctorat de l'Université de Lorraine

(Spécialité: Automatique, Traitement du Signal et des Images, Génie Informatique)

par

Flora Vernerey

Composition du jury

Président :	Franck Plestan	Ecole Centrale de Nantes, L2SN, France
Rapporteurs :	Franck Plestan	Ecole Centrale de Nantes, L2SN, France
	Bernard Brogliato	INRIA Rhône-Alpes, Grenoble, France
Examinateurs :	Florentina Nicolau	ENSEA, Laboratoire Quartz, Cergy-Pontoise, France
	Andrea Iannelli	University of Stuttgart, IST, Allemagne
Encadrants :	Pierre Riedinger	Université de Lorraine, CRAN, France
	Jamal Daafouz	Université de Lorraine, CRAN, France

Centre de Recherche en Automatique de Nancy (CRAN) — UMR 7039

Mis en page avec la classe thesul.

Remerciements

Le travail de recherche présenté dans ce manuscrit aurait été impossible sans les nombreuses personnes qui m'ont entourée pendant ces quatre dernières années. Je tiens à leur exprimer à présent ma profonde reconnaissance.

Avant tout, je souhaite remercier mes encadrants, Pierre Riedinger et Jamal Daafouz, pour m'avoir donné une opportunité de découvrir le monde de la recherche. Merci à vous deux pour tout le temps que vous m'avez consacré durant ces dernières années. En particulier, merci pour votre patience et vos encouragements. J'ai apprécié notre collaboration et j'espère que vous contribuerez encore longtemps au contrôle harmonique.

Je voudrais aussi remercier les membres de mon jury de thèse pour avoir accepté d'évaluer mon travail. En particulier, merci à Franck Plestan et Bernard Brogliato pour les questions intéressantes que vous avez soulevées dans vos rapports, ainsi qu'à Florentina Nicolau et Andrea Iannelli pour nos échanges durant la soutenance. Je suis également reconnaissante à Romain Postoyan et Daniele Astolfi d'avoir fait partie de mon comité de suivi individuel.

Un autre remerciement mérite d'être adressé à Andrea pour m'avoir accueillie pendant trois mois au sein de son laboratoire en Allemagne et pour les nombreux échanges que nous avons eus à distance avant cette visite. J'aimerais remercier tous les membres de l'IST pour leur accueil, en particulier Jasmin pour son sourire chaque fois que l'on se croisait pendant la journée, ainsi que Meisam et Massimiliano pour leur gentillesse à mon égard. Je me souviens de nos discussions et du temps passé ensemble avec plaisir.

Au sein du CRAN, j'ai fait de nombreuses rencontres: lors de ma soutenance, j'ai été très émue d'être soutenue par tant de personnes extraordinaires et je tiens donc à adresser un merci général à toutes les personnes que j'ai eu la chance de croiser au cours de ma thèse. Jihane a partagé mon bureau pendant plusieurs mois dont je garde un très beau souvenir (j'espère qu'on se reverra bientôt). Je suis fière d'avoir effectué ma thèse aux côtés de Valessa et Mira. Vous êtes non seulement des chercheuses brillantes, mais aussi des personnes en or. Je compte également Elena et Bouchra comme modèles de chercheuses et d'enseignantes. Je remercie Letizia pour sa belle personnalité et pour m'avoir fait goûter à ses spécialités italiennes. Merci Julie d'avoir toujours été de très bonne compagnie à l'heure du déjeuner et de m'avoir offert un livre pour combler mes lacunes en cuisine (je vais tester toutes les recettes, promis). Personne d'autre n'aurait pensé à célébrer mes accomplissements de voleuse de fourchettes et je vais m'assurer que mon trophée reste en un seul morceau. Merci Sarah d'avoir rendu plus drôle le TP d'automatique, dommage qu'on n'ait pas eu plus de cours ensemble. Je serai toujours partante pour échanger du thé avec toi (comme ça on pourra en acheter des nouveaux plus souvent). Merci Maxime d'avoir partagé ta super toolbox et tes idées sur le contrôle harmonique avec moi. Merci Anthony pour tout ce que tu as fait pour améliorer la vie du laboratoire et des doctorants. Merci Gustave d'avoir été un très bon accompagnateur au Canada, j'ai hâte de voir combien de papiers tu es capable de soumettre à la même conférence. Merci Gumi pour ton soutien, j'espère que nous trouverons toutes les deux une voie dans laquelle nous nous sentirons à notre place. Merci Aurélien d'être toujours prêt à partager tes passions, j'espère pouvoir assister à l'un de tes concerts un jour. Merci au futur docteur Weihao de toujours croire en moi et de me le faire savoir, je suis certaine que nous pourrons bientôt avoir des conversations entières en français! Merci Hugo, Gustavo, Valentin et Hernando pour les discussions au moment du café, elles m'ont toujours aidée à me

changer les idées. Merci Aymane d'avoir toujours supporté que je radote sur la taille de ton repas, et de m'avoir offert un Pokémon auquel je m'identifie (surtout en fin de thèse). Merci Mouad de m'avoir encouragée sur la dernière ligne droite de ma thèse, je croise les doigts pour que tes cours aient toujours lieu l'après-midi à l'avenir. Je tiens à remercier Mathieu et Clément pour m'avoir fait rire en jugeant mes créations culinaires, le fait que je sois encore parmi vous prouve que c'est comestible (sauf les pâtes à la patate douce, j'avoue avoir abusé sur ce coup-là). Merci à la fournée de doctorants constituée de Pierre, Thomas, Hassan, Jonathan et Etienne pour avoir été toujours sympathiques et ouverts à la discussion. Merci Robert de m'avoir fait découvrir des nouvelles recettes, j'espère que nous pourrons randonner ensemble un jour. Merci Francisco de m'avoir ramené un beau souvenir du Mexique, cela m'a beaucoup touchée.

Merci Christine pour tout ce que tu fais pour les membres du laboratoire au quotidien (je garderai le gilet ENSEM précieusement), et pour les bons moments passés ensemble à la pause déjeuner. Je tiens également à mentionner Yasmina, qui a veillé à ce que mon bureau soit le plus propre possible tout en s'inquiétant de mon bien-être. Je n'oublie pas non plus les membres de la commission parité, qui font de leur mieux pour sensibiliser le laboratoire à ces problématiques et faire connaître les métiers de la recherche aux jeunes. Au cours de ma thèse et de mon ATER, j'ai eu l'opportunité d'enseigner au sein de l'ENSEM, ce qui m'a permis de me sortir la tête de mes recherches. Parmi mes collègues enseignants, je remercie Maya, Samia, Clarice, Steven, Valérie, Gaël, Karima, Ayoub, Sarah, Jérémie et Jérome de m'avoir épaulée pour la réalisation de TD ou TP. Merci Gaël d'avoir assisté à ma soutenance, c'était une belle surprise. Avec Pauline, vous m'avez beaucoup aidée à préparer le TP sur ce logiciel incroyable qu'est CPN Tools. Merci également à Nicolae, Constantin, Radu, Benoît, Gilles et Marc pour leur gentillesse à mon égard.

Je voudrais également remercier mes amies de lycée: Melissa (mon infirmière et entraîneuse de latin préférée), Xavière (dont les talents créatifs et de cosplay sont sans égal), Elie (j'aspire à devenir aussi sage que toi), Alexane (la meilleure Ranger) et Alizée (le moteur de nos rencontres). Mes études à l'ENSEM m'ont permis de rencontrer Pauline et Marie, que je remercie pour tous les encouragements au cours de ma thèse. En particulier, merci Marie pour tous les moments passés ensemble à discuter, préparer des cookies ou peindre des oeufs de Pâques.

Il m'est bien sûr impossible de conclure cette page de remerciements sans mentionner ma famille: mes parents Aleksandra et Frédéric, mon frère Charles et ma sœur Agatha. Ils m'ont soutenue dans mes choix depuis le début, m'offrant un refuge lors des périodes difficiles. Merci maman de toujours tout donner pour tes enfants (comme disait le poème, je te dis merci maman, pour tout l'amour que chaque jour, tu donnes à ton petit enfant). Tu es la plus belle femme que je connaisse. Tu as beaucoup de mérite et j'espère pouvoir te rendre au centuple tout ce que tu m'as donné. Kocham cię całym sercem. Merci papa de m'avoir toujours conduite à la gare, même si le sacrifice d'un pneu de ta voiture chérie a été nécessaire (elle aura contre toute attente survécu à cette thèse). Je te suis très reconnaissante de m'avoir toujours encouragée dans mes études sans jamais rien m'imposer, et j'espère trouver une vocation comme la tienne. Merci Charles de m'avoir fait découvrir les jeux vidéos et les mathématiques (deux thématiques qui n'ont a priori rien à voir mais qui font encore partie de mon quotidien) et d'avoir répondu présent à ma soutenance. Merci ma gu d'être ma plus fervente supportrice (enfin j'espère) et de toujours me faire rire. Quand tu étais bébé, je n'arrivais pas à imaginer à quoi tu ressemblerais à l'âge adulte mais je n'aurais pas pu créer une meilleure sœur. Enfin, je remercie mes grands-parents de m'avoir accueillie chez eux pendant de nombreuses vacances. Grâce à eux, j'ai pu essayer de nombreuses activités et profiter de ce que la région autour de Morteau avait à offrir.

Abstract

This thesis addresses identification and control problems associated with continuous-time linear time-periodic (LTP) systems. Understanding the properties of such systems is important because of their ability to represent many interesting phenomena. However, their time-varying nature introduces significant complexities compared to their linear time-invariant (LTI) counterparts. This work leverages the equivalence between LTP systems and harmonic LTI systems to benefit from an LTI framework for studying LTP systems. A difficulty nevertheless arises due to the infinite dimension inherent in harmonic systems. The objective of this thesis is to develop methods for rigorously handling this infinite dimension when solving problems in the harmonic domain.

In the first part of this thesis, we propose a method for identifying LTP systems. Identifying a model for an LTP system is equivalent to determining the Fourier coefficients that characterize its state dynamics. We demonstrate that this identification problem, which is infinite-dimensional in the harmonic domain, can be reduced to a finite-dimensional linear least-squares problem by exploiting the Toeplitz structure inherent in harmonic systems. The convergence of the finite-dimensional approximation to the solution of the infinite-dimensional problem is established.

Problems related to the stability and robust control of LTP systems can be formulated as semidefinite optimization problems in the harmonic framework. However, the associated Toeplitz Block LMIs (TBLMIs) are infinite-dimensional. By exploiting this structure, we propose in the second part of this thesis a consistent truncation method that reduces the problem to a finite-dimensional convex optimization problem. This truncation allows us to approximate the solution of the infinite-dimensional problem with arbitrary precision. Furthermore, we establish a link between the harmonic framework and the time domain, highlighting the advantages of the former compared to Periodic Differential LMIs (PDLMIs).

In the final part of this thesis, we formulate robust harmonic control problems H_2 and H_∞ as TBLMIs, to which the previous resolution method applies. In order to achieve this, we extend the definitions of the H_2 and H_∞ norms to the harmonic space. Then, control methods for LTI systems can be applied. From the harmonic state feedback, a periodic state feedback can be determined in the time domain.

Résumé

Cette thèse est consacrée à l'identification et au contrôle des systèmes linéaires continus variant périodiquement dans le temps (LTP). Comprendre les propriétés de tels systèmes est essentiel, en raison de leur rôle dans la modélisation de nombreux dispositifs d'ingénierie soumis à des régimes périodiques. Cependant, leur dépendance au temps pose des difficultés qui n'apparaissent pas dans le cas des systèmes linéaires invariants dans le temps (LTI). Ce travail exploite l'équivalence entre les systèmes LTP et les systèmes LTI harmoniques afin de bénéficier d'un cadre LTI pour étudier les systèmes LTP. Une difficulté apparaît néanmoins en raison de la dimension infinie inhérente aux systèmes harmoniques. L'objectif de cette thèse est de développer des méthodes permettant de traiter rigoureuseusement cette dimension infinie lors de la résolution de problèmes dans le domaine harmonique.

Dans la première partie de la thèse, nous proposons une méthode pour identifier les systèmes LTP. L'identification d'un modèle pour un système LTP équivaut à déterminer les coefficients de Fourier qui caractérisent la dynamique du vecteur d'état. Nous démontrons que ce problème d'identification, de dimension infinie dans le domaine harmonique, peut être réduit à un problème de moindres carrés linéaires de dimension finie en exploitant la structure Toeplitz inhérente aux systèmes harmonique. La convergence de l'approximation en dimension finie vers la solution du problème de dimension infinie est établie.

Les problèmes liés à la stabilité et au contrôle robuste des systèmes LTP peuvent être formulés comme des problèmes d'optimisation semi-définie dans le domaine harmonique. Cependant, les LMIs de structure bloc Toeplitz (TBLMIs) associées sont de dimension infinie. En exploitant cette structure, nous proposons dans la deuxième partie de cette thèse une méthode de troncature consistante qui réduit le problème à un problème d'optimisation convexe de dimension finie. Cette troncature permet d'approximer la solution du problème de dimension infinie avec une précision arbitraire. Par ailleurs, nous établissons un lien entre le cadre harmonique et le domaine temporel, en soulignant les avantages du premier par rapport aux LMIs différentielles périodiques (PDLMIs).

Dans la dernière partie de la thèse, nous formulons des problèmes de contrôle harmonique robuste H_2 et H_∞ comme des TBLMIs sur lesquelles la méthode de résolution précédente s'applique. Pour ce faire, nous étendons les définitions des normes H_2 et H_∞ à l'espace harmonique. Alors, les méthodes de contrôle pour les systèmes LTI peuvent être appliquées. A partir du retour d'état harmonique, un retour d'état périodique peut être déterminé dans le domaine temporel.

Contents

Introduction **xi**

Chapter 1
State of the art **1**

1.1 Preliminaries on Harmonic modeling 2
1.1.1 The harmonic space 2
1.1.2 Equivalence between LTP and harmonic LTI systems 4
1.1.3 Toeplitz Block versus Block Toeplitz formulation 4
1.2 Identification of LTP systems 5
1.2.1 Lifting and subspace identification 5
1.2.2 Harmonic transfer function 7
1.3 Solving periodic differential and harmonic equations 7
1.3.1 Solving periodic differential equations 7
1.3.2 Solving harmonic equations 9
1.4 Periodic control 10
1.4.1 Tracking and rejection of periodic signals 11
1.4.2 Robust control of periodic systems 12

Chapter 2
A Harmonic Framework for the Identification of Linear Time-Periodic systems **17**

2.1 Problem statement 18
2.2 From an infinite-dimensional problem to a finite-dimensional least-squares problem 19
2.2.1 Approximating the periodic operators 19
2.2.2 A central strip identification problem 22
2.2.3 Solving the central strip least squares identification problem 24
2.2.4 Validation 26

2.3 Illustrative examples . . . 27
2.3.1 A finite phasor-order example . . . 27
2.3.2 An infinite phasor-order example . . . 32
2.3.3 A wind turbine . . . 33
2.4 Conclusion . . . 35

Chapter 3
A Consistent Truncation for solving Infinite-Dimensional Toeplitz Block LMI 37

3.1 Equivalence between TBLMIs and PDLMIs . . . 38
3.1.1 TBLMI . . . 38
3.1.2 PDLMI . . . 39
3.1.3 TBLMIs are the harmonic counterparts of PDLMIs . . . 39
3.2 Solving an infinite-dimensional harmonic convex optimization problem . . . 41
3.2.1 Average Trace operator . . . 42
3.2.2 Truncation of a TBLMI . . . 43
3.2.3 Truncated and banded approximation of TBLMI . . . 45
3.2.4 Solving **COP** up to an arbitrary error . . . 47
3.3 Illustrative examples . . . 51
3.3.1 Validation on a periodic differential Riccati inequality with a known solution 51
3.3.2 Validation of a regularization approach on a periodic differential Lyapunov equation . . . 53
3.4 Conclusion . . . 55

Chapter 4
A TBLMI Framework for Harmonic Robust Control 57

4.1 Framework for harmonic robust control . . . 58
4.1.1 Harmonic transfer and transition functions . . . 58
4.1.2 Harmonic H_2 and H_∞ norms . . . 60
4.2 Harmonic H_2 and H_∞ optimal control . . . 63
4.2.1 Harmonic H_2 optimal control . . . 64
4.2.2 Harmonic H_∞ optimal control . . . 66
4.2.3 Reconstruction of the periodic feedback gain . . . 67
4.3 Illustrative examples . . . 68
4.3.1 H_2 harmonic control-LQR case . . . 69
4.3.2 H_∞ harmonic control . . . 72
4.4 Conclusion . . . 74

Conclusion and perspectives 77

Appendixs

Appendix A
Systems identified in Chapter 2

A.1 Example 2.3.1: a system with a finite degree 81
A.2 Example 2.3.2: a system with an infinite degree 82
A.3 Example 2.3.3: a wind turbine 83

Appendix B
Résumé détaillé en français

B.1 Préliminaires sur la modélisation harmonique 86
B.2 Identification des systèmes LTP 87
B.3 Résolution des TBLMIs de dimension infinie 87
B.4 Contrôle harmonique robuste 88
B.5 Perspectives 89
B.6 Contributions 90
B.7 Publications 90

Bibliography **93**

List of Figures

2.1 Boxplot of the fit percentage - process noise with $\sigma_w = 10^{-3}$ . . . 29
2.2 Boxplot of the identification error - process noise with $\sigma_w = 10^{-3}$ . . . 29
2.3 Boxplot of the identification error - process noise with $\sigma_w = 10^{-1}$ . . . 30
2.4 Boxplot of the identification error when $3\sigma = \frac{5}{100}|x_i(t)|$ . . . 31
2.5 Comparison of the true and estimated trajectories of the infinite phasor-order example . . . 33
2.6 Moduli of the true and estimated phasors of A of the infinite-phasor order example with noise on the state measurements. . . . 34
2.7 Validation of the banded approximation on a new trajectory for the infinite-phasor order example . . . 35
2.8 Comparison of the true and estimated trajectories of the wind turbine. . . . 35
2.9 Mean identification error convergence for the wind turbine. . . . 36

3.1 Multiplication of two finite dimensional banded Toeplitz matrices . . . 44
3.2 Steps of the approximation scheme for solving infinite-dimensional TBLMIs. . . . 48
3.3 Comparison of $A(t)$ and its regularized version $A_\varepsilon(t)$ for $\varepsilon \in \{0.001, 0.01, 0.05, 0.1, 0.2\}$ 54
3.4 Comparison of $Q(t)$ and its regularized version $Q_\varepsilon(t)$ for $\varepsilon \in \{0.001, 0.01, 0.05, 0.1, 0.2\}$ 54

4.1 The robust periodic control problem is solved with our TBLMI framework instead of solving PDLMIs. . . . 68
4.2 Numerical comparisons for Periodic Gain K by solving PDRE, HARE and TBLMI associated to the LQ problem . . . 70
4.3 Moduli of harmonics of $K = [K_1, K_2]$ for Problem $\mathbf{COP_{p,q,r}}$ associated to (4.39), (4.40) and (4.29) with $r = 40$, $p = 2r$ and $q = r$. . . . 71
4.4 T-periodic gain $K(t)$ over a period $T = 1$ for Problem (4.39) . . . 72
4.5 T-periodic gain $K(t)$ over a period $T = 1$ for Problem (4.29) . . . 73
4.6 Closed-loop response with harmonic LQ control achieved by solving (4.39) for $r = 10, 20, 30$. . . . 74
4.7 Moduli of gain-phasors $K = [K_1, K_2]$(Harmonic H_∞) . . . 75
4.8 T-periodic gain $K(t)$ over a period $T = 1$(Harmonic H_∞) . . . 76
4.9 Closed loop response with optimal harmonic H_∞ control for $r = 10, 20, 30$ . . . 76

A.1 $A(t)$ in Example 2.3.1 . . . 81
A.2 $B(t)$ in Example 2.3.1 . . . 82
A.3 $A(t)$ in Example 2.3.2 . . . 82
A.4 $B(t)$ in Example 2.3.2 . . . 83
A.5 $M(t)$ in Example 2.3.3 . . . 83
A.6 $C(t)$ in Example 2.3.3 . . . 84

A.7 $K(t)$ in Example 2.3.3 84

B.1 Les problèmes de contrôle robuste harmonique sont résolus avec notre approche TBLMI au lieu de résoudre des PDLMIs. 89

Introduction

Periodicity arises naturally in various engineering and scientific disciplines [1]. From the mechanical vibrations of car engines to oscillations in electronic circuits, and the rhythmic dynamics of biological processes, periodic behavior is a pervasive and fundamental phenomenon [2–4]. Therefore, it is essential to understand, analyze and control these periodic behaviours in order to ensure stability, optimize system performance and enhance the predictability of various applications. Applications include, for example, helicopter control in forward flight, fatigue mitigation in wind turbines, and satellite positioning.

While many physical systems are inherently nonlinear, they can often be approximated as Linear Time-Periodic (LTP) systems by linearizing them along a periodic trajectory [3]. LTP systems form a subclass of linear time-varying systems whose parameters vary periodically in time. As a result, they are more complex than Linear Time-Invariant (LTI) systems, but their periodic structure renders them amenable to Floquet theory for analysis of their properties. However, while Floquet theory provides insight on the stability of periodic systems, it is not a constructive framework and therefore cannot be directly used for control design.

Harmonic modeling is a frequency-domain alternative to Floquet theory for studying the properties of LTP systems. Sliding Fourier decomposition can be exploited to map an LTP system onto an equivalent LTI system, known as a harmonic system. The latter describes the behavior of the harmonics of the signals that characterize the system over time. Harmonics are prevalent in the context of power systems, telecommunications, mechanical systems and electronic devices. Since they lead to oscillations, instability, and increased energy consumption, reducing their impact represents a critical concern in control engineering. The harmonic model provides insight into the interactions between the harmonics of the signals under investigation. Understanding these interactions is crucial to achieve satisfactory performance and robustness in control applications.

The central premise of this thesis is that many challenging problems in the time domain, such as identification and robust control of LTP systems, as well as resolution of periodic differential LMIs, can be transformed into equivalent problems in the harmonic domain. There, the LTP system is replaced by a time-invariant one, which circumvents the difficulties posed by a time-varying model. However, the resulting harmonic LTI system is infinite dimensional, which implies that an intermediate step is required to rigorously deal with this infinite dimension. This thesis adapts traditional identification and robust control LTI methods to the harmonic framework by proposing efficient truncation and approximation schemes.

Outline of the thesis

This thesis introduces a unified harmonic-domain framework for the identification and control of continuous-time LTP systems and is organized into four chapters. After reviewing the state of the art in Chapter 1, the contributions of this thesis are developed in the remaining three chapters as follows.

Chapter 2 presents the first contribution of the thesis: a data-driven identification framework for continuous-time LTP systems that overcomes several limitations of existing methods. By exploiting the harmonic equivalence introduced in [5], the identification problem is reformulated in terms of a single equivalent LTI system, referred to as the harmonic system. This approach avoids the need for state-derivative estimation and does not require lifting the dynamics into multiple LTI subsystems. Most importantly, it applies to both stable and unstable systems and accommodates transient data, rather than relying on periodic steady-state operation. The chapter provides a rigorous analysis of the infinite-dimensional nature of the harmonic representation and establishes conditions under which finite-dimensional approximations converge to the true system.

Chapter 3 is dedicated to the resolution of periodic differential LMIs (PDLMIs) arising in analysis and control of LTP systems. By working in the harmonic domain, PDLMIs are shown to be equivalent to infinite-dimensional Toeplitz block LMIs (TBLMIs). While such objects are infinite dimensional, their algebraic structure is particularly well suited to periodic problems. This chapter establishes a formal equivalence between periodic solutions of differential LMIs and solutions of TBLMIs, and proposes a consistent truncation strategy that yields computationally tractable semidefinite programs. The key result is that the truncated problems admit solutions that converge to the true infinite-dimensional solution, thereby providing a sound numerical framework for problems that were previously considered intractable.

Building on the tools developed in the previous chapters, the third and final contribution of this thesis is detailed in Chapter 4 and addresses periodic control problems in the harmonic domain. Stability analysis and robust H_2 and H_∞ control synthesis for LTP systems are formulated as infinite-dimensional semidefinite optimization problems involving TBLMIs. Leveraging the truncation framework developed earlier, these problems can be solved in practice while preserving equivalence with their time-domain PDLMIs. A key outcome is that, within the harmonic framework, periodic control problems assume a form that closely resembles classical LTI robust control, enabling the use of well-established techniques and extensions to uncertainty descriptions.

Publications

The work carried out in this thesis has resulted in the following publications.

Book chapter

1. F. Vernerey, P. Riedinger and J. Daafouz, "Harmonic Modeling and Control," in R. Postoyan, P. Frasca, E. Panteley, L. Zaccarian (dir.), *Hybrid and Networked Dynamical Systems*, Springer, 2024. [6]

Journal paper

1. F. Vernerey, P. Riedinger and J. Daafouz, "A TBLMI Framework for Harmonic Robust Control," in IEEE Transactions on Automatic Control, vol. 70, no. 4, pp. 2537-2551, April 2025. [7]

Conference papers

1. F. Vernerey, P. Riedinger, A. Iannelli and J. Daafouz, "A Harmonic Framework for the Identification of Linear Time-Periodic Systems," 2024 American Control Conference (ACC), Toronto, ON, Canada, 2024, pp. 4645-4650. [8]

2. F. Vernerey, P. Riedinger and J. Daafouz, "On Solving Infinite-Dimensional Toeplitz Block LMIs," 2023 62nd IEEE Conference on Decision and Control (CDC), Singapore, Singapore, 2023, pp. 4717-4722. [9]

1

State of the art

Contents

1.1 Preliminaries on Harmonic modeling 2
1.1.1 The harmonic space 2
1.1.2 Equivalence between LTP and harmonic LTI systems 4
1.1.3 Toeplitz Block versus Block Toeplitz formulation 4
1.2 Identification of LTP systems 5
1.2.1 Lifting and subspace identification 5
1.2.2 Harmonic transfer function 7
1.3 Solving periodic differential and harmonic equations 7
1.3.1 Solving periodic differential equations 7
1.3.2 Solving harmonic equations 9
1.4 Periodic control 10
1.4.1 Tracking and rejection of periodic signals 11
1.4.2 Robust control of periodic systems 12

Introduction

This chapter aims at presenting the state of the art on the main axes of this thesis, namely harmonic modeling, identification and control of continuous-time LTP systems, as well as methods for the resolution of periodic differential equations and harmonic equations.

The modeling of LTP systems is of significant interest for both analysis and control design given the wide range of systems that can be described by periodic dynamics, as seen in the introduction. However, the time-varying nature of LTP systems introduces a high degree of complexity compared to LTI systems, for which numerous tools and methodologies have been developed. Consequently, the main strategy in LTP system identification is to reformulate the problem to that of identifying one or several LTI systems, from which a model of the LTP system can be derived. This approach allows to take advantage of the existing tools for LTI system identification [10], for example through lifting techniques or frequency-domain methods [2].

In control design, two complementary tools that are often encountered are Riccati equations and Linear Matrix Inequalities (LMIs). Riccati equations are particularly prevalent in optimal

control and estimation. On the other hand, LMIs offer a broader and more flexible framework, capable of addressing a wider range of control problems including robust control and multi-objective optimization. Although LMI methods are standard for LTI systems, their application to periodic systems involves the resolution of Periodic Differential LMIs (PDLMIs), which must hold over a period of the system and are therefore challenging to solve. Despite ongoing research and significant advances in the resolution of differential LMIs [11–13], a universally efficient and scalable solution remains an open problem. An alternative solution is to exploit the equivalence between LTP systems and harmonic LTI systems to reformulate the previous problem in the harmonic framework. In the context of harmonic control, one of the central challenges lies in solving infinite-dimensional Riccati equations. This issue was addressed in [14], which highlighted the importance of obtaining practical solutions with minimal approximation error to preserve stabilization properties.

This chapter is organized as follows. First, preliminaries on harmonic modeling are provided in Section 1.1. Then, methods for the identification of LTP systems are presented in Section 1.2. We give an overview of resolution methods for periodic differential equations and harmonic equations in Section 1.3. Section 1.4 is dedicated to periodic control. To conclude, the objectives to be achieved in this thesis are presented in a final section and the thesis plan is detailed.

1.1 Preliminaries on Harmonic modeling

In this section, we aim to present the most important properties of harmonic modeling. The result on which the entire thesis is based is that Linear Time-Periodic (LTP) systems can be transformed into Linear Time-Invariant (LTI) systems with an appropriate operation on their entries. This equivalence can be exploited to benefit from an LTI framework, for example to solve identification and control problems. However, harmonic systems are inherently infinite-dimensional. Dealing with that infinite characteristic to provide practical solutions to such problems is what we aim to achieve in this thesis.

1.1.1 The harmonic space

The main tool in harmonic modeling is the Sliding Fourier Decomposition (SFD). For a given integer n, consider $x \in L^2_{loc}(\mathbb{R}, \mathbb{C}^n)$ a complex-valued function of time. The SFD of x over a window of length T is defined by the time-varying infinite sequence $X = (\cdots, X_{-1}, X_0, X_1, \cdots) := \mathcal{F}(x) \in C^a(\mathbb{R}, \ell^2(\mathbb{C}^n))$ (see [5]) whose n-dimensional components X_k (named $k-$th phasor) satisfy:

$$X_k(t) := \frac{1}{T} \int_{t-T}^{t} x(\tau) e^{-\mathrm{j}\omega k \tau} d\tau$$

for $k \in \mathbb{Z}$, with $\omega := \frac{2\pi}{T}$. The Toeplitz transformation of a matrix function $A \in L^2_{loc}(\mathbb{R}, \mathbb{C}^{n\times m})$, denoted $\mathcal{A} := \mathcal{T}(A)$, defines a block Toeplitz and infinite dimensional matrix as follows:

$$\mathcal{A} := \mathcal{T}(A) = \begin{bmatrix} \ddots & & \vdots & & \iddots \\ & A_0 & A_{-1} & A_{-2} & \\ \cdots & A_1 & A_0 & A_{-1} & \cdots \\ & A_2 & A_1 & A_0 & \\ \iddots & & \vdots & & \ddots \end{bmatrix}, \tag{1.1}$$

where $(A_k)_{k\in\mathbb{Z}}$ denotes the phasor sequence of A. For clarity reasons, when considering a lowercase vector-valued function $x \in L^2_{\mathrm{loc}}(\mathbb{R}, \mathbb{C}^n)$, we adopt the following convention: $X := \mathcal{F}(x)$

represents the Fourier transform of x, while $\mathcal{X} \coloneqq \mathcal{T}(x)$ represents the Toeplitz form of x. When a T-periodic vector x or matrix function A are considered, both $X \coloneqq \mathcal{F}(x)$ and $\mathcal{A} \coloneqq \mathcal{T}(A)$ are constant. Note also that when x is a real signal, $X_k = \overline{X}_{-k}$ for any k.

Definition 1 *We say that X belongs to H if X is an absolutely continuous function (i.e $X \in C^a(\mathbb{R}, \ell^2(\mathbb{C}^n))$ and fulfills for any k the following condition:*

$$\dot{X}_k(t) = \dot{X}_0(t)e^{-j\omega kt} \ a.e. \tag{1.2}$$

Similarly to the Riesz-Fisher theorem which establishes a one-to-one correspondence between the spaces L^2 and ℓ^2, the following theorem establishes a one-to-one correspondence between the spaces L^2_{loc} and H (see [5]).

Theorem 1 *For a given $X \in L^\infty_{loc}(\mathbb{R}, \ell^2(\mathbb{C}^n))$, there exists a representative $x \in L^2_{loc}(\mathbb{R}, \mathbb{C}^n)$ of X, i.e. $X = \mathcal{F}(x)$, if and only if $X \in H$.*

Proof 1 *See [5].*

The following theorem states that the essential supremum of a T-periodic function in L^∞ is equal to the induced ℓ^2 norm of its infinite-dimensional Toeplitz transformation.

Theorem 2 *Consider a T-periodic matrix function $A \in L^2([0\ T], \mathbb{C}^{n\times n})$. Then, $\mathcal{A} \coloneqq \mathcal{T}(A)$ is a constant bounded operator on ℓ^2 if and only if $A \in L^\infty([0\ T], \mathbb{C}^{n\times n})$. Moreover, the operator norm induced by the ℓ^2-norm satisfies :*

$$\|\mathcal{A}\|_{\ell^2} \coloneqq \sup_{\|X\|_{\ell^2}=1} \|\mathcal{A}X\|_{\ell^2} = \|A\|_{L^\infty} \tag{1.3}$$

Proof 2 *See Part V p.p. 562-574 of [15].*

The following essential rules hold [15]:

1. For a matrix function $A \in L^\infty_{loc}$ and a vector $x \in L^2_{loc}$:

$$\mathcal{F}(Ax) = \mathcal{T}(A)\mathcal{F}(x) = \mathcal{A}X \tag{1.4}$$

   where $X \coloneqq \mathcal{F}(x)$ and $\mathcal{A} \coloneqq \mathcal{T}(A)$.

2. For two matrix functions $A \in L^\infty_{loc}$ and $B \in L^\infty_{loc}$:

$$\mathcal{T}(AB) = \mathcal{T}(A)\,\mathcal{T}(B) = \mathcal{A}\mathcal{B}. \tag{1.5}$$

According to the SFD, all these transformations lead to absolutely continuous functions of time and such that $t \mapsto \mathcal{A}X(t) \in \ell^2$ and $t \mapsto \mathcal{A}\mathcal{B}(t)$ is a bounded operator on ℓ^2.

1.1.2 Equivalence between LTP and harmonic LTI systems

Thanks to Theorem 1, it is established in [5] that any system having solutions in Carathéodory sense can be transformed by a sliding Fourier decomposition into an infinite dimensional system for which a one-to-one correspondence between their respective trajectories is established, provided that the trajectories in the infinite dimensional space belong to the subspace H. Moreover, when a $T-$periodic system is considered, the resulting infinite dimensional system is time-invariant. With a mild assumption (as detailed in [5]), any n-dimensional differential system of the form:

$$\dot{x} = f(t, x)$$

with Caratheodory solutions can be represented in a harmonic form as follows:

$$\dot{X} = \mathcal{F}(f(t, x)) - \mathcal{N}X$$

where

$$\mathcal{N} := diag(\mathrm{j}\omega k \otimes Id_n,\ k \in \mathbb{Z}) \tag{1.6}$$

with $\otimes$ the Kronecker product and Id_n the identity matrix of size n. For polynomial systems, $\mathcal{F}(f(t, x))$ can be easily computed using the arithmetic rules (1.4) and (1.5).

Consider $T-$periodic functions $A(\cdot)$ and $B(\cdot)$ respectively of class $L^2([0\,T], \mathbb{C}^{n\times n})$ and $L^\infty([0\,T], \mathbb{C}^{n\times m})$ and let:

$$\dot{x}(t) = A(t)x(t) + B(t)u(t) \quad x(0) = x_0 \tag{1.7}$$

If x is a solution associated to the control $u \in L^2_{loc}(\mathbb{R}, \mathbb{C}^m)$ of the linear time-periodic (LTP) system (1.7), then $X := \mathcal{F}(x)$ is a solution associated to $U := \mathcal{F}(u)$ of the linear time-invariant (LTI) system:

$$\dot{X}(t) = (\mathcal{A} - \mathcal{N})X(t) + \mathcal{B}U(t), \quad X(0) = \mathcal{F}(x)(0) \tag{1.8}$$

where $\mathcal{A} = \mathcal{T}(A)$, $\mathcal{B} = \mathcal{T}(B)$. Reciprocally, if $X \in H$ is a solution to (1.8) with $U \in H$, then their representatives x and u (i.e. $X = \mathcal{F}(x)$ and $U = \mathcal{F}(u)$) are a solution to (1.7). In addition, it is proved in [5] that one can reconstruct time trajectories from the exact formula:

$$x(t) = \mathcal{F}^{-1}(X)(t) = \sum_{k=-\infty}^{+\infty} X_k(t)e^{\mathrm{j}\omega kt} + \frac{T}{2}\dot{X}_0(t) \tag{1.9}$$

1.1.3 Toeplitz Block versus Block Toeplitz formulation

The formulas up until this section have a Block Toeplitz (BT) formulation, which means that the components of the vector X and operator $\mathcal{A}$ are grouped according to phasor order. This BT formulation is well-suited to identification problems, as will be clear in Chapter 2.

For control purposes, we employ a Toeplitz Block (TB) matrix representation rather than the BT matrix representation. The primary motivation behind this choice lies in its ability to yield a harmonic equation structure akin to that found in the time domain, as exemplified in (1.10). For a $n \times m$ matrix function $A = (a_{ij})$ ($\in L^2_{loc}(\mathbb{R}, \mathbb{C}^{n\times m})$), we define the associated infinite dimensional TB matrix function as

$$\mathcal{A} := \mathcal{T}(A) = \begin{bmatrix} \mathcal{A}_{11} & \dots & \mathcal{A}_{1m} \\ \vdots & & \vdots \\ \mathcal{A}_{n1} & \dots & \mathcal{A}_{nm} \end{bmatrix} \tag{1.10}$$

with $\mathcal{A}_{ij} \coloneqq \mathcal{T}(a_{ij})$, $i = 1,\cdots,n,\ j = 1,\cdots,m$.

If $x = (x_1,\cdots,x_n) \in L^2_{loc}(\mathbb{R},\mathbb{C}^n)$ is a complex valued vector function, then $X \coloneqq \mathcal{F}(x) = \big(\mathcal{F}(x_1),\cdots,\mathcal{F}(x_n)\big)$ maintains the order of the state components. The $k-$th phasor of X has the following TB form: $X_k = (X_{1,k},\cdots,X_{n,k})$ with

$$X_k(t) \coloneqq \frac{1}{T}\int_{t-T}^{t} x(\tau)e^{-\mathrm{j}\omega k\tau}d\tau.$$

This choice better suits our objectives for analysis and control design. To obtain a BT structure as in [5, 16], one has to consider the transformation operator $\mathcal{F}(x) = (\cdots,X_{-1},X_0,X_1,\cdots)$, where X_k refers to the $k-th$ phasors, instead of $\mathcal{F}(x) = (\mathcal{F}(x_1),\cdots,\mathcal{F}(x_n))$. Note also when a TB representation is chosen that $\mathcal{N}$ in (1.6) must be rewritten :

$$\mathcal{N} \coloneqq Id_n \otimes diag(\mathrm{j}\omega k,\ k \in \mathbb{Z}) \tag{1.11}$$

instead of $\mathcal{N} \coloneqq diag(\mathrm{j}\omega k \otimes Id_n,\ k \in \mathbb{Z})$. Obviously, we can readily switch between these two representations by applying an appropriate permutation matrix.

1.2 Identification of LTP systems

This section provides an overview of established methods for the identification of LTP systems. These methods can be divided into discrete-time and continuous-time approaches. A distinction is also made between the time-domain and frequency-domain approaches, as is usual in the field of system identification. Many similar ideas are shared across these categories.

Let a linear discrete-time periodic system be described by:

$$\begin{aligned} x_{k+1} &= A_k x_k + B_k u_k \\ y_k &= C_k x_k + D_k u_k \end{aligned} \tag{1.12}$$

where A, B, C and D are $p-$periodic ($A(k+p) = A(k)$), and let a linear continuous-time periodic system be characterized by:

$$\begin{aligned} \dot{x}(t) &= A(t)x(t) + B(t)u(t) \\ y(t) &= C(t)x(t) + D(t)u(t) \end{aligned} \tag{1.13}$$

where A, B, C and D are $T-$periodic ($A(t+T) = A(t)$).

1.2.1 Lifting and subspace identification

The most common strategy in LTP system identification consists in converting the original problem into an identification problem for LTI systems. For instance, lifting techniques exploit the periodic nature of the LTP system to construct one or several equivalent LTI systems, which are then identified instead of the LTP system. Therefore, periodicity is eliminated from the identification problem. For discrete-time systems of the form (1.12), this is achieved by stacking trajectories over one period to obtain a single higher-dimensional LTI representation [17, 18]. In [17], the input and output are stacked over a period p so that the LTI system that maps x_k to x_{k+p} is written as follows:

$$\begin{aligned} x_{k+p} &= A_k^L x_k + B_k^L U_k^L \\ Y_k^L &= C_k^L x_k + D_k^L U_k^L \end{aligned}$$

where the exponent L stands for *lifted*:

$$A_k^L = \prod_{q=0}^{p-1} A_{k+p-1-q}$$
$$B_k^L = \begin{pmatrix} \prod_{q=0}^{p-2}(A_{k+p-1-q})B_k & \prod_{q=0}^{p-3}(A_{k+p-1-q})B_{k+1} & \cdots & A_{k+p-1}B_{k+p-2} & B_{k+p-1} \end{pmatrix}$$
$$U_k^L = \begin{pmatrix} u_k \\ u_{k+1} \\ \vdots \\ u_{k+p-1} \end{pmatrix}, \; Y_k^L = \begin{pmatrix} y_k \\ y_{k+1} \\ \vdots \\ y_{k+p-1} \end{pmatrix}$$

The matrices C_k^L and D_k^L are not detailed here, but they are easily derived from (1.12). The lifted LTI system has the same state dimension as the original LTP system, but the input and output dimensions are multiplied by the period p. In [18], this lifting technique is used to identify autonomous LTP systems.

In the context of continuous-time systems, lifting consists of extracting sub-trajectories from a main trajectory, with a complete period separating two consecutive samples for each sub-trajectory [19]. To put it simply, trajectories sampled at times $\{t_k, t_k+T, t_k+2T...\}$ for $k = 1, ..., N$ and $t_k \in [0, T]$ lead to N LTI systems. Indeed, the following relationships result from the periodicity of A and B and (1.13):

$$\begin{aligned} \dot{x}(t_k) &= A(t_k)x(t_k) + B(t_k)u(t_k) \\ \dot{x}(t_k+T) &= A(t_k+T)x(t_k+T) + B(t_k+T)u(t_k+T) = A(t_k)x(t_k+T) + B(t_k)u(t_k+T) \\ &\vdots \\ \dot{x}(t_k+qT) &= A(t_k+qT)x(t_k+qT) + B(t_k+qT)u(t_k+qT) = A(t_k)x(t_k+qT) + B(t_k)u(t_k+qT) \end{aligned}$$

so $A(t_k)$ and $B(t_k)$ are the constant state and input matrices associated with the k-th LTI system. Therefore, the number of systems to identify increases with the sampling frequency of the main trajectory, but classical LTI methods can be used for identification of these systems.

Lifting schemes have proven successful in the time domain [2, 18] and the frequency domain [19]. These techniques are better suited for discrete-time systems since they lead to finite-dimensional LTI systems without approximation, whereas lifting a continuous-time system requires discretization [19]. For instance, in the latter paper, the authors sample rotorcraft data with respect to azimut and identify several LTI models from the corresponding frequency responses. However, the frequency response of the lifted system can be affected by aliasing [2].

The lifting technique is often followed with a subspace identification method which relies on the singular value decomposition of Hankel matrices that contain trajectories of the system. It allows to determine state-space parameters of the system and has been applied to identification of discrete-time LTP systems both in the time domain [17, 18, 20–22] and more recently in the frequency domain [23, 24]. In [24], restrictions on the input-output dimension and input form are relaxed by leveraging the idea to employ the frequency response of a time-lifted system with a linear time-invariant structure. In addition to state-space models, modal parameters that stem from Floquet theory may also be determined [25–27].

In many approaches, the unknown parameters are determined with a least-squares approach [28–30]. The Fourier coefficients of A and B are determined in [30] from Fourier transforms of

the state and input signals at different frequencies. A requirement is that steady-state is reached, as in [31]. This can be a limiting factor, particularly in control applications.

1.2.2 Harmonic transfer function

Another approach is centered on the concept of the Harmonic Transfer Function (HTF), which was first introduced in [32]. Similarly as for LTI systems, the HTF relates the Fourier transforms of the input and output signals: $\hat{Y}(s) = \hat{\mathcal{G}}(s)\ \hat{U}(s)$. In contrast to LTI systems, for which a single input frequency produces an output with the same frequency, several output frequencies that are separated by multiples of the fundamental frequency arise in the case of LTP systems.

The HTF can be identified from Fourier transforms of input/output signals [27]. However, the HTF is an infinite-dimensional operator, with the following structure:

$$\hat{\mathcal{G}}(s) = \begin{pmatrix} \ddots & \vdots & \vdots & \vdots & \iddots \\ \cdots & G_0(s-j\omega_0) & G_{-1}(s) & G_{-2}(s+j\omega_0) & \cdots \\ \cdots & G_1(s-j\omega_0) & G_0(s) & G_{-1}(s+j\omega_0) & \cdots \\ \cdots & G_2(s-j\omega_0) & G_1(s) & G_0(s+j\omega_0) & \cdots \\ \iddots & \vdots & \vdots & \vdots & \ddots \end{pmatrix} \tag{1.14}$$

where $\omega_0 = \frac{2\pi}{T}$ is the fundamental frequency of the periodic system. Therefore, practical implementations require truncation [33–35]. In general, a small number of harmonics allow to model accurately LTP systems.

In [27], the modal parameters of the HTF are determined from the power spectrum of the output signal only, but the input spectrum is required to be flat. The structure of (1.14) implies that the output $\hat{Y}(s)$ can be written as the sum of weighted $\hat{U}(s-jk\omega_0)$ for $k \in \mathbb{Z}$. This means that the LTP system can be assimilated to a multi input single output LTI system with a theoretically infinite number of parallel LTI systems. The weights correspond to the coefficients of the HTF, which are identified with a local polynomial method in [33]. In [34], an optimal problem is solved to identify the HTF while penalizing non-smooth estimations. Close to the pumping frequency of the system, the prediction error of the identified model dramatically increases when the input is single sinusoidal.

1.3 Solving periodic differential and harmonic equations

This section provides an overview of methods to solve periodic differential equations and harmonic equations. While there are an uncountable number of finite-dimensional constraints in the former, the latter are characterized by a finite number of infinite-dimensional constraints. Although strategies exist to handle infinite-dimensional problems, the resolution of harmonic equations generally requires restrictive assumptions.

1.3.1 Solving periodic differential equations

Periodic differential equations (PDEs) are equations in which equality holds between periodic functions over a period, and they involve the derivative of the unknown periodic function. They arise in many areas, for instance when one wants to check the controllability or observability

of an LTP system [36]. In the context of control, the most well-known PDEs are the periodic Lyapunov and Riccati differential equations described respectively by

$$\textbf{PLDE}: -\dot{P}(t) = P(t)A(t) + A(t)'P(t) + Q(t), \forall t \in [0,T], \qquad P(0) = P(T)$$

and

$$\textbf{PRDE}: -\dot{P}(t) = P(t)A(t) + A(t)'P(t) - P(t)B(t)R^{-1}(t)B(t)'P(t) + Q(t), \forall t \in [0,T]$$

where $P(t) = P(t)' > 0, \forall t \in [0,T]$ and $P(0) = P(T)$.

The main difficulties that arise when solving such equations are the estimation of the derivative $\dot{P}$ and the fact that an infinite number of constraints should be satisfied. Indeed, an equality holds at each time instant over a period, while P should also be positive definite on the same interval. Methods that tackle these challenges exist [36, 37].

For general differential LMIs, a strategy is to subdivide the time domain into several intervals in which the solution has a particular form. In [13], it is clear that searching for a piecewise-quadratic solution is preferable to a piecewise-affine structure. Indeed, the former class can ensure that the solution is continuously differentiable and fewer optimization variables are needed to find a precise solution. For PDLMIs, it is logical to look for a solution with a periodic structure and therefore characterized by its Fourier series.

The solution of the PRDE can be derived from the state transition matrix associated with an Hamiltonian matrix defined as $H(t) = \begin{pmatrix} A(t) & R(t) \\ Q(t) & -A(t)' \end{pmatrix}$. Indeed, from an equation of the form $\begin{pmatrix} \dot{M}(t) \\ \dot{N}(t) \end{pmatrix} = H(t) \begin{pmatrix} M(t) \\ N(t) \end{pmatrix}$, provided that M is invertible, the solution of the PRDE is given by $P(t) = -N(t)M^{-1}(t)$ [38]. However, the Hamiltonian system is unstable, which means that the numerical computation of $N(t)$ and $M(t)$ is not straightforward.

The paper [39] highlights the limits of several methods for solving periodic Riccati, Lyapunov and Sylvester differential equations. A naive approach, the one-shot periodic generator method, consists of computing the solution at time $t = 0$ by solving an algebraic equation, then numerically integrating $P(t)$ over a period so that it satisfies $P(T) = P(0)$. This method can lead to large errors because the ordinary differential equations that are integrated are unstable. There are also difficulties when the period T is large.

A better method is the multi-point periodic generator method introduced in [36], which relies on exact discretization to reformulate PDEs as algebraic equations. A first approach is to write the transition matrix associated with the Hamiltonian as the product of several transition matrices: $\Phi_H(T,0) = \Phi_H(T,T-\Delta)...\Phi_H(2\Delta,\Delta)\Phi_H(\Delta,0)$ where Δ is the time step. Instead of calculating that product, properties of orthogonal matrices can be used to extract the value of the solution of the PRDE at discrete time instants. Since the length of the time interval on which the ordinary differential equations associated with $\Phi_H(k\Delta,(k-1)\Delta)$ must be integrated is restricted to Δ (which is assumed to be small), this reduces numerical errors even in the case of an unstable $A(t)$. Another multi-shot approach is to exploit a recursive relationship between the solution at two successive time instants, similarly to what is done in [38]. The multi-point method can also be used to solve PLDEs, which then reduce to solving as many discrete-time

periodic Lyapunov equations as there are sampling points. Contrary to the one-shot periodic generator method, its multi-point counterpart can handle large periods. The paper [40] shows that a symplectic integrator should be used in the latter case.

In [38], a recursive strategy is also adopted to determine the solution of the PRDE. First, the Hamiltonian matrix is expressed as its truncated Fourier series. The transition matrix satisfying $\dot{\Phi}(t,\tau) = H(t)\Phi(t,\tau)$ can then be estimated at discrete time instants by exploiting Magnus series. Indeed, the latter depend on the Fourier coefficients of $H(t)$, which are known. A formula allows to write the solution of the PRDE in a recursive manner from the values of $\Phi(t,\tau)$ over a period. Therefore, if the solution of the PRDE is known at some time instant, this formula allows to compute the values of the solution at each time instant over a period. A similar reasoning can be used to solve PLDEs.

Although the methods described above are effective for solving differential equations, they do not extend to the case of PDLMIs that appear in robust control. The paper [37] proposes a method for solving PDLMIs. The solution of a periodic Riccati LMI is expressed as a periodic function belonging to $C^1([0,T])$ to allow its derivative to be written as a function of the same Fourier coefficients: $P(t) = \sum_{k=-M}^{M} P_k e^{j\omega kt}$ and $\dot{P}(t) = \sum_{k=-M}^{M} j\omega k P_k e^{j\omega kt}$. Then, the constraints are discretized over a period so that the solution which is determined satisfies only a finite number of constraints. A semidefinite finite-dimensional problem can finally be solved to determine the Fourier coefficients of the solution. This method avoids the numerical issues that are often associated with larger periods T, insofar as there is no need to integrate unstable differential equations. However, the size of the problem increases with the sampling frequency.

In general, there exist methods for solving periodic differential equations and LMIs, but they often consist of determining the solution at discrete time instants over a period and can involve complex calculations. We aim to propose a method whose principle is closer to [37] in the sense that the Fourier coefficients of the solution are determined instead of computing the values of the function itself. However, [37] presents a time-domain formulation, whereas we want to offer a way to solve the problem in the harmonic framework, avoiding the need for discretization or integration.

1.3.2 Solving harmonic equations

Solving harmonic equations such as the harmonic Lyapunov equation

$$\mathcal{P}(\mathcal{A}-\mathcal{N}) + (\mathcal{A}-\mathcal{N})^*\mathcal{P} + \mathcal{Q} = 0$$

or the harmonic Riccati equation

$$\mathcal{P}(\mathcal{A}-\mathcal{N}) + (\mathcal{A}-\mathcal{N})^*\mathcal{P} - \mathcal{P}\mathcal{B}\mathcal{R}^{-1}\mathcal{B}^*\mathcal{P} + \mathcal{Q} = 0$$

with $\mathcal{P} > 0$, and where all operators except $\mathcal{N}$ (which is diagonal) have a Toeplitz block (TB) structure, is challenging. The main difficulty stems from the infinite dimensionality of these equations, but they have the advantage of being algebraic equations, as opposed to periodic differential equations.

In [16], an iterative algorithm is proposed to solve the harmonic Riccati equation with the assumption $\mathcal{A}-\mathcal{N}$ Hurwitz. With the Floquet factorization of the transition matrix $\Phi(t,0) =$

$W(t)e^{Ft}$, the following relationship holds: $\mathcal{A}-\mathcal{N} = \mathcal{W}(\mathcal{F}-\mathcal{N})\mathcal{W}^{-1}$, where $\mathcal{W} = \mathcal{T}(W(t))$ and $\mathcal{F} = \mathcal{T}(F)$. Then, the harmonic Riccati equation can be reformulated as:

$$\underline{\mathcal{P}}(\mathcal{F}-\mathcal{N}) + (\mathcal{F}-\mathcal{N})^*\underline{\mathcal{P}} = -\underline{\mathcal{Q}} + \underline{\mathcal{L}}$$

where

$$\begin{aligned}\underline{\mathcal{P}} &= \mathcal{W}^*\mathcal{P}\mathcal{W}\\ \underline{\mathcal{B}} &= \mathcal{W}^{-1}\mathcal{B}\\ \underline{\mathcal{Q}} &= \mathcal{W}^*\mathcal{Q}\mathcal{W}\\ \underline{\mathcal{L}} &= \underline{\mathcal{P}}\underline{\mathcal{B}}\mathcal{R}^{-1}\underline{\mathcal{B}}^*\underline{\mathcal{P}}\end{aligned}$$

The iterative algorithm to find the solution to this problem is given by:

$$\begin{aligned}\underline{\mathcal{P}}_{(k+1)}(\mathcal{F}-\mathcal{N}) + (\mathcal{F}-\mathcal{N})^*\underline{\mathcal{P}}_{(k+1)} &= -\underline{\mathcal{Q}} + \underline{\mathcal{L}}_{(k)}\\ \underline{\mathcal{L}}_{(k)} &= \underline{\mathcal{P}}_{(k)}\underline{\mathcal{B}}\mathcal{R}^{-1}\underline{\mathcal{B}}^*\underline{\mathcal{P}}_{(k)}\end{aligned}$$

where the index $\cdot_{(k)}$ indicates the value of the variable at the k-th iteration of the algorithm. The previous formulation involves infinite-dimensional operators. Therefore, only the principal submatrix of each Toeplitz matrix is considered for the practical implementation of this algorithm. Each block of a submatrix of order q has a finite dimension $(2q+1)\times(2q+1)$ and contains at most $2q+1$ Fourier coefficients associated with the Toeplitz operator. Since the matrix $\mathcal{F}-\mathcal{N}$ is block diagonal, the product of the principal submatrices of order q associated with $\underline{\mathcal{P}}_{(k+1)}$ and $\mathcal{F}-\mathcal{N}$ is exactly equal to the submatrix of order q of the product $\underline{\mathcal{P}}_{(k+1)}(\mathcal{F}-\mathcal{N})$. The computation of the submatrix of order q associated with the product $\underline{\mathcal{P}}_{(k)}\underline{\mathcal{B}}\mathcal{R}^{-1}\underline{\mathcal{B}}^*\underline{\mathcal{P}}_{(k)}$ is not as straightforward given that the product of truncated Toeplitz matrices is not equal to the truncation of the infinite-dimensional product (see Figure 3.1 in Chapter 3). To avoid approximation, a solution is to compute the product of the corresponding periodic functions in the time domain ($\underline{L}_{(k)}(t) = \underline{P}_{(k)}(t)\underline{B}(t)\mathcal{R}^{-1}(t)\underline{B}(t)'\underline{P}_{(k)}(t)$), then to derive the associated Toeplitz transformation. Then, convergence of the iterative method is guaranteed. However, this method relies on a Floquet factorization, which is not always straightforward to determine. Moreover, the matrix $\mathcal{A}-\mathcal{N}$ is required to be Hurwitz, restricting the applicability of this method to stable dynamics only, which is a significant limitation.

The method proposed in [14] has the advantage of not requiring Floquet factorization to solve the harmonic Lyapunov equation and being valid also for non-Hurwitz $\mathcal{A}-\mathcal{N}$. The idea is to vectorize certain quantities so that the Fourier coefficients of the solution are given by a simple formula. For a sufficiently high truncation order on the solution, the solution to the original problem is obtained up to an arbitrarily small error. Since harmonic Riccati equations can be rewritten as Lyapunov equations, combining a Kleinman-like algorithm with the previous method allows to solve the former. However, this method requires prior knowledge of a Toeplitz matrix $\mathcal{K}$ such that $\mathcal{A}-\mathcal{B}\mathcal{K}-\mathcal{N}$ is stable for initialization.

1.4 Periodic control

Periodic control concerns the design of controllers for periodic systems as well as for non-periodic systems subject to periodic references or disturbances [4]. The control of periodic systems is inherently challenging, as standard tools developed for linear time-invariant (LTI) systems cannot

be directly applied. This section first reviews regulation methods for tracking periodic references and rejecting periodic disturbances, and then provides an overview of robust control techniques for linear time-periodic (LTP) systems.

1.4.1 Tracking and rejection of periodic signals

The regulation of periodic references and the rejection of periodic disturbances constitute a classical problem in control theory and are fundamentally governed by the internal model principle [41]. This principle states that exact asymptotic tracking or disturbance rejection can only be achieved if the controller embeds a dynamical model capable of reproducing the exogenous signal to be regulated. For periodic signals, this implies the inclusion of oscillatory dynamics corresponding to the harmonics of the signal within the control loop.

A well-established control strategy derived from the internal model principle is repetitive control, which has been extensively studied for linear time-invariant (LTI) systems [42–44]. Repetitive control incorporates a generator of periodic signals into the feedback loop, typically realized as a time-delay operator of the form

$$C(s) = \frac{e^{-Ls}}{1 - e^{-Ls}},$$

where L denotes the period of the signal to be tracked or rejected. This structure embeds an internal model of all harmonics of the fundamental frequency, yielding infinite loop gain at integer multiples of that frequency and thereby enabling perfect rejection of periodic disturbances. While L is commonly chosen equal to the signal period, it has been shown that selecting a slightly smaller delay can improve robustness and transient performance [44]. Despite its theoretical appeal, the ideal repetitive controller is not directly implementable in practice, as the presence of infinite gain at infinitely many harmonics can lead to closed-loop instability. Consequently, practical implementations rely on low-pass filtering to limit the effective bandwidth of the internal model, resulting in approximate disturbance rejection over a prescribed frequency range [42].

An alternative and closely related class of controllers is provided by proportional–resonant (PR) controllers [45]. Unlike repetitive control, PR controllers embed internal models only for a finite set of harmonics, thereby yielding a finite-dimensional realization. Specifically, PR controllers enforce infinite loop gain at selected frequencies $k\omega_0$, where $\omega_0 = 2\pi/T$ is the fundamental angular frequency and k belongs to a finite index set H. A typical PR controller is given by

$$C(s) = K_p + \sum_{k \in H} \frac{2K_{r,k}s}{s^2 + (k\omega_0)^2},$$

where K_p is the proportional gain and $K_{r,k}$ are resonant gains associated with the targeted harmonics. This structure allows independent tuning of each harmonic component, offering improved robustness and design flexibility compared to repetitive control. From an internal-model perspective, PR controllers can be interpreted as finite-dimensional approximations of the ideal repetitive controller, in which only a selected subset of harmonics is embedded.

The internal model embedded in PR controllers admits a natural state-space interpretation that aligns with the general output regulation framework. Consider the rejection of the k-th harmonic component in an output signal $y \in \mathbb{R}^p$. This can be achieved by augmenting the plant

with an internal model generating sinusoidal signals at frequency $k\omega_0$. In complex form, this internal model is described by

$$\dot{z}(t) = jk\omega_0 z(t) + y(t),$$

which combines oscillatory dynamics with integral action. An equivalent real-valued realization is obtained by introducing the auxiliary state $r_k \in \mathbb{R}^{2p}$, governed by

$$\dot{r}_k(t) = \begin{pmatrix} 0 & -k\omega_0 I_p \\ k\omega_0 I_p & 0 \end{pmatrix} r_k(t) + \begin{pmatrix} I_p \\ 0 \end{pmatrix} y(t).$$

By stacking such subsystems for all harmonics $k \in H$, one obtains a finite-dimensional internal model whose stabilization ensures asymptotic rejection of the selected harmonic components.

Beyond the LTI setting, internal-model-based regulation has been extended to nonlinear systems subject to periodic disturbances [46, 47]. In this context, the regulation error can be systematically reduced by enriching the internal model with additional harmonic components, at the cost of increased controller complexity [47]. These ideas have been successfully applied to switched and hybrid systems, such as single-phase rectifier bridges, where periodic disturbances arise naturally from the system's operating principle [5]. Closely related techniques are also employed in phase-periodic systems, where modulation-based approaches eliminate specific harmonic components by projecting the regulation error onto sinusoidal basis functions [48]. In such formulations, the internal model is expressed in terms of a phase variable φ, leading to dynamics of the form

$$\dot{z}(\varphi) = \begin{pmatrix} \cos(k\varphi) \\ \sin(k\varphi) \end{pmatrix} y(\varphi),$$

which provides an equivalent mechanism for harmonic rejection.

1.4.2 Robust control of periodic systems

The previous methods allow to deal with periodic perturbations that affect systems which are not necessarily periodic but in this thesis, we are more interested in determining robust periodic control laws for LTP systems of the following form:

$$\dot{x}(t) = A(t)x(t) + B(t)u(t) + B_w(t)w(t) \tag{1.15}$$
$$y(t) = C(t)x(t) + D(t)u(t) \tag{1.16}$$
$$z(t) = C_z(t)x(t) + D_{zu}(t)u(t) \tag{1.17}$$

where w is a disturbance and z is a performance variable.

Robust control of periodic systems has many practical applications. For instance, [49] exploits adaptive dynamic programming to solve a periodic H_∞ problem for magnetic attitude control, whereas in [50], the load of a wind turbine is reduced with a linear quadratic Gaussian (LQG) controller. The same ideas that apply to control for LTI systems also apply here, but we must be careful when extending LTI methods to LTP systems, as difficulties arise due to their time-varying nature. Regarding traditional time-domain methods for robust control, the lifting method [4] offers a well-established approach in the discrete-time domain [51–54]. The harmonic spectrum of a discrete-time periodic signal is intrinsically finite. Consequently, discrete-time periodic linear systems have a finite harmonic state-space representation. However, we focus on

the continuous-time setting, which presents significant challenges [36, 40, 55, 56].

As seen in Section 1.2, Floquet theory can be used to derive an infinite-dimensional harmonic state space representation, from which a harmonic transfer function (HTF) is deduced [32]. Such a frequency domain representation allows to define operators for H_2 and H_∞ robust control but, as the related frequency response operators are infinite dimensional, the numerical implementation is not straightforward [57]. For instance, the H_2 norm of an HTF $\hat{\mathcal{G}}$ is defined in [57] as

$$\|\hat{\mathcal{G}}\|_{H_2}^2 = \frac{1}{2\pi}\int_{-\frac{\omega}{2}}^{\frac{\omega}{2}} trace(\hat{\mathcal{G}}(j\phi)^*\hat{\mathcal{G}}(j\phi))\ d\phi.$$

However, since $\hat{\mathcal{G}}$ is infinite dimensional, a truncation must be performed on this operator to compute an estimation of its H_2 norm. If a Floquet decomposition such that $\mathcal{A}-\mathcal{N} = \mathcal{W}(\mathcal{F}-\mathcal{N})\mathcal{W}^{-1}$ is known, neglecting the high-order harmonics of the operators in $\hat{\mathcal{G}}$ allows to determine an estimate of the H_2 norm. This estimation converges to the true norm when the truncation order (namely the order of the last harmonic to be retained) is high enough.

In [55], the H_2 norm associated with the transfer function $\hat{\mathcal{G}}(s) = \mathcal{C}(s\mathcal{I}-(\mathcal{A}-\mathcal{N}))^{-1}\mathcal{B}$ can be computed in the time domain from the solutions of the following periodic differential Lyapunov equations if A is stable:

$$\dot{P}(t) = P(t)A(t)' + A(t)P(t) + B(t)B(t)' \tag{1.18}$$

$$-\dot{Q}(t) = A(t)'Q(t) + Q(t)A(t) + C(t)'C(t) \tag{1.19}$$

The H_2 norm of $\hat{\mathcal{G}}(s)$ is given by:

$$\|\hat{\mathcal{G}}\|_{H_2}^2 = trace(\int_0^T C(t)P(t)C(t)'\ dt) = trace(\int_0^T B(t)'Q(t)B(t)\ dt). \tag{1.20}$$

Notice that P and Q correspond respectively to the controllability and observability Grammians of the system. For formula (1.20) to hold in the particular case of LTI systems, corresponding to $\dot{P} = \dot{Q} = 0$ and all functions in (1.18) and (1.19) being constant, a factor $\frac{1}{T}$ should be taken into account in formula (1.20). Indeed, in the LTI case, the H_2 norm of the system is defined as the trace of CPC' or $B'QB$.

Similarly as for LTI systems, the H_∞ norm associated with LTP systems measures the effect of the disturbance w on the performance variable z in the worst-case scenario. This norm is defined as follows [55]:

$$\|\hat{\mathcal{G}}(s)\|_{H_\infty} := \sup_{\|\hat{U}\|_{L^2}=1} \|\hat{\mathcal{G}}\hat{U}\|_{L^2}$$

where $\hat{\mathcal{G}}$ corresponds to the HTF between the disturbance and performance output. In [57], this norm is estimated numerically by exploiting what the authors call "staircase truncation". Instead of truncating the operators that appear in the HTF so that the truncated operators have as many blocks horizontally and vertically, the proposed truncation leads to rectangular operators. The dimensions of the resulting operators are $(2N+1)\times(2M+1)$ blocks, and if N and M are large enough, the estimation of the associated H_∞ norm converges to the true norm.

In the time domain, robust control of periodic systems can be achieved by solving periodic differential equations such as the ones presented in Section 1.3. Consider the full state feedback

case, namely $y(t) = x(t)$. The optimal periodic H_2 control problem consists in minimizing the H_2 norm of the HTF between w and z. Let the following assumptions hold: the pair $(A(\cdot), B(\cdot))$ is stabilizable, $D_{zu}(t)$ is full column rank for each t and the periodic system (A, B, C_z, D_{zu}) does not have invariant zeros on the imaginary axis [55,56]. Then the optimal solution of the periodic H_2 problem can be determined by finding the unique stabilizing periodic positive semi-definite solution of the following periodic Riccati equation (see Theorem 2.2, p. 331 in [56]):

$$\begin{aligned}\dot{P}(t)&+A'(t)P(t) + P(t)A(t) + C_z'(t)C_z(t)\\ &- (B(t)'P(t) + D_{zu}'(t)C_z(t))'(D_{zu}'(t)D_{zu}(t))^{-1}(B(t)'P(t) + D_{zu}'(t)C_z(t)) = 0\end{aligned}$$

and the optimal feedback is given by:

$$K(t) = -(D_{zu}'(t)D_{zu}(t))^{-1}(B'(t)P(t) + D_{zu}'(t)C_z(t)).$$

As for the H_∞ control problem, its objective is to design a stabilizing controller such that the H_∞ norm between w and z is smaller than some threshold γ. If there exists K and P a stabilizing periodic positive semi-definite solution of the following periodic Riccati equation, then the system defined by the closed-loop matrix $A(t)+B(t)K(t)$ is stable and the associated H_∞ norm is smaller than γ [56]:

$$\begin{aligned}\dot{P}(t) &+ (A(t) + B(t)K(t))'P(t) + P(t)(A(t) + B(t)K(t))\\ &+ \frac{1}{\gamma^2}P(t)B_w(t)B_w(t)'P(t) + (C_z(t) + D_{zu}(t)K(t))'(C_z(t) + D_{zu}(t)K(t)) = 0\end{aligned}$$

To solve such periodic Riccati equations, the methods that were summarized in Section 1.3 can be leveraged. Optimal control problems for periodic systems can also be formulated as periodic differential LMIs, but they are not straightforward to solve.

In [49] and [58], an adaptive method is implemented to find the solution of an optimal periodic control problem iteratively even when no model of the system is available. The first paper focuses on H_∞ controller, while the second deals with the periodic LQR problem. However, backward integration of a nonlinear differential equation is necessary in both cases. While [59] provides an adaptive method for the LQR problem in which there is no differential equation to solve, a stabilizing feedback should be available for initialization of the method. The paper [60] relaxes the latter assumption, but the proposed method still requires the resolution of a periodic differential Lyapunov equation at each iteration of the algorithm.

Harmonic control is a significant alternative to time-domain formulations, which transforms time-varying control design problems into time-invariant ones within an infinite-dimensional framework [32, 61–63]. This transformation allows the use of established time-invariant control techniques, making the control of systems with harmonics more manageable and intuitive. However, the transition to infinite dimensionality presents its own set of challenges that are not encountered in finite-dimensional control [5, 14]. For example, any harmonic feedback $U(t) = \mathcal{K}X(t)$ should belong to the space H introduced in the preliminaries for an equivalent feedback $u(t) = \mathcal{F}^{-1}(\mathcal{K}X(t))$ to exist in the time domain. A necessary condition for the latter is that $\mathcal{K}$ has a Toeplitz structure [5].

Harmonic control often involves the resolution of harmonic equations which are infinite-dimensional. In [5, 14], the LQR problem associated with the harmonic system

$$(\mathcal{A} - \mathcal{N})^*\mathcal{P} + \mathcal{P}(\mathcal{A} - \mathcal{N}) - \mathcal{P}\mathcal{B}\mathcal{R}^{-1}\mathcal{B}^*\mathcal{P} + \mathcal{Q} = 0$$

is solved, allowing the tracking of periodic trajectories. In [64], the authors place the poles of the closed-loop matrix $\mathcal{A} - \mathcal{N} - \mathcal{B}\mathcal{K}$ by solving the harmonic Sylvester equation $(\mathcal{A} - \mathcal{N})\mathcal{P} - \mathcal{P}(\Lambda \otimes \mathcal{I} - \mathcal{N}) = \mathcal{B}\mathcal{G}$. Indeed, letting $\mathcal{K} = \mathcal{G}\mathcal{P}^{-1}$ in the previous equation leads to $\mathcal{P}^{-1}(\mathcal{A} - \mathcal{N} - \mathcal{B}\mathcal{K})\mathcal{P} = \Lambda \otimes \mathcal{I} - \mathcal{N}$, which guarantees that the poles of the closed-loop system belong to the set $\sigma = \{\lambda + j\omega k, k \in \mathbb{Z}, \lambda \in diag(\Lambda)\}$. However, because the setting is infinite dimensional, choosing $\mathcal{G}$ to ensure that $\mathcal{P}$ is invertible is not straightforward. If a Floquet factorization of the system is known, a suitable expression of $\mathcal{G}$ can be derived.

Conclusion and Thesis Objectives

Linear time-periodic systems provide a natural modeling framework for a wide range of engineered and physical systems, yet their analysis, identification, and control remain significantly more challenging than their time-invariant counterparts. This chapter has reviewed the state of the art and highlighted several fundamental limitations that persist across existing approaches. In particular, identification methods often rely on restrictive assumptions such as open-loop stability, periodic steady-state operation, or carefully designed excitation signals, and they predominantly target discrete-time models. On the control side, many relevant performance and robustness objectives lead to periodic differential linear matrix inequalities, whose time-varying and infinite-dimensional nature makes them difficult to analyze and solve in practice. While harmonic-domain representations offer a promising alternative by transforming time-periodic problems into algebraic ones, the resulting infinite-dimensional inequalities, typically Toeplitz block LMIs, remain largely unexplored from a computational perspective.

These observations motivate several open questions that guide the remainder of this thesis. Can continuous-time LTP systems be identified directly from data without restrictive stability or steady-state assumptions? Can the infinite-dimensional objects arising in harmonic-domain formulations be handled in a principled and convergent manner? And, ultimately, can periodic control problems, particularly those involving robustness and performance guarantees, be solved using tools that retain the conceptual simplicity and effectiveness of LTI control theory? The aim of the following chapters is to provide answers to these questions.

2

A Harmonic Framework for the Identification of Linear Time-Periodic systems

Contents

2.1 Problem statement 18
2.2 From an infinite-dimensional problem to a finite-dimensional least-squares problem 19
2.2.1 Approximating the periodic operators 19
2.2.2 A central strip identification problem 22
2.2.3 Solving the central strip least squares identification problem 24
2.2.4 Validation 26
2.3 Illustrative examples 27
2.3.1 A finite phasor-order example 27
2.3.2 An infinite phasor-order example 32
2.3.3 A wind turbine 33
2.4 Conclusion 35

Introduction

In this chapter, we develop a novel identification framework that builds upon the equivalence between LTP systems and harmonic LTI systems. A review of identification methods for LTP systems was provided in Section 1.2 of Chapter 1. We address the problem of direct identification of a continuous-time LTP system from sampled data, leveraging harmonic state space properties. The chapter is structured as follows. In Section 2.1 we formulate the identification problem as the estimation of the Fourier coefficients that characterize the LTP dynamics. To solve this problem, we exploit an equivalence result established in [5], linking LTP systems to infinite-dimensional LTI systems characterized by a block Toeplitz structure formed by the Fourier coefficients of the state and input matrices. Due to that equivalence, the initial problem of identifying an LTP system comes down to identifying the associated LTI system. However, the harmonic LTI system is inherently infinite-dimensional, implying that a truncation is necessary. In Section 2.2 we prove

that the infinite-dimensional identification problem can be reduced to a finite-dimensional least-squares problem by choosing a high enough truncation order. We also demonstrate that, under regularity assumptions, the solution to this truncated problem converges to the true solution with an arbitrarily small error. Validation criteria to measure the quality of the identified model are defined. The proposed harmonic framework is tested on several examples in Section 2.3. In particular, its robustness to noise is investigated empirically.

2.1 Problem statement

In this part, we specify the identification problem that we aim to solve in this chapter. In particular, we state the assumptions that must be satisfied in our identification framework. A quick overview of the benefits offered by a harmonic framework is also provided.

We consider the continuous-time LTP system described by the state equation (1.7):

$$\dot{x}(t) = A(t)x(t) + B(t)u(t) \tag{2.1}$$

where A and B are T-periodic, real-valued functions belonging to $L^\infty([0\ T])$, $x(t) \in \mathbb{R}^n$ and $u(t) \in \mathbb{R}^m$. Let $T \leq t_0 \leq t_f$ be two real and positive time instants. The following assumptions are required in the identification approach that is presented in this chapter:

Assumption 1 *The period T of the system is known, and the state x can be measured or estimated over a time interval $[t_0 - T, t_f]$.*

These assumptions are common for state-space identification of LTP systems, see for example [24, 30]. Although identification approaches that rely on input/output measurements are more practical than those that require knowledge of the state of the system, we will show later that a property of the harmonic state derivative vector can be exploited to simplify the identification problem.

Due to their periodicity, the functions A and B can be represented by their Fourier series:

$$A(t) = \sum_{k=-\infty}^{\infty} A_k e^{\mathbf{j}\omega kt} \ a.e. \quad B(t) = \sum_{k=-\infty}^{\infty} B_k e^{\mathbf{j}\omega kt} \ a.e. \tag{2.2}$$

Therefore, the identification of the time-varying functions A and B can be achieved through the identification of their respective Fourier coefficients sequences $(A_k)_{k\in\mathbb{Z}}$ and $(B_k)_{k\in\mathbb{Z}}$.

As established in the preliminaries on harmonic modeling in Chapter 1, studying LTP systems of the form (2.1) essentially involves examining an equivalent infinite-dimensional LTI system as defined in (1.8):

$$\dot{X}(t) = (\mathcal{A} - \mathcal{N})X(t) + \mathcal{B}U(t) \tag{2.3}$$

The Fourier coefficients of A and B appear explicitly in the operators $\mathcal{A}$ and $\mathcal{B}$, which possess a Toeplitz structure as seen in (1.1). Hence, the task of identifying an LTP system can be reformulated as identifying the operators $\mathcal{A}$ and $\mathcal{B}$ of its associated harmonic LTI system. Consequently, the infinite-dimensional identification problem we aim to solve in this chapter, achieving precision to an arbitrarily small error, can be stated as follows:

Problem 1 *Under Assumption 1, identify the Toeplitz operators $\mathcal{A}$ and $\mathcal{B}$ in the harmonic LTI system* (2.3) *from a state/input (x, u) trajectory of the LTP system* (2.1)*. Deduce the periodic functions A and B from their Fourier series* (2.2)*.*

Although numerous identification methods exist for LTI systems, the infinite dimension of the harmonic system represents a challenge to be addressed. Our goal is to provide a computationally tractable approach to identification of (2.3) with a guaranteed bound on the approximation. As we shall see in the sequel, adopting a harmonic approach offers several noteworthy benefits.

The first advantage is inherently tied to the LTI characteristic of the harmonic system insofar as its state and input matrices are time invariant, as opposed to those of the equivalent LTP system. Their Toeplitz structure is particularly noteworthy, given that the information contained within these matrices is redundant. This is confirmed by the structure of the derivative of the harmonic state vector. Indeed, as seen in [5], the derivative of any state phasor satisfies the following relationship:

$$\forall k \in \mathbb{Z}, \dot{X}_k(t) = e^{-j\omega kt}\dot{X}_0(t) \ a.e. \tag{2.4}$$

with

$$\dot{X}_0(t) = \frac{1}{T}(x(t) - x(t-T)), \tag{2.5}$$

which not only means that the vector $\dot{X}$ can be directly inferred from x, eliminating the need for differentiation, but also that $\dot{X}_k(t)$ contains the same information as $\dot{X}_0(t)$. These two last formulas will be very useful to generate harmonic data from time-domain trajectories and simplify the identification problem, as will be clear in what follows. Another advantage pertains to the filtering of high-frequency noise achieved when computing the low-order phasors of (X, U) from state and input trajectories (x, u).

2.2 From an infinite-dimensional problem to a finite-dimensional least-squares problem

In this section, we show how Problem 1 can be reduced to a finite-dimensional least-squares identification problem by exploiting convergence properties of periodic approximations, as well as the Toeplitz structure of the harmonic model. The solution of this finite-dimensional problem satisfies the original problem up to an arbitrarily small error under a regularity assumption on A and B. As a consequence, the identification of the original LTP system is achieved with a guaranteed bound on the approximation in the ideal case of noise-free data.

2.2.1 Approximating the periodic operators

Before deriving a finite-dimensional approximation to Problem 1, we start by proving some technical results. For $p \geq 0$, we define the p-banded periodic approximation of A as $A|_p(t) := \sum_{|k|\leq p} A_k e^{j\omega kt}$ with A_k the $k-$th Fourier coefficient of A. The following assumption is needed to prove the results in this section:

Assumption 2 (Uniform Convergence a.e. of the Fourier series) *The T-periodic matrix function A admits a convergent Fourier series in L^∞, that is:*

$$\lim_{p\to+\infty} \|A|_p(t) - A(t)\|_{L^\infty} = 0.$$

What if Assumption 2 is not satisfied? Assumption 2 may seem restrictive but it is achieved for instance when A is continuous with bounded variations. However, if A belongs to L^∞ but is discontinuous, Assumption 2 is not satisfied. Nevertheless, for any $\varepsilon > 0$, the regularization

$A_\varepsilon = A * \varphi_\varepsilon$ where $\varphi_\varepsilon(s) = \frac{1}{\varepsilon}\varphi\left(\frac{s}{\varepsilon}\right)$ and where φ refers to a bump (or test) function, belongs to C^∞ and thus satisfies Assumption 2.

The key idea is to define a regularized version $A_\varepsilon(t)$ of $A(t)$, parameterized by $\varepsilon > 0$, such that:

1. Assumption 2 is satisfied for every $\varepsilon > 0$;
2. The trajectories of the regularized system converge uniformly to those of the original system on any compact time interval as $\varepsilon \to 0$.

Here, we propose a regularization strategy to obtain such regularized matrices. Let us define the test function $\varphi : \mathbb{R} \to \mathbb{R}$ by:

$$\varphi(t) = \begin{cases} \exp\left(-\dfrac{1}{1-|t|^2}\right), & \text{if } |t| < 1 \\ 0, & \text{if } |t| \geq 1 \end{cases}$$

This function is C^∞, compactly supported, strictly positive inside its support, and satisfies $\int_{\mathbb{R}} \varphi(t)\, dt = 1$. Let $a : \mathbb{R} \to \mathbb{R}$ be a T-periodic function and define its regularized version a_ε:

$$a_\varepsilon(t) = \varphi_\varepsilon * a\ (t) = \int_{-\varepsilon}^{\varepsilon} a(t-\tau)\, \varphi_\varepsilon(\tau)\, d\tau, \tag{2.6}$$

where $\varphi_\varepsilon(\tau) = \frac{1}{\varepsilon}\varphi\left(\frac{\tau}{\varepsilon}\right)$. The function φ_ε is C^∞, compactly supported in $[-\varepsilon, \varepsilon]$, and preserves the normalization property. We have:

1. $a_\varepsilon \in C^\infty(\mathbb{R})$ and T-periodic,
2. $a_\varepsilon \to a$ in $L^p([0,T])$, for any $1 \leq p < \infty$, if $a \in L^p([0,T])$.
3. $a_\varepsilon \to a$ a.e. if $a \in L^\infty([0,T])$

If we replace a T-periodic matrix $A \in L^\infty(\mathbb{R}; \mathbb{R}^{n\times n})$ by its regularized version $A_\varepsilon(t)$ whose coefficients are given by $a_{\varepsilon_{ij}} = \varphi_\varepsilon * a_{ij}$, then $A_\varepsilon(t) \in C^\infty$ and its Fourier series converges uniformly.

Let $A \in L^\infty(\mathbb{R}; \mathbb{R}^{n\times n})$ be a T-periodic matrix and consider:

$$\dot{x}(t) = A(t)x(t), \quad x(0) = x_0. \tag{2.7}$$

with its regularized version:

$$\dot{x}_\varepsilon(t) = A_\varepsilon(t)x_\varepsilon(t), \quad x_\varepsilon(0) = x_0. \tag{2.8}$$

We use a density argument to demonstrate that, for sufficiently small ε, the trajectories of the regularized system remain arbitrarily close to those of the original system.

Theorem 3 *For any initial condition $x(0) = x_\varepsilon(0)$, the solution x_ε of the regularized system* (2.8) *converges uniformly to the solution x of the original system* (2.7) *on any compact time interval $[0\ t_f]$. In other words,*

$$\sup_{t\in[0,t_f]} \|x(t) - x_\varepsilon(t)\| \longrightarrow 0 \quad \text{as } \varepsilon \to 0.$$

Proof 3 *Define* $\delta_\varepsilon(t) \coloneqq x(t) - x_\varepsilon(t)$. *Then,*

$$\dot{\delta}_\varepsilon(t) = A(t)\delta_\varepsilon(t) + \big(A(t) - A_\varepsilon(t)\big)x_\varepsilon(t),$$

and it follows:

$$\|\dot{\delta}_\varepsilon(t)\| \leq \|A(t)\|\ \|\delta_\varepsilon(t)\| + \|A(t) - A_\varepsilon(t)\|\ \|x_\varepsilon(t)\|.$$

Let $C \coloneqq \|A(t)\|_{L^\infty} < +\infty$, *and assume that* $\|x_\varepsilon(t)\| \leq M$ *on* $[0, t_f]$ *(justification follows). Then:*

$$\frac{d}{dt}\|\delta_\varepsilon(t)\| \leq C\|\delta_\varepsilon(t)\| + M\|A(t) - A_\varepsilon(t)\|.$$

By Grönwall's inequality (non-homogeneous version):

$$\|\delta_\varepsilon(t)\| \leq \int_0^t M\|A(\tau) - A_\varepsilon(\tau)\|e^{C(t-\tau)}d\tau.$$

Taking the supremum over $[0, t_f]$*:*

$$\sup_{t\in[0,t_f]} \|\delta_\varepsilon(t)\| \leq Me^{Ct_f}\|A - A_\varepsilon\|_{L^1([0,t_f])}.$$

Since $A_\varepsilon \to A$ *in* $L^1([0, t_f])$, *and because* $A \in L^\infty([0, t_f]) \subset L^p([0, t_f])$ *for all* $p \geq 1$, *we conclude:*

$$\sup_{t\in[0,t_f]} \|x(t) - x_\varepsilon(t)\| \longrightarrow 0.$$

Now, let us justify the bound on $x_\varepsilon(t)$ *on* $[0\ t_f]$. *Since* $\dot{x}_\varepsilon(t) = A_\varepsilon(t)x_\varepsilon(t)$, *applying Grönwall's inequality again, we get:*

$$\|x_\varepsilon(t)\| \leq \|x_0\| \exp\left(\int_0^t \|A_\varepsilon(\tau)\|d\tau\right).$$

Since $A_\varepsilon \to A$ *in* $L^1([0, t_f])$ *and* $A \in L^\infty$, *the norms* $\|A_\varepsilon\|_{L^1([0,t_f])}$ *are uniformly bounded since*

$$\begin{aligned}\|A_\varepsilon\|_{L^1([0,t_f])} &\leq \|A_\varepsilon - A\|_{L^1([0,t_f])} + \|A\|_{L^1([0,t_f])} \\ &\leq \|A_\varepsilon - A\|_{L^1([0,t_f])} + \|A\|_{L^\infty([0,t_f])}t_f.\end{aligned}$$

Therefore, $\|x_\varepsilon(t)\| \leq M$ *for some constant* M *independent of* ε *on* $[0\ t_f]$. ∎

This density result shows that even if A and B do not satisfy Assumption 2, it is still possible to assume that they have smooth representations A_ε and B_ε that satisfy Assumption 2 and lead to an arbitrarily small error in the obtained trajectories. This justifies the fact that we deal in the sequel only with periodic matrix functions that belong to L^∞ and such that Assumption 2 is satisfied.

The following theorem establishes the convergence of the periodic approximation of any periodic function in $L^\infty([0\ T])$ under Assumption 2.

Theorem 4 *If* $A \in L^\infty([0, T])$ *and satisfies Assumption 2 then:*

$$\lim_{p\to+\infty} \|\mathcal{A} - \mathcal{A}|_p\|_{\ell^2} = 0$$

where $\mathcal{A} \coloneqq \mathcal{T}(A)$ *and* $\mathcal{A}|_p \coloneqq \mathcal{T}(A|_p)$.

Proof 4 *This is a direct consequence of Assumption 2 and Theorem 2.* ∎

From this result, it follows that replacing the pair $(\mathcal{A}, \mathcal{B})$ by the p-banded operators $(\mathcal{A}|_p, \mathcal{B}|_p)$ leads to the following approximation of the harmonic state dynamic:

Corollary 1 *Let (x, u) be a trajectory of (1.7) such that A and B satisfy Assumption 2 and $(X, U) \coloneqq \mathcal{F}(x, u)$. For any $\epsilon > 0$, there exists p such that for any compact time interval I*

$$\sup_{t \in I} \frac{\|\Psi_p(X(t), U(t))\|_{\ell^2}}{\|(X(t), U(t))\|_{\ell^2}} \leq 2\epsilon \tag{2.9}$$

where $\Psi_p(X(t), U(t)) \coloneqq (\mathcal{A} - \mathcal{N})X(t) + \mathcal{B}U(t) - ((\mathcal{A}|_p - \mathcal{N})X(t) + \mathcal{B}|_p U(t))$ is the harmonic state derivative error due to banding the state and input operators to the order p.

Proof 5 *As the operator norms are sub-multiplicative, we have for any t:*

$$\begin{aligned}
&\|(\mathcal{A} - \mathcal{N})X(t) + \mathcal{B}U(t) - ((\mathcal{A}|_p - \mathcal{N})X(t) + \mathcal{B}|_p U(t))\|_{\ell^2} \\
&\qquad \leq \|\mathcal{A} - \mathcal{A}|_p\|_{\ell^2} \|X(t)\|_{\ell^2} + \|\mathcal{B} - \mathcal{B}|_p\|_{\ell^2} \|U(t)\|_{\ell^2} \\
&\qquad \leq (\|\mathcal{A} - \mathcal{A}|_p\|_{\ell^2}\| + \|\mathcal{B} - \mathcal{B}|_p\|_{\ell^2})\|(X(t), U(t))\|_{\ell^2}
\end{aligned}$$

then, as X and U are absolutely continuous functions of the time, the supremum on any compact set exists and using Theorem 4 the result follows. ∎

Definition 2 *The degree $d^o A \in \mathbb{Z}^+ \cup \{+\infty\}$ of A is defined as the greatest non vanishing phasor of A.*

Corollary 1 shows that if $d^o A$ and $d^o B$ are not finite but A and B satisfy Assumption 2, it is still possible to obtain an accurate approximated solution to the identification problem by imposing a sufficiently large band order p. Indeed for a given $\epsilon > 0$ and $p(\epsilon)$ such that Corollary 1 holds, the solution $(\tilde{\mathcal{A}}, \tilde{\mathcal{B}})$ of the normalized linear least-squares optimization problem:

$$\min_{\mathcal{A}|_p, \mathcal{B}|_p} \sup_{t \in I} \frac{\|\dot{X}(t) - ((\mathcal{A}|_p - \mathcal{N})X(t) + \mathcal{B}|_p U(t))\|_{\ell^2}^2}{\|(X(t), U(t))\|_{\ell^2}^2}$$

where the unknowns $\mathcal{A}|_p$ and $\mathcal{B}|_p$ are block p-banded (i.e. $A_k \coloneqq 0$ and $B_k \coloneqq 0$ for $k > p$) and Toeplitz matrices, will necessarily satisfy relation (2.9).

2.2.2 A central strip identification problem

The previous results and formula (2.4) allow us to show that Problem 1 can be simplified and reduced to a finite-dimensional problem. This problem is referred to as the "central strip identification problem," insofar as it only leverages information from the "0-row" of (2.3).

Theorem 5 *Problem 1 can be reduced to the central strip identification problem which involves the identification of the Fourier coefficients $(A_k)_{k \in \mathbb{Z}}$ and $(B_k)_{k \in \mathbb{Z}}$ in:*

$$\dot{X}_0(t) = \sum_{k \in \mathbb{Z}} A_k X_{-k}(t) + \sum_{k \in \mathbb{Z}} B_k U_{-k}(t). \tag{2.10}$$

Moreover, if there exists a finite $p \geq 0$ such that (2.9) holds, the central strip identification problem reduces to the identification of $(A_k)_{|k| \leq p}$ and $(B_k)_{|k| \leq p}$ in:

$$\dot{X}_0(t) = \sum_{k=-p}^{p} A_k X_{-k}(t) + \sum_{k=-p}^{p} B_k U_{-k}(t)$$

which is a finite dimensional problem that involves $n(n+m)(2p+1)$ real unknowns.

Proof 6 *Since the phasors of $\dot{X}$ are related with $\dot{X}_0$ by the relationship $\dot{X}_q(t) = e^{-j\omega qt}\dot{X}_0(t)$ for any q, and as the 0-row of (2.3) can be written*

$$\dot{X}_0(t) = \sum_{k\in\mathbb{Z}} A_k X_{-k}(t) + \sum_{k\in\mathbb{Z}} B_k U_{-k}(t),$$

it follows that the $q-$strip of (2.3) corresponding to $\dot{X}_q(t)$ satisfies

$$\dot{X}_q(t) = e^{-j\omega qt}\Big(\sum_{k\in\mathbb{Z}} A_k X_{-k}(t) + \sum_{k\in\mathbb{Z}} B_k U_{-k}(t)\Big)$$

and is no more informative than $\dot{X}_0$ when it comes to the identification of the Fourier coefficients of A and B. Thus, only the central strip is sufficient to identify the harmonic system (2.3). Moreover, if there exists a finite $p \geq 0$ such that (2.9) holds, there are $n^2(2p+1) + nm(2p+1)$ complex unknowns to be determined in this problem, given that the phasors of A and B exhibit the following dimensions: $\forall k \in \mathbb{Z}, A_k \in \mathbb{C}^{n\times n}$ and $B_k \in \mathbb{C}^{n\times m}$. As A and B are real-valued functions, their phasors of negative and positive order are complex conjugates of each other: $\forall k \in \mathbb{Z}, A_{-k} = \overline{A_k}$. Furthermore, since any phasor of order 0 is real valued, this means that Problem 1 amounts to identifying $n(n+m)(2p+1)$ real unknowns. ■

Notice that focusing only on the central strip allows to avoid taking into account the operator $\mathcal{N}$ since the value of its 0-row is zero as seen in (1.6). Moreover, if $d^oA = d^oB = 0$, the identified model is LTI.

Finally, combining Corollary 1 and Theorem 5 leads to the following finite-dimensional least-squares problem:

Theorem 6 *For any $u \in L^2_{loc}$ and any $\epsilon > 0$, if A and B satisfy Assumption 2, there exists p such that the finite dimensional normalized central strip identification problem on interval I given by:*

$$\min_{A_k,B_k,|k|\leq p} \sup_{t\in I} \frac{\|\dot{X}_0(t) - \sum_{k=-p}^{p}(A_k X_{-k}(t) + B_k U_{-k}(t))\|^2}{\|(X(t),U(t))\|^2_{\ell^2}} \tag{2.11}$$

where $\|\cdot\|$ refers to the 2-norm, leads to an approximated solution $\tilde{A}(t) := \sum_{k=-p}^{p}\tilde{A}_k e^{\mathbf{j}\omega kt}$ and $\tilde{B}(t) := \sum_{k=-p}^{p}\tilde{B}_k e^{\mathbf{j}\omega kt}$ that satisfies:

$$\sup_{t\in I} \frac{\|\dot{X}_0(t) - \sum_{k=-p}^{p}(\tilde{A}_k X_{-k}(t) + \tilde{B}_k U_{-k}(t))\|}{\|(X(t),U(t))\|_{\ell^2}} \leq 2\epsilon \tag{2.12}$$

and relation (2.12) still holds true if I in (2.11) and (2.12) is replaced by a discrete set $I_d \subset I$.

Proof 7 *Let us define the central strip selecting operator $\mathcal{C}_0 := [\cdots\ 0\ Id_n\ 0\ \cdots]$ such that $X_0 = \mathcal{C}X$ where $X := \mathcal{F}(x)$. Obviously $\|\mathcal{C}_0\| = 1$ where $\|\cdot\|$ is the standard Euclidian norm (2-norm) since*

$$\sup_{\|X\|_{\ell^2}=1} \|\mathcal{C}_0 X\| = \sup_{\|X\|_{\ell^2}=1} \|X_0\| = 1$$

is achieved for $X = [\cdots, 0, X_0, 0, \cdots]$ with $\|X_0\| = 1$. Now, for a given u, and $\epsilon > 0$, under Assumption 2, we know that there exists p such that Corollary 1 is satisfied and thus relation (2.9) holds. Therefore,

$$\frac{\|\mathcal{C}_0\Psi_p(X(t),U(t))\|}{\|(X(t),U(t))\|_{\ell^2}} \leq \|\mathcal{C}_0\| \sup_{t\in I} \frac{\|\Psi_p(X(t),U(t))\|_{\ell^2}}{\|(X(t),U(t))\|_{\ell^2}} \leq 2\epsilon. \tag{2.13}$$

As $\mathcal{C}_0\Psi_p(X(t),U(t)) = \dot{X}_0(t) - \sum_{k=-p}^{p}(A_k X_{-k}(t) + B_k U_{-k}(t))$, we see that the minimizer of (2.11) satisfies necessarily (2.12). Finally, if in (2.11) I is replaced by a discrete set $I_d \subset I$, the minimizer of (2.11) satisfies necessarily (2.12) on I_d. ■

Remark 1 (Normalization) *Note that computing* $\|(X(t),U(t))\|_{\ell^2}$ *in* (2.11) *can be simply achieved by computing* $\|(x(t),u(t))\|_{L^2([t-T\ t])}$ *as Parseval theorem implies*

$$\|X(t)\|_{\ell^2} = \|x\|_{L^2([t-T\ t])} = (\frac{1}{T}\int_{t-T}^{t} x^2(\tau)d\tau)^{\frac{1}{2}}.$$

2.2.3 Solving the central strip least squares identification problem

Having successfully converted the infinite-dimensional harmonic identification problem into an approximate finite-dimensional counterpart, we can now detail the conditions that are essential for achieving a precise solution from a discrete-time sequence of data. The theoretical results in this part allow the true system to be recovered up to an arbitrarily small error from noise-free data. We will show in Section 2.3 that the proposed identification framework can handle some noise.

Constructing the data matrices in the harmonic domain

In practice, only samples of the state and input trajectories are available. For a sufficiently large number N, consider a sampled state/input trajectory (x,u) of the LTP system (2.1) with sampling time $\delta t = T/N$ over the time interval $I := [t_0-T, t_f]$. Suppose that an anti-aliasing filter was applied. Let $p < \infty$ be the degree of the system that we want to identify. The computation of phasors $(X_k(t),U_k(t))$ for $|k| \le p$ in the time interval $[t_0,t_f]$ can be performed efficiently by using a Fast Fourier Transform (FFT) algorithm, especially if N is a power of 2. Notice that to determine the phasors of a signal at time t, it should be available on the interval $[t-T,t]$. This explains why the state and input phasors are computed from time t_0. Moreover, $\dot{X}_0$ can be determined using (2.5). Then, these data are normalized following Remark 1 that is, for $|k| \le p$:

$$(X_k(t),U_k(t))_{\mathbf{N}} := \frac{(X_k(t),U_k(t))}{M(t)} \text{ and } \dot{X}_{0_{\mathbf{N}}}(t) := \frac{\dot{X}_0(t)}{M(t)}$$

where $M(t) := \|(x(t),u(t))\|_{L^2([t-T\ t])}$. Let L be the number of samples available for identification. The computed phasors are stored in the following data matrices:

$$\mathbf{X_1} := \begin{pmatrix} \dot{X}_{0_{\mathbf{N}}}(t_0) & \cdots & \dot{X}_{0_{\mathbf{N}}}(t_f) \end{pmatrix} \in \mathbb{R}^{n\times L}$$

$$\mathbf{X_0} := \begin{pmatrix} X_{-p_{\mathbf{N}}}(t_0) & \cdots & X_{-p_{\mathbf{N}}}(t_f) \\ \vdots & & \vdots \\ X_{p_{\mathbf{N}}}(t_0) & \cdots & X_{p_{\mathbf{N}}}(t_f) \end{pmatrix} \in \mathbb{C}^{n(2p+1)\times L}$$

$$\mathbf{U_0} := \begin{pmatrix} U_{-p_{\mathbf{N}}}(t_0) & \cdots & U_{-p_{\mathbf{N}}}(t_f) \\ \vdots & & \vdots \\ U_{p_{\mathbf{N}}}(t_0) & \cdots & U_{p_{\mathbf{N}}}(t_f) \end{pmatrix} \in \mathbb{C}^{m(2p+1)\times L}$$

Conditions for solving the identification problem from data

Once the data matrices $(\mathbf{X_1},\mathbf{X_0},\mathbf{U_0})$ have been constructed, the p-banded central strip identification problem given by (2.11) can be formulated as follows:

Problem 2 *From data* $(\mathbf{X_1},\mathbf{X_0},\mathbf{U_0})$*, solve the least-squares problem:*

$$\min_{A_k,B_k,\ |k|\le p} \|\mathbf{X_1} - [A_p,\cdots,A_{-p},B_p,\cdots,B_{-p}]\begin{bmatrix}\mathbf{X_0}\\ \mathbf{U_0}\end{bmatrix}\|^2 \tag{2.14}$$

where $\|\cdot\|$ *refers to* $2-$*norm.*

There exists a unique solution of (2.14) under the following rank condition:

Proposition 1 *A unique solution of* (2.14) *can be recovered from the data* $(\mathbf{X_0}, \mathbf{U_0})$ *if and only if*

$$rank \begin{pmatrix} \mathbf{X_0} \\ \mathbf{U_0} \end{pmatrix} = (n+m)(2p+1). \tag{2.15}$$

Proof 8 *This is a standard condition for solving linear least squares problems, insofar as* $\begin{pmatrix} \mathbf{X_0} \\ \mathbf{U_0} \end{pmatrix}$ *having full row rank guarantees that the matrix* $\begin{pmatrix} \mathbf{X_0} \\ \mathbf{U_0} \end{pmatrix}\begin{pmatrix} \mathbf{X_0} \\ \mathbf{U_0} \end{pmatrix}^*$ *is invertible.* ■

To ensure that the rank condition (2.15) is met, a necessary condition is that the sample size, denoted as L, exceeds the value of $(n+m)(2p+1)$. Let $X_{-p:p_{\mathbf{N}}}(t)$ and $U_{-p:p_{\mathbf{N}}}(t)$ be column vectors that contain the normalized phasors of X and U from order $-p$ to p at time t.

Solution of the data-based identification problem

The solution of the data-based least squares identification problem (2) can now be stated.

Theorem 7 *For a given* p*, if the data* $(\mathbf{X_0}, \mathbf{U_0})$ *satisfy the rank condition* (2.15)*, the solution of the least-squares problem* (2.14) *is given by*

$$[\tilde{A}_p, \cdots, \tilde{A}_{-p}, \tilde{B}_p, \cdots, \tilde{B}_{-p}] := \mathbf{X_1} \begin{bmatrix} \mathbf{X_0} \\ \mathbf{U_0} \end{bmatrix}^{\dagger}$$

where $\begin{bmatrix} \mathbf{X_0} \\ \mathbf{U_0} \end{bmatrix}^{\dagger}$ *refers to the pseudo-inverse of* $\begin{bmatrix} \mathbf{X_0} \\ \mathbf{U_0} \end{bmatrix}$ *and is uniquely determined. Moreover, for a given* $\epsilon > 0$*, if* p *satisfies Corollary 1 on* $I := [t_0, t_f]$ *then relation* (2.12) *is satisfied at least at every sample time* $t := t_0 + k\delta t$ *of* I *and we have:*

$$\max_t \| ([\tilde{A}_p, \cdots, \tilde{A}_{-p}, \tilde{B}_p, \cdots, \tilde{B}_{-p}] - [A_p, \cdots, A_{-p}, B_p, \cdots, B_{-p}]) \begin{bmatrix} X_{-p:p_{\mathbf{N}}}(t) \\ U_{-p:p_{\mathbf{N}}}(t) \end{bmatrix} \| \leq 4\epsilon. \tag{2.16}$$

Proof 9 *As condition* (2.15) *is satisfied, the minimizer of* (2.14) *is uniquely defined. If* p *is such that Corollary 1 is satisfied on* I *then relation* (2.12) *is satisfied on every sample time* $t := t_0 + k\delta t$ *(as stated in Theorem 6). Using* (2.12) *and* (2.13)*, it follows that for any sample time* $t := t_0 + k\delta t$*:*

$$\begin{aligned} &\| ([\tilde{A}_p, \cdots, \tilde{A}_{-p}, \tilde{B}_p, \cdots, \tilde{B}_{-p}] - [A_p, \cdots, A_{-p}, B_p, \cdots, B_{-p}]) \begin{bmatrix} X_{-p:p_{\mathbf{N}}}(t) \\ U_{-p:p_{\mathbf{N}}}(t) \end{bmatrix} \| \\ &\leq \| \sum_{k=-p}^{p} (\tilde{A}_k X_{-k_{\mathbf{N}}}(t) + \tilde{B}_k U_{-k_{\mathbf{N}}}(t)) - \dot{X}_{0_{\mathbf{N}}}(t) \| + \| \dot{X}_{0_{\mathbf{N}}}(t) - \sum_{k=-p}^{p} (A_k X_{-k_{\mathbf{N}}}(t) + B_k U_{-k_{\mathbf{N}}}(t)) \| \leq 4\epsilon. \end{aligned}$$

■

Corollary 2 *Let* (2.15) *hold. This implies that there exists a subsequence of sampling time* t_{i_k} *of length* $(n+m)(2p+1)$ *such that the matrix* V *whose columns are formed by* $(X_{-p:p_{\mathbf{N}}}(t_{i_k}), U_{-p:p_{\mathbf{N}}}(t_{i_k}))$ *is invertible. Then, the following bound holds:*

$$\| [\tilde{A}_p, \cdots, \tilde{A}_{-p}, \tilde{B}_p, \cdots, \tilde{B}_{-p}] - [A_p, \cdots, A_{-p}, B_p, \cdots, B_{-p}] \| \leq 4\epsilon M$$

where $M = (n+m)(2p+1)\|V^{-1}\|$.

Proof 10 *As the rank condition* (2.15) *is achieved, an invertible matrix* V *can be extracted from the columns of* $(\mathbf{X_0}, \mathbf{U_0})$. *As for any* $Y \in \mathbb{R}^r$ *with* $r = (n+m)(2p+1)$ *s.t.* $\|Y\| = 1$, *there exists* Λ *s.t.* $Y = V\Lambda$, *the following relation holds (using* (2.16)*):*

$$\|([\tilde{A}_p, \cdots, \tilde{A}_{-p}, \tilde{B}_p, \cdots, \tilde{B}_{-p}] - [A_p, \cdots, A_{-p}, B_p, \cdots, B_{-p}])Y\| \leq 4\epsilon \sum_i |\Lambda_i|$$

Using norm equivalence in finite dimension, we have:

$$\begin{aligned}\|([\tilde{A}_p, \cdots, \tilde{A}_{-p}, \tilde{B}_p, \cdots, \tilde{B}_{-p}] - [A_p, \cdots, A_{-p}, B_p, \cdots, B_{-p}])Y\| &\leq 4\epsilon r \|\Lambda\| \\ &\leq 4\epsilon r \|V^{-1}Y\| \\ &\leq 4\epsilon r \|V^{-1}\|\end{aligned}$$

Taking the supremum on Y *leads to the result.* ∎

Corollary 1 establishes the existence of a solution for a high enough order p without providing a constructive approach. A sufficient condition for the bound (2.12) to hold is that $p \geq max(d^oA, d^oB)$. If these degrees are unknown, Problem (2.14) can be solved with increasing values of p until the difference between two successive solutions is smaller than some specified threshold and the higher-order phasors of the solution approach zero. If $\max(d^oA, d^oB) = \infty$ and A or B is discontinuous, a smooth approximation of these functions can be determined.

Furthermore, the rank condition (2.15) acts as a necessary and sufficient condition for the uniqueness of a solution in Problem 2 when dealing with noise-free data. However, it is essential to highlight that this rank condition becomes insufficient in the presence of noisy measurements, which is unavoidable when dealing with real systems. In that case, the true system matrices can no longer be exactly recovered by solving the least-squares problem 2. To mitigate the impact of noise, selecting a larger value for the number of samples L is crucial for solving Problem 2. We demonstrate the effect of noise on the identification method in Section 2.3.

2.2.4 Validation

After solving the least-squares Problem 2 for a particular value of p, the quality of the resulting model must be evaluated. This section outlines how the identified model can be assessed. The choice of the validation approach depends on the available information on the system. Two validation methods are considered in this work. In the first one, a model of the system is available for direct comparison, while the other approach only relies on validation data.

When the true phasors are available for comparison

Assume that the p first Fourier coefficients that characterize the LTP dynamics are available, so that we can directly compare their values with the estimated ones. The relative identification error between the true and estimated Fourier coefficients of A and B is defined as follows:

$$err := 100 \cdot \frac{\|[A_p, \cdots, A_{-p}, B_p, \cdots, B_{-p}] - [\tilde{A}_p, \cdots, \tilde{A}_{-p}, \tilde{B}_p, \cdots, \tilde{B}_{-p}]\|_2}{\|[A_p, \cdots, A_{-p}, B_p, \cdots, B_{-p}]\|_2}(\%) \tag{2.17}$$

A threshold ε must be defined to indicate if the obtained values of the phasors are close enough to the true ones. This threshold depends on the intended application of the identified model. Note that this error metric does not take into account the error on harmonics of order

higher than p. Indeed, our identification scheme aims at estimating the p-banded operator that best explains the data. If $p = \max(d^oA, d^oB) < \infty$ and the data are free from noise, exact identification of the nonzero phasors of A and B is possible if the rank condition (2.15) holds. Suppose that p is underestimated, e.g. $p \ll max(d^oA, d^oB)$. Then, the computation of (2.17) would reveal the inadequacy of p since err would be large. In Chapter 4, we will present a robust framework that could be adapted to deal with such model uncertainties.

When a set of validation data is available

It is crucial to recognize that in real-world scenarios, the theoretical values of the phasors that characterize a system are often unknown. Moreover, any model is imperfect by nature. Consequently, it is preferable to evaluate the prediction ability of the identified model on a new trajectory. This validation procedure involves the use of a different dataset separate from the one used for identification, named *validation dataset*. One can simulate the identified LTP system on a new trajectory with the same input as in the validation dataset, facilitating a comparison between the true and estimated trajectories.

To quantify the quality of the prediction with the estimated model, a fit percentage, defined for each component of the state, can be computed with:

$$Fit_i = 100 \cdot (1 - \frac{\|x_i - \tilde{x}_i\|_2}{\|x_i - \overline{x_i}\|_2}) \ (\%) \tag{2.18}$$

where x_i is the trajectory of the i-th component of the state from the validation set, $\overline{x_i}$ is its mean and $\tilde{x}_i$ is the trajectory obtained with the identified model. The closer Fit_i is to 100%, the better the prediction ability of the identified model.

In both cases, if the validation procedure indicates that the model is far from ideal, a larger value of p or L could help improve the quality of the model. A risk that should be taken into account in the case of noisy data is that considering a too large p might lead to overfitting.

2.3 Illustrative examples

In this section, the proposed harmonic identification framework is tested on a range of examples. We begin by verifying the theoretical exactness of the method in an ideal, noise-free scenario with a stable system of finite degree (Subsection 2.3.1). We then investigate the robustness of the method to process and measurement noise and offer solutions to mitigate their effects. Subsequently, we show that our approach extends to infinite-degree systems that do not satisfy Assumption 2 by neglecting high-order coefficients (Subsection 2.3.2). Finally, the practical relevance of the algorithm is demonstrated on an autonomous wind turbine from state data alone (Subsection 2.3.3).

2.3.1 A finite phasor-order example

Let us consider a toy LTP system generated with random phasors for A and B, such that $n = 3$, $m = 2$, $T = 1$ and $d^oA = d^oB = 10$. Consequently, the minimal truncation order that should be chosen to recover all harmonics of the system is $p = 10$. This leads to a total of $n(n+m)(2p+1) = 315$ unknowns. The functions A and B are plotted on Fig. A.1 and A.2.

Noise-free data

In the ideal noise-free case, we verify that the exact recovery of the unknown system parameters is possible, provided that the system is sufficiently excited by the input, as indicated by the fulfillment of condition (2.15). For instance, the input can be chosen as a random signal or a sinusoidal input. In the latter case, the input must be updated at least every period. Indeed, the phasors of a periodic function are constant, preventing the rank condition (2.15) to be satisfied if a periodic input is applied for more than one period. We solve the least squares problem (2.14) for $p = 10$, matching the degree of the system. The number of data samples L is chosen to be the minimum required for identification: $L = (n+m)(2p+1) = 105$. Over 100 simulations, the relative identification error has an order of magnitude of $10^{-8}\%$. This result numerically demonstrates the validity of the proposed identification method in the noise-free case.

Process noise

Let us now assume that the LTP system is affected by process noise, namely $\dot{x}(t) = A(t)x(t) + B(t)u(t) + w(t)$. We consider that this noise satisfies $w \sim \mathcal{N}(0, \sigma_w^2 I_n)$. We define the matrix that contains the normalized 0-th phasor of the noise over the identification time interval as $\mathbf{W_0} \coloneqq \begin{pmatrix} W_{0_\mathbf{N}}(t_0) & \cdots & W_{0_\mathbf{N}}(t_f) \end{pmatrix} \in \mathbb{R}^{n \times L}$. Obviously, this matrix is unknown, but $W_0(t) = \frac{1}{T}\int_{t-T}^{t} w(\tau)d\tau$, which means that this phasor corresponds to the average noise over a period. The data matrices are related with the following relationship if $\max(d^o A, d^o B) \leq p$:

$$\mathbf{X_1} = [A_p, \cdots, A_{-p}, B_p, \cdots, B_{-p}] \begin{bmatrix} \mathbf{X_0} \\ \mathbf{U_0} \end{bmatrix} + \mathbf{W_0} \tag{2.19}$$

Since we solve the least-squares problem (2.14), the noise will lead to imperfect estimations of the Fourier coefficients of A and B. Let us observe the effect of the noise on the identification procedure and propose solutions to improve its performance.

For $\sigma_w = 10^{-3}$, we generate 100 trajectories of the system with Gaussian inputs and 100 trajectories with sinusoidal inputs for $N = 64$ so that $\delta t = \frac{1}{64}$. Data from 2 periods of the system are exploited for identification. We compute the identification error with (2.17) and the fit percentage with (2.18). The same trajectory is used as the validation trajectory for all simulations.

Boxplots of the fit percentage and identification error are plotted on Fig. 2.1 and Fig. 2.2, allowing to compare the effect of the input on these metrics. In both cases, the effect of noise on the identified phasors is negligible, given that the identification error is lower than 2% and the new trajectory is accurately predicted.

Now, we consider $\sigma_w = 10^{-1}$ and for $N = 64$, we use data from 5 different trajectories for each simulation because a single trajectory of 2 periods leads to a large error. The boxplot of the identification error over 100 trials is represented on Fig. 2.3. Exploiting data from several trajectories leads to a significant reduction in identification error. This can be seen in Table 2.1, which contains the mean values of Fit_i and the associated standard deviation σ_i for $i = 1, ..., n$. If 5 trajectories are considered, the mean value of the fit is greater than 99% and its standard deviation is low, demonstrating the robustness of our identification approach with respect to process noise.

Measurement noise

Now that the impact of process noise on the proposed identification method has been studied, we consider that the state is affected by measurement noise: $\tilde{x}(t) = x(t) + w(t)$ where $\tilde{x}$ is the

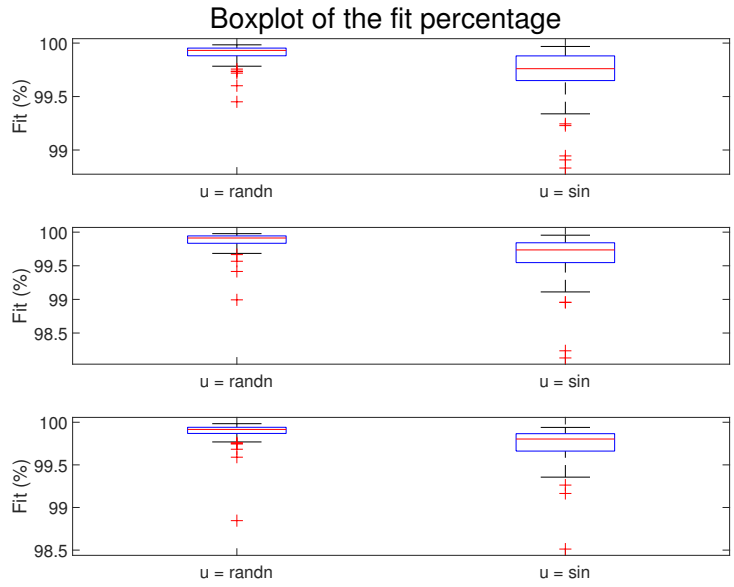

Figure 2.1: Boxplot of the fit percentage - process noise with $\sigma_w = 10^{-3}$

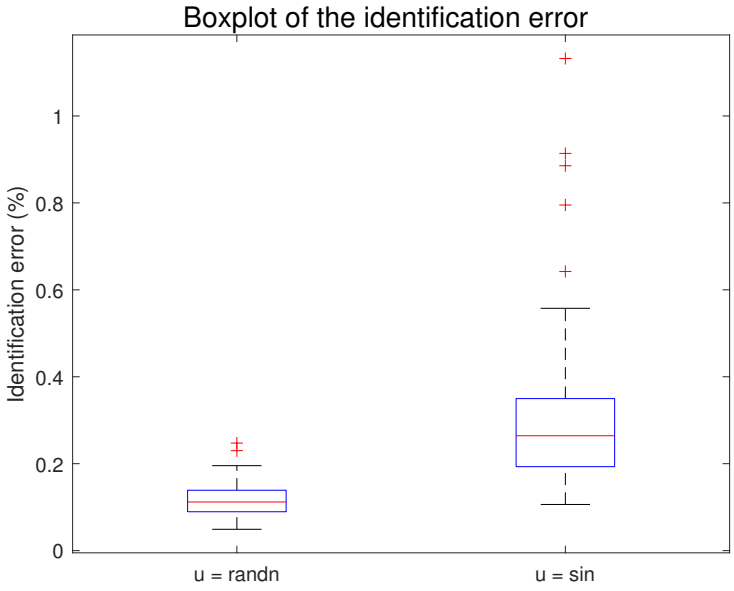

Figure 2.2: Boxplot of the identification error - process noise with $\sigma_w = 10^{-3}$

	u = randn, 1 traj	u = randn, 5 traj	u = sin, 1 traj	u = sin, 5 traj
$Fit_1(\%)$	94.8061	99.3580	65.0857	99.9281
$Fit_2(\%)$	92.5728	99.1935	56.3192	99.9122
$Fit_3(\%)$	94.9201	99.3474	66.4404	99.9224
$\sigma_1(\%)$	3.8573	0.2662	62.5118	0.0298
$\sigma_2(\%)$	6.5358	0.4104	60.9853	0.0438
$\sigma_3(\%)$	4.1529	0.2773	41.5066	0.0321

Table 2.1: Comparison of the mean and standard deviation of the fit percentage over 100 simulations - process noise with $\sigma_w = 10^{-1}$.

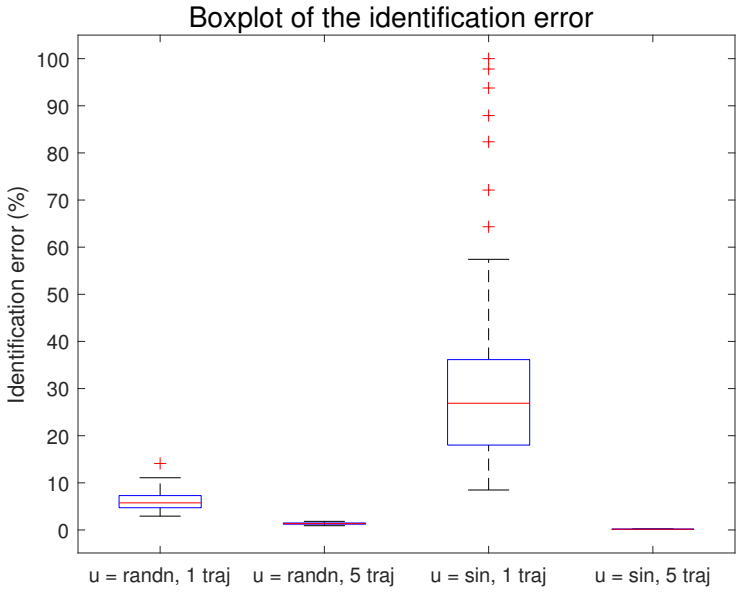

Figure 2.3: Boxplot of the identification error - process noise with $\sigma_w = 10^{-1}$

	u = randn, 5 traj	u = randn, 10 traj	u = sin, 5 trajectories	u = sin, 10 trajectories
$Fit_1(\%)$	96.6854	98.1514	95.4223	97.7454
$Fit_2(\%)$	96.3355	97.8336	94.8065	97.6572
$Fit_3(\%)$	96.9638	98.1696	95.7342	97.9280
$\sigma_1(\%)$	1.5829	0.7209	2.8825	0.8531
$\sigma_2(\%)$	1.6635	1.1693	3.0961	1.1824
$\sigma_3(\%)$	1.5427	0.7235	2.6192	0.8465

Table 2.2: Comparison of the mean and standard deviation of the fit percentage over 100 simulations - measurement noise with $3\sigma = \frac{5}{100}|x_i(t)|$.

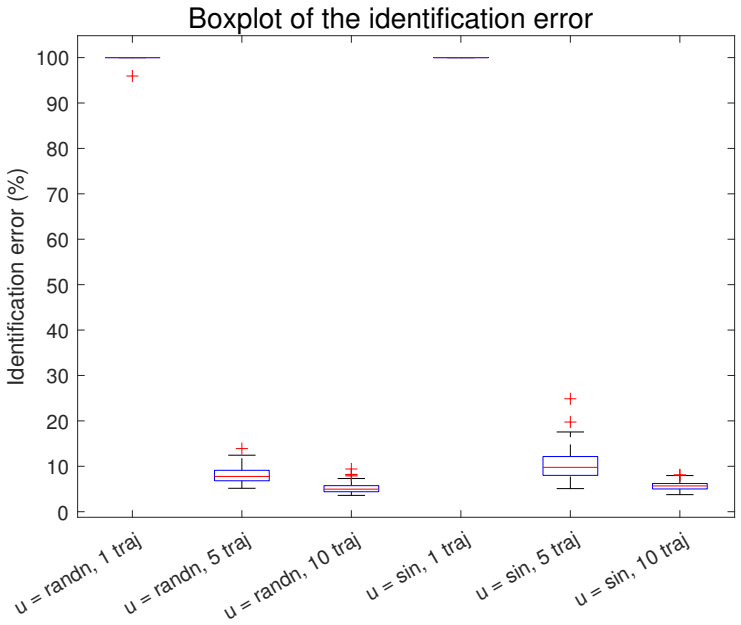

Figure 2.4: Boxplot of the identification error when $3\sigma = \frac{5}{100}|x_i(t)|$

measured state but the true state is x.

This type of noise affects the resolution of the identification problem insofar as errors will appear in both $\mathbf{X_1}$ and $\mathbf{X_0}$. Although a theoretical analysis is beyond the scope of this section, we note that the integral action of the phasor computation inherently filters high-frequency noise. Indeed, since only p phasors of X and U must be computed to identify p Fourier coefficients of A and B, the frequency components of the noise of order greater than p will not affect the resolution of the least-squares problem provided that an anti-aliasing filter was applied.

Suppose that at each time instant t and for $i = 1, ..., n$, the noise in the state x_i conforms to a Gaussian distribution $N(0, \sigma^2)$ where $3\sigma = \frac{5}{100}|x_i(t)|$. We evaluate the robustness of the identification protocol against such noise in a similar way as in the previous part. The results can be found in Table 2.2 and Fig. 2.4. One trajectory encompassing two periods of the system is not sufficient to obtain satisfactory results, but considering more trajectories can reduce the identification error to a tolerable level.

In summary, even if the data are contaminated with noise, an approximation of the true state trajectories remains possible.

2.3.2 An infinite phasor-order example

Consider the example discussed in [14]:

$$\dot{x} = \begin{pmatrix} a_{11}(t) & a_{12}(t) \\ a_{21}(t) & a_{22}(t) \end{pmatrix} x + \begin{pmatrix} b_{11}(t) \\ 0 \end{pmatrix} u \tag{2.20}$$

$$\begin{aligned}
a_{11}(t) &= 1 + \frac{4}{\pi} \sum_{k=0}^{\infty} \frac{1}{2k+1} \sin(\omega(2k+1)t), \\
a_{12}(t) &= 2 + \frac{16}{\pi^2} \sum_{k=0}^{\infty} \frac{1}{(2k+1)^2} \cos(\omega(2k+1)t), \\
a_{21}(t) &= -1 + \frac{2}{\pi} \sum_{k=1}^{\infty} \frac{(-1)^k}{k} \sin(\omega k t + \frac{\pi}{4}), \\
a_{22}(t) &= 1 - 2\sin(\omega t) - 2\sin(3\omega t) + 2\cos(3\omega t) + 2\cos(5\omega t), \\
b_{11}(t) &= 1 + 2\cos(2\omega t) + 4\sin(3\omega t) \text{ with } \omega = 2\pi.
\end{aligned}$$

We represent A and B on Fig. A.3 and Fig. A.4. The corresponding Toeplitz matrix $\mathcal{A}$ possesses an infinite number of phasors and does not exhibit a banded structure. Moreover, Assumption 2 is not satisfied because some components of A are discontinuous. Nevertheless, its higher-order phasors converge towards zero, which suggests that a banded approximation can be determined.

Given the inherent instability of this system, we use data obtained from multiple trajectories for phasor identification (see [65]). Each state x_i is affected by measurement noise as described in the previous example, so that $3\sigma = \frac{5}{100}|x_i(t)|$. With a truncation order set at $p = 25$, a time step of $\delta t = \frac{T}{256}$ and using 16 trajectories, each with a length of 512 time points, the identification error ranges from 4.6% to 9.8% among the 100 trials. The validation of the identification results on a new trajectory is visually demonstrated in Fig. 2.5.

Let us plot the true and estimated moduli of the phasors for A on Fig. 2.6 for one of the simulations. Since we tackled the identification problem with a finite truncation order $p = 25$ and there was noise in the identification data, the effects of this noise are discernible, particularly on the higher-order phasors. This phenomenon is to be expected, as the chosen noise injects high-frequency content into the signal. However, the amplitude of these components is obviously limited. Figure 2.5 shows that the predictive accuracy of the estimated phasors is acceptable. To improve the results, a threshold can be set on the phasor modulus so that phasors below this threshold are eliminated.

A key practical aspect of the proposed framework is the choice of truncation order p, which represents a trade-off between model fidelity and computational complexity. To investigate this, we now repeat the identification of the infinite-degree system using a significantly lower order, namely $p = 10$. This choice reduces the number of unknown parameters (126 parameters to be identified as opposed to 306 unknown parameters when $p = 25$), simplifying the least-squares problem. The identification was performed over 100 Monte Carlo trials with sinusoidal inputs, each using data from 10 trajectories. The resulting mean identification error is equal to 2.62% and its standard deviation is equal to 0.43%. This indicates that the lower-order harmonics contain most of the information about the system.

Figure 2.7 compares the trajectories predicted by these 100 identified low-order models and the validation trajectory. The true and estimated trajectories are respectively represented in bold

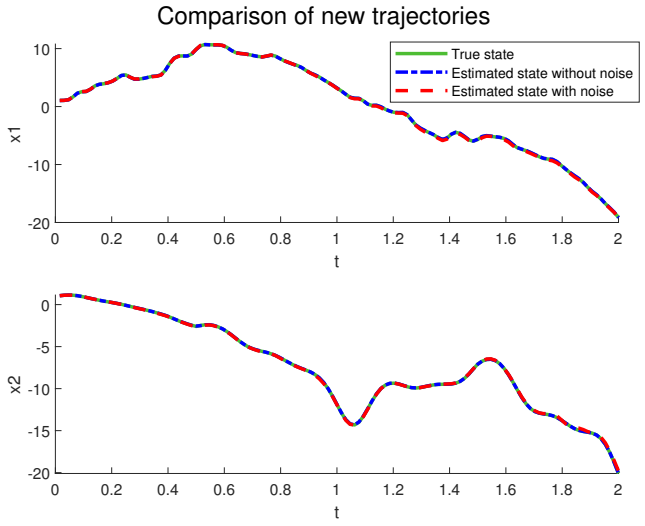

Figure 2.5: Comparison of the true and estimated trajectories of the infinite phasor-order example

and dotted lines. While some deviation from the true trajectory is visible, this was expected insofar as high-order coefficients were neglected. However, the general shape of the state is preserved. This result is particularly significant, as it shows that a low-order harmonic model can accurately approximate a much more complex system.

In summary, even with a theoretically infinite number of phasors and non-smooth functions that do not respect Assumption 2, it is possible to obtain an approximation for the non-negligible phasors so that future trajectories of the system can be accurately predicted.

2.3.3 A wind turbine

Consider the three-bladed wind turbine discussed in [28]. We first review its key attributes. The equation governing the motion of the turbine can be expressed as follows:

$$M(t)\ddot{q}(t) + C(t)\dot{q}(t) + K(t)q(t) = 0$$

where M, C and K are the system's mass, damping and stiffness matrices, and $q(t) = \begin{pmatrix} \zeta_1(t) \\ \zeta_2(t) \\ \zeta_3(t) \\ y_c(t) \end{pmatrix}$ contains the lag angles of each blade and the horizontal displacement of the hub. The rated rotor speed is $\Omega_r = 1.2\ rad.s^{-1}$. The functions M, C and K are periodic with period $T = \frac{2\pi}{\Omega_r}$. We plot them on Fig. A.5, A.6 and A.7. These functions are very smooth, implying that they are entirely characterized by a low number of harmonics.

This autonomous system can be described by the state equation: $\dot{x}(t) = A(t)x(t)$ where

$$x(t) = \begin{pmatrix} q(t) \\ \dot{q}(t) \end{pmatrix}, \quad A(t) = \begin{pmatrix} 0_{4,4} & I_4 \\ -M(t)^{-1}K(t) & -M(t)^{-1}C(t) \end{pmatrix}$$

This system is characterized by a state dimension $n = 8$. In this context, we assume a truncation order of $p = 4$, resulting in the determination of $n^2(2p+1) = 576$ unknowns. The step size is set to $\delta t = \frac{T}{256}$.

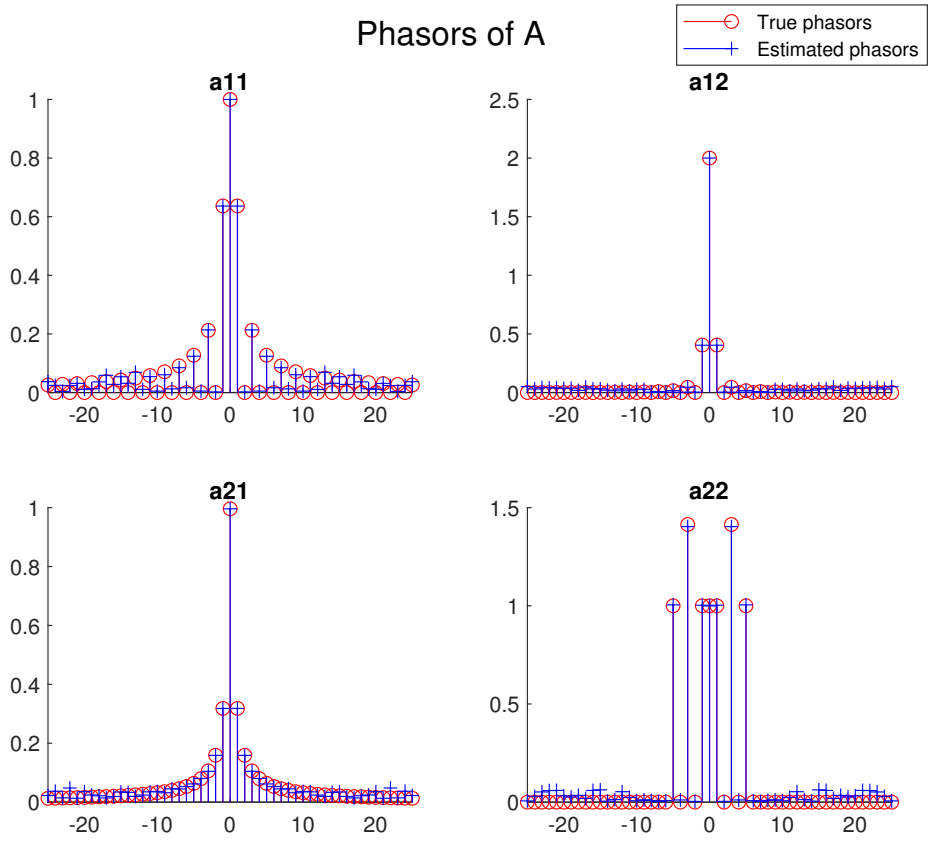

Figure 2.6: Moduli of the true and estimated phasors of A of the infinite-phasor order example with noise on the state measurements.

Due to the marginal instability of this system (its eigenvalues are very close to the imaginary axis) and its autonomous nature, we rely on data from 15 trajectories, each with a length of 256, to identify its phasors. The state measurements are corrupted by noise. At each time instant t and for $i = 1, ..., n$, the noise affecting state x_i follows a Gaussian distribution $N(0, \sigma^2)$ where $3\sigma = \frac{5}{100}|x_i(t)|$, so that a certain signal-to-noise ratio is achieved.

The identification protocol proves successful across all initial conditions, with the relative error (2.17) ranging from a minimum of 0.9% to a maximum of 6.3% among the 100 trials. Furthermore, the validation of these identification results on a new trajectory is depicted in Fig. 2.8.

Subsequently, we increase the number of samples for identification to observe its effect on the performance of the identification method. For each value of L, 100 models are identified from different datasets, allowing to compute a mean identification error value. The curve of the mean identification error is represented on Fig. 2.9. This shows that the precision of the solution is improved by a larger value of L.

The previous results show that our identification framework is well suited for autonomous systems. Given that the system under investigation is a wind turbine, achieving precise identification is of significant relevance, particularly in the context of control applications.

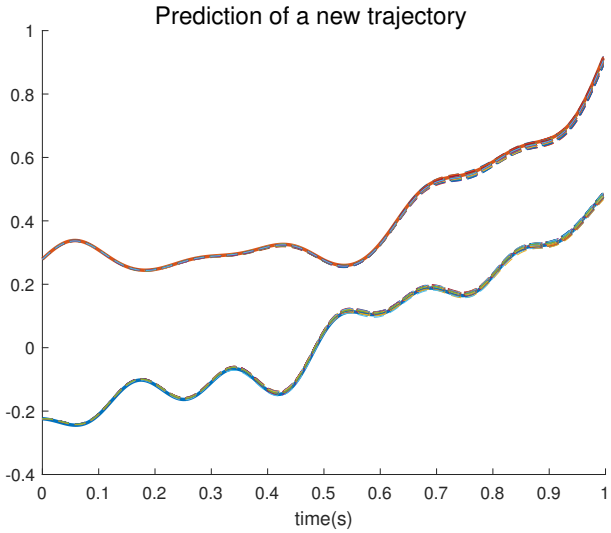

Figure 2.7: Validation of the banded approximation on a new trajectory for the infinite-phasor order example

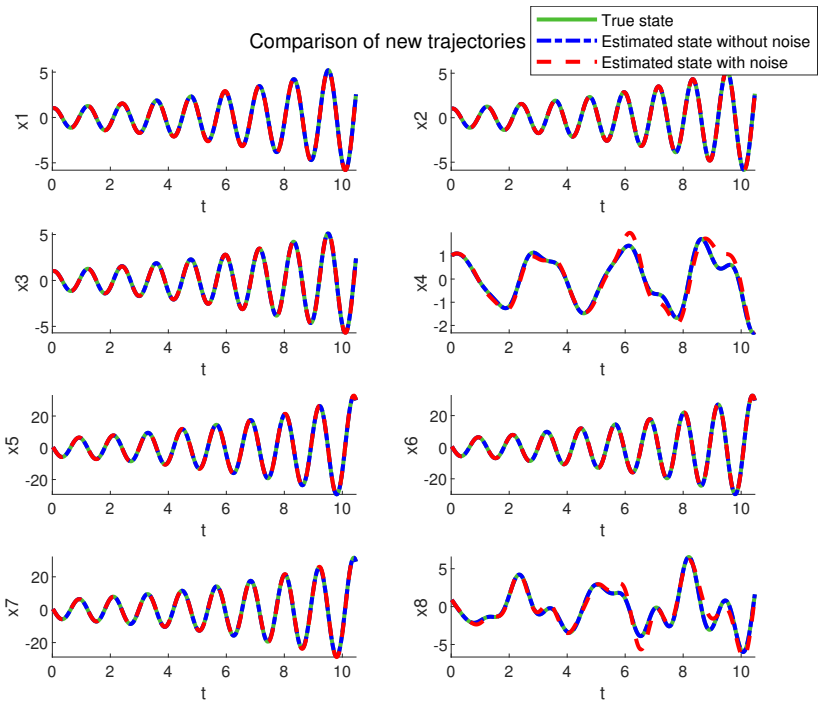

Figure 2.8: Comparison of the true and estimated trajectories of the wind turbine.

2.4 Conclusion

In this chapter, a novel harmonic framework has been presented for the identification of continuous-time LTP systems. This method enables the identification of the state and input matrices of any

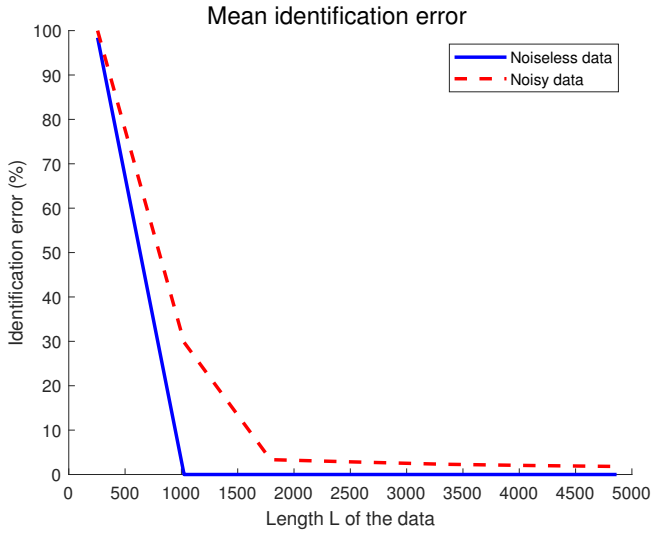

Figure 2.9: Mean identification error convergence for the wind turbine.

LTP system up to an arbitrarily small error under sufficient regularity assumptions. We exploit the equivalence between LTP systems in the time domain and infinite-dimensional LTI systems in the harmonic domain. Leveraging the block Toeplitz structure of the latter, the identification problem can be reduced to a finite-dimensional linear least-squares problem, whose solution corresponds to the unknown Fourier coefficients. Our approach offers significant advantages, including avoiding signal derivative calculations, and performs effectively in noisy scenarios even for unstable systems, as shown in numerical simulations. The main limit of the proposed approach is the assumption that the state can be estimated.

3

A Consistent Truncation for solving Infinite-Dimensional Toeplitz Block LMI

Contents

3.1 Equivalence between TBLMIs and PDLMIs 38
3.1.1 TBLMI 38
3.1.2 PDLMI 39
3.1.3 TBLMIs are the harmonic counterparts of PDLMIs 39
3.2 Solving an infinite-dimensional harmonic convex optimization problem 41
3.2.1 Average Trace operator 42
3.2.2 Truncation of a TBLMI 43
3.2.3 Truncated and banded approximation of TBLMI 45
3.2.4 Solving **COP** up to an arbitrary error 47
3.3 Illustrative examples 51
3.3.1 Validation on a periodic differential Riccati inequality with a known solution 51
3.3.2 Validation of a regularization approach on a periodic differential Lyapunov equation 53
3.4 Conclusion 55

Introduction

In this chapter, we propose a general framework for solving Toeplitz Block LMIs (TBLMIs) of infinite dimension. These TBLMIs are the harmonic counterparts of periodic differential LMIs (PDLMIs), making the resolution of the former a valuable area of research. A review of resolution methods for periodic differential equations and harmonic equations was provided in Section 1.3. The chapter is structured as follows. In Section 3.1, the equivalence between PDLMIs in the time domain and TBLMIs in the harmonic domain is formally established. This means that solving a PDLMI can be achieved by solving its harmonic counterpart. However, the latter is an infinite-dimensional LMI, which implies that the solution to this problem must be approximated.

In Section 3.2, we introduce a consistent truncation procedure that enables the recovery of the infinite-dimensional solution to a TBLMI-based convex optimization problem, with an error that can be made arbitrarily small under regularity assumptions on the entries. This is achieved by solving a finite-dimensional truncated problem. A trace operator, specifically designed for Toeplitz block operators so that it is bounded on ℓ^2, corresponds to the objective function. Our framework is not limited to smooth systems. We introduce a regularization scheme that extends its applicability to entries in L^∞ (the space of essentially bounded functions). This allows to handle a wide variety of periodic systems, whereas existing literature typically assumes these matrices are at least piecewise continuous. To validate the resolution method presented in this chapter, we solve two PDLMIs in Section 3.3. The solutions obtained with the TBLMI approach are close to the true ones, which confirms the interest of this method to solve PDLMIs.

3.1 Equivalence between TBLMIs and PDLMIs

In this section, we define rigorously the concepts of Toeplitz Block LMIs (TBLMIs) and Periodic Differential LMIs (PDLMIs), then we prove that solving a PDLMI in the time domain is equivalent to solving a TBLMI in the harmonic domain.

3.1.1 TBLMI

A TBLMI is an infinite-dimensional LMI of the form:

$$\mathcal{M}(x) = \mathcal{M}_0 + \sum_{i=1}^{+\infty} x_i \mathcal{M}_i > 0 \tag{3.1}$$

where $x_i \in \mathbb{R}$, $i = 1, 2, \cdots$ are the unknown variables and where the Hermitian matrices $\mathcal{M}_i$ are $n \times n$ infinite-dimensional TB operators. A sequence $x = (x_1, x_2, \cdots)$ is a solution of the TBLMI (3.1) if $\mathcal{M}(x)$ is a positive definite and bounded operator on ℓ^2, i.e. for any $y \in \ell^2$, $y \neq 0$, $y^* \mathcal{M}(x) y > 0$ and there exists $C > 0$ s.t. $\|\mathcal{M}(x)\|_{\ell^2} \leq C$.

Often, the variables of an LMI are matrices, as in the harmonic Lyapunov inequality:

$$(\mathcal{A} - \mathcal{N})^* \mathcal{P} + \mathcal{P}(\mathcal{A} - \mathcal{N}) < 0 \tag{3.2}$$

where $\mathcal{A}$ and $\mathcal{N}$ are given and $\mathcal{P}$ is the variable (bounded on ℓ^2 with $\mathcal{P} = \mathcal{P}^*$). In the context of control theory, this inequality can be encountered when analyzing the stability of the harmonic system described by $\dot{X}(t) = (\mathcal{A} - \mathcal{N})X(t)$.

Obviously, (3.2) can be rewritten in the form (3.1) with scalar unknowns by considering a basis $\mathcal{V}_i$, $i = 0, \cdots, +\infty$ for Hermitian and $n \times n$ TB matrices as follows:

$$\mathcal{M}_i = (\mathcal{A} - \mathcal{N})^* \mathcal{V}_i + \mathcal{V}_i (\mathcal{A} - \mathcal{N}) \text{ and } \mathcal{P} = \sum_{i=0}^{+\infty} x_i \mathcal{V}_i. \tag{3.3}$$

For the sake of simplification, consider the case where $n = 1$ and let $\mathcal{I}_k$ be the k-shifted identity matrix with $k \in \mathbb{N}$. Then, a basis denoted as $\mathcal{V}_i$ can be obtained from the following set:

$$\{(\mathcal{I}_{-k} + \mathcal{I}_k),\ \mathrm{j}(-\mathcal{I}_{-k} + \mathcal{I}_k) : k \in \mathbb{N}\}.$$

For any index i, $\mathcal{M}_i$ is a TB operator as $\mathcal{N}^* \mathcal{V}_i + \mathcal{V}_i \mathcal{N}$ is a TB operator and the product of TB operators results in a TB operator.

In the sequel, we consider the following definition of TBLMI:

Definition 3 *Let $\mathbb{S}$ be a finite set of subscripts. Any TBLMI has an equivalent formulation given by* (3.1) *and is defined by:*

$$\mathcal{L}(\mathcal{P}; \mathcal{A}_s, s \in \mathbb{S}) < 0 \tag{3.4}$$

where the entries $\mathcal{A}_s, s \in \mathbb{S}$, are given and $\mathcal{P}$ refers to the TB unknown operator.

The Lyapunov inequality (3.2) is a TBLMI and corresponds to $\mathcal{L}(\mathcal{P}; \mathcal{A}) < 0$. Although the role of $\mathcal{N}$ in this inequality is not immediately apparent, its significance will be fully elucidated in the forthcoming theorem.

3.1.2 PDLMI

In the time domain, the counterpart of (3.2) is the *differential* Lyapunov inequality:

$$\dot{P} + A^T P + PA < 0 \tag{3.5}$$

with $P \in L^\infty([0\ T])$ and $P = P^T > 0$ *a.e.* An intriguing question arises: Is there a connection between TBLMIs and PDLMIs? To address this question, we define precisely the notion of PDLMI in the time domain and then establish its equivalence with a TBLMI in the harmonic domain.

Definition 4 *Let $\mathbb{S}$ be a finite set of subscripts and consider $T-$periodic matrix functions A_s, $s \in \mathbb{S}$, all belonging to L^∞. A PDLMI is defined by:*

$$L(\dot{P}(t), P(t); A_s(t), s \in \mathbb{S}) < 0 \text{ a.e.} \tag{3.6}$$

where the function L is given by

$$L(\dot{P}(t), P(t); A_s(t), s \in \mathbb{S}) = \dot{P} + G(P(t); A_s(t), s \in \mathbb{S}),$$

and where the function G is linear with respect to the unknown P and is also a polynomial matrix-valued function with respect to its defining entries $A_s, s \in \mathbb{S}$. We assume that the mapping from t to $L(\dot{P}(t), P(t); A_s(t), s \in \mathbb{S})$ belongs to L^∞_{loc}, implying that for any vector function $x \in L^2([t-T, t])$, the inner product:

$$< x, Lx >_{L^2([t-T\ t])} < 0$$

holds, or equivalently, $L(t) < 0$ a.e.. In simpler terms, this means that L defines a negative definite linear operator on L^2_{loc}.

A solution, denoted as $P(\cdot) : \mathbb{R} \to \mathbb{R}^{n \times n}$, to (3.6)*, if it exists, is expected to be an absolutely continuous and symmetric matrix function.*

Note that absolute continuity of the solution is a minimum requirement for its derivative to exist almost everywhere.

3.1.3 TBLMIs are the harmonic counterparts of PDLMIs

The following result establishes the connection between TBLMIs and PDLMIs: TBLMIs are the harmonic counterpart of PDLMIs.

Theorem 8 *$P(t)$ is a $T-$periodic solution to (3.6) if and only if $\mathcal{P} := \mathcal{T}(P)$ is a constant, hermitian and bounded operator on ℓ^2 and satisfies the infinite dimensional TBLMI:*

$$\mathcal{L}(\mathcal{P}; \mathcal{A}_s, s \in \mathbb{S}) < 0 \tag{3.7}$$

with $\mathcal{A}_s := \mathcal{T}(A_s)$, $s \in \mathbb{S}$, and where

$$\mathcal{L}(\mathcal{P}; \mathcal{A}_s, s \in \mathbb{S}) := L(-\mathcal{N}^*\mathcal{P} - \mathcal{P}\mathcal{N}, \mathcal{P}; \mathcal{A}_s, s \in \mathbb{S}).$$

Proof 11 *If P is absolutely continuous, $\dot{P}$ exists almost everywhere and is integrable, thus $\mathcal{F}(\dot{P})$ can be defined. Moreover, as $P(t)$ and $L(\dot{P}(t), P(t); A_s(t), s \in \mathbb{S})$ are L^∞_{loc}, the operators $\mathcal{P} := \mathcal{T}(P)$ and $\mathcal{T}(L(\dot{P}(t), P(t); A_s(t), s \in \mathbb{S}))$ are bounded operators on ℓ^2 (see Theorem 2). As any LMI is a polynomial matrix-valued function with respect to all its entries, the Toeplitz transformation $\mathcal{T}(L)$ of L is obtained by replacing all the terms in the PDLMI by their Toeplitz transformation and $\dot{P}$ by $\dot{\mathcal{P}} - \mathcal{N}^*\mathcal{P} - \mathcal{P}\mathcal{N}$ (see Proof of Theorem 5 in [5] for more details). This leads formally to:*

$$\begin{aligned} &\mathcal{T}\big(L(\dot{P},P; A_s, s \in \mathbb{S})\big) \\ &\qquad = L(\dot{\mathcal{P}} - \mathcal{N}^*\mathcal{P} - \mathcal{P}\mathcal{N}, \mathcal{P}; \mathcal{A}_s, s \in \mathbb{S}). \end{aligned} \tag{3.8}$$

As it is assumed that $P(t)$ is $T-$periodic, it follows that $\mathcal{P}$ is constant. Hence, $\dot{\mathcal{P}} = 0$ and (3.8) is a constant bounded operator on ℓ^2. Moreover, it can be readily demonstrated through the application of the Parseval-Plancherel theorem that for any $x \in L^2([t-T\ t])$:

$$\begin{aligned} &< x, L(\dot{P}, P; A_s, s \in \mathbb{S})x >_{L^2([t-T\ t])}(t) \\ &:= \frac{1}{T}\int_{t-T}^{t} x' L(\dot{P}, P; A_s, s \in \mathbb{S})x \ d\tau \\ &= X(t)^* L(\dot{\mathcal{P}} - \mathcal{N}^*\mathcal{P} - \mathcal{P}\mathcal{N}, \mathcal{P}; \mathcal{A}_s, s \in \mathbb{S})X(t) < 0 \end{aligned}$$

where $X := \mathcal{F}(x)$. Finally, replacing $\dot{\mathcal{P}}$ by zero leads to (3.7). The converse is obvious since the bounded operators on ℓ^2, $\mathcal{P}$ and $\mathcal{A}_s, s \in \mathbb{S}$, are constant and thus trivially belong to H (see Theorem 1). ■

We can establish the following result regarding the regularity of the solution to a PDLMI:

Theorem 9 *The Fourier series of the periodic solution to a PDLMI converges uniformly. Moreover, its Fourier coefficients satisfy*

$$|P_k| = O\Big(\frac{1}{k^{1+\alpha}}\Big), \qquad \alpha > \tfrac{1}{2}.$$

Proof 12 *Given that $L(\dot{P}, P(t); A_s(t), s \in \mathbb{S})$ is assumed to belong to L^∞, there exists a bounded operator $Q \in L^\infty$ such that the following equality holds almost everywhere:*

$$\dot{P} + G(P(t); A_s(t), s \in \mathbb{S}) + Q(t) = 0.$$

Since G is a polynomial in the matrix-valued functions $P(t)$ and $A_s(t)$, which are both in L^∞ (P is absolutely continuous), it follows that $G(P(t); A_s(t), s \in \mathbb{S}) \in L^\infty$ and thus

$$\dot{P} \in L^\infty.$$

In particular, this implies that $\dot{P} \in L^2$. *Hence,* P, *being periodic and absolutely continuous, admits a Fourier series that converges uniformly. Moreover, as* $(j\omega k P_k)_{k\in\mathbb{Z}}$ *correspond to the Fourier coefficients of* $\dot{P}$ *and since the series is square summable (Parseval-Plancherel Theorem), it means that* P_k *is at least*

$$O\left(\frac{1}{k^{1+\alpha}}\right), \qquad \alpha > \tfrac{1}{2}$$

when $k \to +\infty$.

The result of Theorem 8 highlights the potential of the harmonic framework to streamline the resolution of PDLMIs. Indeed, the development of reliable and consistent methods for solving infinite-dimensional TBLMIs presents a promising alternative to the notoriously intricate PDLMIs-based approaches. This is of great practical interest insofar as PDLMIs can be encountered in the context of stability analysis and control design synthesis.

The primary challenge when solving TBLMIs lies in their infinite-dimensional nature. In practical terms, achieving a solution requires truncation, but the latter must be carried out consistently. By *consistency*, we mean that the approximate solution at a given truncation order should converge to the solution of the original problem as the order increases. Without this consistency, there is no assurance of optimality or stability with the approximate solution.

In the upcoming section, our objective is to introduce a precise definition of a consistent truncation scheme. The latter enables us to solve TBLMIs with an arbitrarily small margin of error. Given the well-known challenges in solving differential LMIs, as highlighted in Section 1.3 and in particular in [11–13, 55], addressing the case of PDLMIs through a harmonic formulation is particularly relevant.

3.2 Solving an infinite-dimensional harmonic convex optimization problem

Given the effectiveness of convex optimization techniques in solving most robust optimal control problems for linear systems, this section focuses on deriving an approximate solution to the following convex optimization problem (**COP**):

$$\begin{aligned} \mathbf{COP}: \min_{\mathcal{P}^*=\mathcal{P}>0} \; & tr_0(\mathcal{P}) \\ & \mathcal{L}(\mathcal{P}; \mathcal{A}_s, s \in \mathbb{S}) \leq 0 \end{aligned}$$

where tr_0 is the average trace operator defined in Subsection 3.2.1 due to TB operators not being trace-class.

We assume that this convex optimization problem is feasible and that the optimal solution is unique, bounded on ℓ^2 and continuous with respect to the entries $\mathcal{A}_s, s \in \mathbb{S}$. **COP** is an infinite-dimensional problem in the sense that the dimension of the involved entries and unknowns is infinite.

The main objective here is to show how **COP** can be solved up to an arbitrarily small error. This objective is achieved through a three-step approach. In the first step, we establish the concept of a truncated TBLMI. The second step details the process of combining truncation with banded approximation operations, thereby reducing the problem to a finite-dimensional form. In the third and final step, we prove that the solution to **COP** can be reliably obtained up to an arbitrarily small error by solving a finite optimization problem.

3.2.1 Average Trace operator

In optimal control, the objective function to minimize is often the trace of the solution. Since TB operators are not a trace class [66], a new trace operator should be defined. Indeed, for a $n \times n$ TB bounded operator on ℓ^2, we have

$$tr(|\mathcal{M}|) := \sum_{k\in\mathbb{Z}} < e_k, (\mathcal{M}^*\mathcal{M})^{\frac{1}{2}} e_k > = \sum_{k\in\mathbb{Z}} \sum_{i=1}^{n} m_i = +\infty \tag{3.9}$$

where $(m_i)_{i\in[\![1,n]\!]}$ denote the n diagonal values of $(\mathcal{M}^*\mathcal{M})^{\frac{1}{2}}$ and (e_k) is an orthonormal basis for $(\ell^2)^n$. Nevertheless, a solution to circumvent this challenge consists in considering the vector space of matrix functions in $L^\infty([0,T])$ endowed with the conventional scalar product:

$$\begin{aligned} < M, N > &:= \frac{1}{T} \int_0^T tr(M'(\tau)N(\tau))d\tau \\ &= \frac{1}{T} \sum_{i,j=1}^{n} \int_0^T M_{ij}(\tau)N_{ij}(\tau)d\tau \end{aligned} \tag{3.10}$$

for which it is straightforward to show that the induced norm satisfies:

$$\|M\|_{L^2([0\ T])} \leq \|M\|_F \leq \sqrt{n}\|M\|_{L^\infty([0\ T])} \tag{3.11}$$

where $\|.\|_F$ corresponds to the Frobenius norm: $\|M\|_F := < M, M >^{\frac{1}{2}}$.

As any component of M can be rewritten using its Fourier series (since $L^\infty([0\ T]) \subset L^2([0\ T])$):

$$M_{ij}(t) = \sum_{k\in\mathbb{Z}} m_{ij,k} e^{\mathrm{j}\omega kt} \ a.e.,$$

it follows, using (3.10), that:

$$< Id, M > = \sum_{i=1}^{n} m_{ii,0}.$$

This allows to define the average-trace operator as follows.

Definition 5 *The average trace operator for TB bounded operators on ℓ^2 is defined by*

$$tr_0(\mathcal{M}) := \sum_{i=1}^{n} m_{ii,0} \tag{3.12}$$

where $m_{ii,0}$ refers to the diagonal value located on the $i-th$ diagonal block of $\mathcal{M}$.

Theorem 10 *For any constant, $n\times n$ TB and bounded operator on ℓ^2, denoted by $\mathcal{M}$, $tr_0(\mathcal{M}^*\mathcal{M})^{\frac{1}{2}}$ defines an operator-norm that satisfies:*

$$\|\mathcal{M}\|_{\ell^2} \leq tr_0(\mathcal{M}^*\mathcal{M})^{\frac{1}{2}} = \|M\|_F \leq \sqrt{n}\|\mathcal{M}\|_{\ell^2} \tag{3.13}$$

where $M := \mathcal{T}^{-1}(\mathcal{M})$.

Proof 13 *The result is deduced from* (3.11)*, Theorem 2 and recalling that Plancherel Theorem implies:*

$$\begin{aligned} \|M\|_{L^2([0\ T])} &:= \sup_{\|x\|_{L^2}=1} \|Mx\|_{L^2([0\ T])} \\ &= \sup_{\|X\|_{\ell^2}=1} \|\mathcal{M}X\|_{\ell^2} := \|\mathcal{M}\|_{\ell^2} \end{aligned}$$

where $X := \mathcal{F}(x)$ and $\mathcal{M} := \mathcal{T}(M)$. ∎

In Definition 5, the average trace of a TB operator can be interpreted as a mean value of the trace operator, that is

$$\begin{aligned} tr_0(\mathcal{M}) &= \lim_{N\to+\infty} \frac{1}{2N+1} \sum_{|k|\leq N} \sum_{i=1}^{n} < e_{ki}, \mathcal{M}_{ii} e_{ki} > \\ &= \lim_{N\to+\infty} \frac{1}{2N+1} \sum_{|k|\leq N} \sum_{i=1}^{n} m_{ii,0} = \sum_{i=1}^{n} m_{ii,0} < +\infty \end{aligned} \tag{3.14}$$

where $\mathcal{M}_{ii}$ refers to the *ith* Toeplitz diagonal block of $\mathcal{M}$ and (e_{ki}) is an orthonormal basis of ℓ^2 associated to the $i-th$ diagonal block. Since the average trace operator is finite, it makes sense to minimize such a function to solve an optimization problem involving TB operators.

3.2.2 Truncation of a TBLMI

The transition from infinite-dimensional to finite-dimensional TBLMI is not straightforward because some rules that apply in infinite dimension no longer hold in finite dimension. In this part, we define a truncation operator for TBLMIs that preserves their Toeplitz structure by taking into account Hankel error terms.

Consider a $n \times m$ matrix function $A \in L^2_{loc}(\mathbb{R}, \mathbb{R}^{n\times m})$ and its TB transformation

$$\mathcal{A} := \mathcal{T}(A) = \begin{bmatrix} \mathcal{A}_{11} & \dots & \mathcal{A}_{1m} \\ \vdots & & \vdots \\ \mathcal{A}_{n1} & \dots & \mathcal{A}_{nm} \end{bmatrix} \tag{3.15}$$

with $\mathcal{A}_{ij} := \mathcal{T}(a_{ij})$, $i = 1, \cdots, n,\ j = 1, \cdots, m$.

Definition 6 *The $n \times m$ Hankel block matrices $\mathcal{H}(A^+)$, $\mathcal{H}(A^-)$ associated to $\mathcal{A}$ are given by:*

$$\mathcal{H}(A^{\pm}) := \begin{bmatrix} \mathcal{H}(A^{\pm}_{11}) & \cdots & \mathcal{H}(A^{\pm}_{1m}) \\ \vdots & & \vdots \\ \mathcal{H}(A^{\pm}_{n1}) & \cdots & \mathcal{H}(A^{\pm}_{nm}) \end{bmatrix} \tag{3.16}$$

where for $i = 1, \cdots, n,\ j = 1, \cdots, m$

$$\mathcal{H}(A^+_{ij}) := \begin{bmatrix} a_{ij,1} & a_{ij,2} & \cdots \\ a_{ij,2} & \ddots & \\ \vdots & & \ddots \end{bmatrix}$$

$$\mathcal{H}(A^-_{ij}) := \begin{bmatrix} a_{ij,-1} & a_{ij,-2} & \cdots \\ a_{ij,-2} & \ddots & \\ \vdots & & \ddots \end{bmatrix}$$

with $a_{ij,k}$, $k \in \mathbb{Z}$ the phasor sequence of a_{ij}.

Definition 7 *Consider $n \times m$ infinite-dimensional TB matrices $\mathcal{A} := \mathcal{T}(A)$. The truncation operator Π_r at order r is defined by:*

$$\Pi_r(\mathcal{A}) := \begin{bmatrix} \Pi_r(\mathcal{A}_{11}) & \dots & \Pi_r(\mathcal{A}_{1m}) \\ \vdots & & \vdots \\ \Pi_r(\mathcal{A}_{n1}) & \dots & \Pi_r(\mathcal{A}_{nm}) \end{bmatrix} \tag{3.17}$$

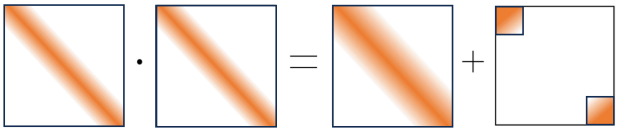

Figure 3.1: Multiplication of two finite dimensional banded Toeplitz matrices

where $\Pi_r(\mathcal{A}_{ij})$ *refers to the* $(2r+1)\times(2r+1)$ *principal submatrix of* $\mathcal{A}_{ij}$*. For the associated Hankel matrices as defined by* (3.16)*, we denote by* $\mathcal{H}_{(r_1,r_2)}(\cdot)$ *the finite dimensional matrix obtained by selecting the first* $(2r_1+1)$ *rows and* $(2r_2+1)$ *columns in each of its* $n\times m$ *infinite dimensional blocks.*

Deriving algebraic rules for infinite-dimensional TB matrix functions of compatible size is straightforward, given that both the sum and the product of two TB matrices result in another TB matrix. In finite dimension, the situation is more complicated as outlined in the following result, proved in [14], which explains why the product of two finite dimensional Toeplitz matrices is not a Toeplitz matrix.

Theorem 11 *Consider two infinite dimensional TB matrix functions* $\mathcal{A}$ *and* $\mathcal{B}$*. The following relations are fulfilled:*
If $\mathcal{A}$ *and* $\mathcal{B}$ *are both formed by* $n\times m$ *blocks:*

$$\Pi_r(\mathcal{A}+\mathcal{B}) = \Pi_r(\mathcal{A}) + \Pi_r(\mathcal{B}). \tag{3.18}$$

If $\mathcal{A}$ *and* $\mathcal{B}$ *are formed respectively by* $n\times p$ *and* $p\times m$ *blocks:*

$$\begin{aligned}\Pi_r(\mathcal{A}\mathcal{B}) = \Pi_r(\mathcal{A})\Pi_r(\mathcal{B}) &+ \mathcal{H}_{(r,\eta)}(A^+)\mathcal{H}_{(\eta,r)}(B^-)\\ &+ \mathcal{J}_{n,r}\mathcal{H}_{(r,\eta)}(A^-)\mathcal{H}_{(\eta,r)}(B^+)\mathcal{J}_{m,r}\end{aligned} \tag{3.19}$$

where:

- J_r *is the* $(2r+1)\times(2r+1)$ *flip matrix having 1 on the anti-diagonal and zeros elsewhere,*
- $\mathcal{J}_{n,r} := Id_n \otimes J_r$,
- $\eta := \min\{\xi \in \mathbb{Z}^+ \cup \{+\infty\} : \xi \geq \frac{1}{2}(\min(d^oA, d^oB) - 1)\}$ *with* d^oA *the largest non vanishing Fourier coefficient of* A*.*

An illustration of the above theorem is given in Fig. 3.1 for $n = p = m = 1$ when d^oA and d^oB are less than r so that $\Pi_r(\mathcal{A})$ and $\Pi_r(\mathcal{B})$ are banded matrices. In this case, the matrices $E^+ := \mathcal{H}_{(r,\eta)}(A^+)\mathcal{H}_{(\eta,r)}(B^-)$ and $E^- := J_r\mathcal{H}_{(r,\eta)}(A^-)\mathcal{H}_{(\eta,r)}(B^+)J_r$ have disjoint supports located in the upper leftmost corner and in the lower rightmost corner, respectively. As a consequence, $\Pi_r(\mathcal{A})\Pi_r(\mathcal{B})$, which corresponds to the product of two finite-dimensional Toeplitz matrices, can be represented as the sum of the truncated Toeplitz matrix $\Pi_r(\mathcal{A}\mathcal{B})$ and two correcting terms E^+ and E^-.

We can now provide a precise definition for an $r-$truncation of a generic TBLMI (3.7).

Definition 8 *For a given $r > 0$, the $r-$truncated TBLMI of* (3.7) *is defined by:*

$$\Pi_r(\mathcal{L}(\mathcal{P}; \mathcal{A}_s, s \in \mathbb{S})) < 0. \tag{3.20}$$

Applying the truncation operator Π_r on a TBLMI consists of applying it to each term of the LMI, then taking the sum of the truncated terms. For example, the $r-$truncated TBLMI associated to the harmonic Lyapunov inequality (3.2) is:

$$\begin{aligned}\Pi_r((\mathcal{A}-\mathcal{N})^*\mathcal{P} + \mathcal{P}(\mathcal{A}-\mathcal{N}) < 0) = &\Pi_r((\mathcal{A}-\mathcal{N})^*)\Pi_r(\mathcal{P}) + \Pi_r(\mathcal{P})\Pi_r(\mathcal{A}-\mathcal{N}) \\ &+ \mathcal{H}_{(r,\eta)}(A^{*+})\mathcal{H}_{(\eta,r)}(P^-) + \mathcal{H}_{(r,\eta)}(P^+)\mathcal{H}_{(\eta,r)}(A^-) \\ &+ \mathcal{J}_{n,r}(\mathcal{H}_{(r,\eta)}(A^{*-})\mathcal{H}_{(\eta,r)}(P^+) \\ &+ \mathcal{H}_{(r,\eta)}(P^-)\mathcal{H}_{(\eta,r)}(A^+))\mathcal{J}_{n,r} < 0\end{aligned}$$

with $\eta := \min\{\xi \in \mathbb{Z}^+ \cup \{+\infty\} : \xi \geq \frac{1}{2}(\min(d^o A, d^o P) - 1)\}$.

The following result asserts that if the infinite-dimensional TBLMI (3.7) is feasible, then a solution to the truncated TBLMI (3.20) can always be found for any order r.

Theorem 12 *If $\mathcal{P}$ solves the infinite-dimensional TBLMI (3.7) then $\mathcal{P}$ solves the r-truncated TBLMI (3.20) at any order r.*

Proof 14 *Consider a solution $\mathcal{P}$ to* (3.7)*, then for any $r > 0$, the principal submatrix $\Pi_r(\mathcal{L}(\mathcal{P}; \mathcal{A}_s, s \in \mathbb{S}))$ of $\mathcal{L}(\mathcal{P}; \mathcal{A}_s, s \in \mathbb{S})$ is necessarily negative definite. Hence, one of the solutions to the resulting $r-$truncated TBLMI is, in fact, $\mathcal{P}$ itself.* ■

Due to the properties (3.18) and (3.19) of the truncation operator, it is possible to explicitly expand $\Pi_r(\mathcal{L}(\mathcal{P}; \mathcal{A}_s, s \in \mathbb{S}))$ without resorting to any approximation. This expansion results in a finite-dimensional problem, provided that all the values obtained for η in (3.19) are finite. However, if some values of η turn out to be infinite, then (3.20) will contain terms involving infinite-dimensional Hankel matrices. In the following, we will demonstrate how to transform this infinite-dimensional problem into a finite one by utilizing a banded approximation for the matrix entries.

3.2.3 Truncated and banded approximation of TBLMI

The aim of this part is to show that (3.7) can be approximated by a banded version (see (3.21)) whose r-truncation (see (3.22)) is now tractable numerically since only a finite number of unknowns must be taken into account.

As in Chapter 2, the uniform convergence of the periodic approximation of each entry is necessary to prove the following technical results.

Assumption 3 *(Uniform convergence of the Fourier series of the entries of the TBLMI) The T-periodic matrix function $A \in L^\infty$ admits a uniformly convergent Fourier series approximation in the L^∞-norm, that is: $\lim_{p\to+\infty} \|A|_p(t) - A(t)\|_{L^\infty} = 0$, where $A|_p$ refers to its partial Fourier series given by $A|_p(t) = \sum_{|k|\leq p} A_k e^{j\omega kt}$.*

Theorem 13 *Assume that $\mathcal{A}$ is a bounded operator on ℓ^2 that satisfies Assumption 3 and denote by $\mathcal{A}_{b(p)}$ its $p-$banded version obtained by deleting all its phasors of order higher than p. The following results hold true:*

1. *The operator* $\mathcal{A}_{b(p)}$ *converges to* $\mathcal{A}$ *in* ℓ^2*-operator norm i.e.*

$$\lim_{p\to+\infty} \|\mathcal{A} - \mathcal{A}_{b(p)}\|_{\ell^2} = 0$$

2. *If* $\mathcal{P}$ *is a solution to* (3.7) *then there exists* p_0 *such that for any* $p \geq p_0$*,*

$$\mathcal{L}(\mathcal{P}; \mathcal{A}_{s_{b(p)}}, s \in \mathbb{S}) < 0 \tag{3.21}$$

3. *For given* p *and* r*, the* $r-$*truncated and* $p-$*banded TBLMI:*

$$\Pi_r(\mathcal{L}(\mathcal{P}; \mathcal{A}_{s_{b(p)}}, s \in \mathbb{S})) < 0 \tag{3.22}$$

involves a finite number of unknown phasors of $\mathcal{P}$*.*

Proof 15 *The first assertion was proven with Theorem 4 in Chapter 2.*
Now for assertion 2), as the entries $\mathcal{A}_s, s \in \mathbb{S}$ *are assumed bounded on* ℓ^2*, the only term of the TBLMI not bounded on* ℓ^2 *is* $\mathcal{N}$*. Fortunately, as* $\mathcal{N}$ *is diagonal,* $\mathcal{N} = \mathcal{N}_{b(p)}$ *for any* $p \geq 0$ *and thus* $\mathcal{N}$ *does not play any role. If* $\mathcal{P}$ *is a solution to* (3.7)*, then by assumption* $\mathcal{L}(\mathcal{P}; \mathcal{A}_s, s \in \mathbb{S})$ *must be a bounded operator on* ℓ^2*. By continuity property of LMIs with respect to their entries, there exists a constant* C *depending of* $\mathcal{P}$ *and* $\mathcal{A}_s$*,* $s \in \mathbb{S}$*, such that for any* $p > 0$

$$\begin{aligned}\|\mathcal{L}(\mathcal{P}; \mathcal{A}_s, s \in \mathbb{S}) - \mathcal{L}(\mathcal{P}; &\mathcal{A}_{s_{b(p)}}, s \in \mathbb{S})\|_{\ell^2} \\ &\leq C \sum_{s\in\mathbb{S}} \|\mathcal{A}_s - \mathcal{A}_{s_{b(p)}}\|_{\ell^2}.\end{aligned}$$

From the first assertion, we conclude that for any $\epsilon > 0$*, there exists* p_0 *such that for* $p \geq p_0$*,*

$$\|\mathcal{L}(\mathcal{P}; \mathcal{A}_s, s \in \mathbb{S}) - \mathcal{L}(\mathcal{P}; \mathcal{A}_{s_{b(p)}}, s \in \mathbb{S})\|_{\ell^2} < \epsilon$$

and relation (3.21) *follows for sufficiently small* ϵ*.*
Finally, to show the last assertion, as all $\mathcal{A}_{s_{b(p)}}$*,* $s \in \mathbb{S}$*, in* $\mathcal{L}(\mathcal{P}; \mathcal{A}_{s_{b(p)}}, s \in \mathbb{S}) < 0$ *are banded, only the unknown* $\mathcal{P}$ *is possibly not banded. As the product of infinite dimensional banded TB operators is a banded TB operator* [1]*, the terms in the TBLMI involving the operator* $\mathcal{P}$ *have the generic form:* $\mathcal{U}\mathcal{P}\mathcal{V}$ *where* $\mathcal{U}$ *and* $\mathcal{V}$ *are polynomial functions of banded entries* $\mathcal{A}_{s_{b(p)}}, s \in \mathbb{S}$*, and are therefore banded. Applying* Π_r *on* $\mathcal{L}(\mathcal{P}; \mathcal{A}_{s_{b(p)}}, s \in \mathbb{S})$ *leads to computing* $\Pi_r(\mathcal{U}\mathcal{P}\mathcal{V})$*. Using* (3.19)*, we have:*

$$\begin{aligned}\Pi_r(\mathcal{U}\mathcal{P}\mathcal{V}) = \Pi_r(\mathcal{U})\Pi_r(\mathcal{P}\mathcal{V}) &\\ + \mathcal{H}_{(r,\eta_1)}(U^+)\mathcal{H}_{(\eta_1,r)}((PV)^-) &\\ + \mathcal{J}_{n,r}\mathcal{H}_{(r,\eta_1)}(U^-)\mathcal{H}_{(\eta_1,r)}((PV)^+)\mathcal{J}_{n,r} &\end{aligned} \tag{3.23}$$

where η_1 *is the first integer greater than* $\frac{1}{2}d^oU$ *and where* $\Pi_r(\mathcal{P}\mathcal{V})$ *is determined using* (3.19) *with* η *the first integer greater than* $\frac{1}{2}d^oV$*. Noticing that the coefficient of the highest degree invoked in the Hankel matrix* $\mathcal{H}_{(r,\eta)}(\cdot)$ *is of degree* $2(r+\eta)+1$*, it is straightforward to check that only a finite number of phasors of* $\mathcal{P}$ *are necessary to compute both* $\Pi_r(\mathcal{P}\mathcal{V})$ *and* (3.23) *and thus the result follows.* ■

[1] This is not true in finite dimension

We want to emphasize that solving the LMI presented in point 3) provides us with the ability to explicitly calculate the unknown phasors of $\mathcal{P}$ up to a specified order. Given that the phasor sequence belongs to ℓ^2, it is evident that this sequence must diminish for higher-order phasors. In essence, this implies that we can expect to achieve a precise solution as we increase the values of both p and r significantly. In the subsequent section, we will delineate the precise steps to determine the solution to **COP** up to a small arbitrary error. For clarity, these steps are summarized on Figure 3.2.

3.2.4 Solving COP up to an arbitrary error

We are now ready to prove the main result of this chapter. To this end, we define three subproblems: the $p-$banded problem $\mathbf{COP_p}$, the fully banded problem $\mathbf{COP_{p,q}}$ and the $r-$truncated, fully banded problem $\mathbf{COP_{p,q,r}}$. These subproblems constitute the successive steps of our approximation scheme for solving infinite-dimensional TBLMIs, as illustrated in Figure 3.2. The main result states that solving $\mathbf{COP_{p,q,r}}$ is a consistent scheme allowing to approximate the solution to **COP**.
For a given $p > 0$, consider the $p-$banded problem:

$$\begin{aligned}\mathbf{COP_p}: \min_{\mathcal{P}^*=\mathcal{P}>0} & tr_0(\mathcal{P}) \text{ s.t.} \\ & \mathcal{L}(\mathcal{P}; \mathcal{A}_{s_{b(p)}}, s \in \mathbb{S}) \leq 0.\end{aligned}$$

For a given $q > 0$, the fully banded problem is:

$$\begin{aligned}&\mathbf{COP_{p,q}}: \min_{\mathcal{P}^*=\mathcal{P}>0} tr_0(\mathcal{P}) \text{ s.t.} \\ &\mathcal{L}(\mathcal{P}; \mathcal{A}_{s_{b(p)}}, s \in \mathbb{S}) \leq 0, \quad P_{ij,k} = 0, |k| > q,\ i,j = 1,\cdots,n\end{aligned}$$

where for a given $k \in \mathbb{Z}$, $P_{ij,k} = 0$ refers to the kth-phasors of the (i,j)th block of $\mathcal{P}$.
For a given $r > 0$, the $r-$truncated, fully banded optimization problem is:

$$\begin{aligned}&\mathbf{COP_{p,q,r}}: \min_{\mathcal{P}^*=\mathcal{P}} tr_0(\mathcal{P}) \quad \text{s.t.} \quad \Pi_r(\mathcal{P}) > 0, \\ &\Pi_r(\mathcal{L}(\mathcal{P}; \mathcal{A}_{s_{b(p)}}, s \in \mathbb{S})) \leq 0,\ P_{ij,k} = 0, |k| > q,\ i,j = 1,\cdots,n.\end{aligned}$$

Since the unknown TB matrix $\mathcal{P}$ and the entries $\mathcal{A}_{s_{b(p)}}$ are q-banded and p-banded respectively, truncating at order r the LMI results in a finite-dimensional LMI which involves $(2q+1)\frac{n(n+1)}{2}$ scalar unknowns. As the evaluation of $tr_0(\mathcal{P})$ requires only 0-order phasors $P_{ii,0}$, $i = 1,\cdots,n$, it follows that $\mathbf{COP_{p,q,r}}$ is a problem of finite dimension.

Now, assume that all these convex optimization problems are feasible and that the optimal solution is unique, bounded on ℓ^2 and continuous with respect to the entries $\mathcal{A}_s$, $s \in \mathbb{S}$. Given p, q and r, we denote by $\hat{\mathcal{P}}$, $\hat{\mathcal{P}}_p$, $\hat{\mathcal{P}}_{p,q}$ and $\hat{\mathcal{P}}_{p,q,r}$, the solution to **COP**, $\mathbf{COP_p}$, $\mathbf{COP_{p,q}}$ and $\mathbf{COP_{p,q,r}}$ respectively. The next theorem states that solving $\mathbf{COP_{p,q,r}}$ is a consistent scheme allowing to approximate the solution to **COP**.

Theorem 14 *Let the TBLMI entries $\mathcal{A}_s, s \in \mathbb{S}$ of* **COP** *satisfy Assumption 3. For any $\epsilon > 0$, there exist p, q and r_0 such that for any $r > r_0$:*

$$\|\hat{\mathcal{P}}_{p,q,r} - \hat{\mathcal{P}}\|_{\ell^2} = \|\hat{P}_{p,q,r} - \hat{P}\|_{L^\infty} < \epsilon \tag{3.24}$$

where $\hat{\mathcal{P}}_{p,q,r} = \mathcal{T}(\hat{P}_{p,q,r})$ and $\hat{\mathcal{P}} := \mathcal{T}(\hat{P})$.

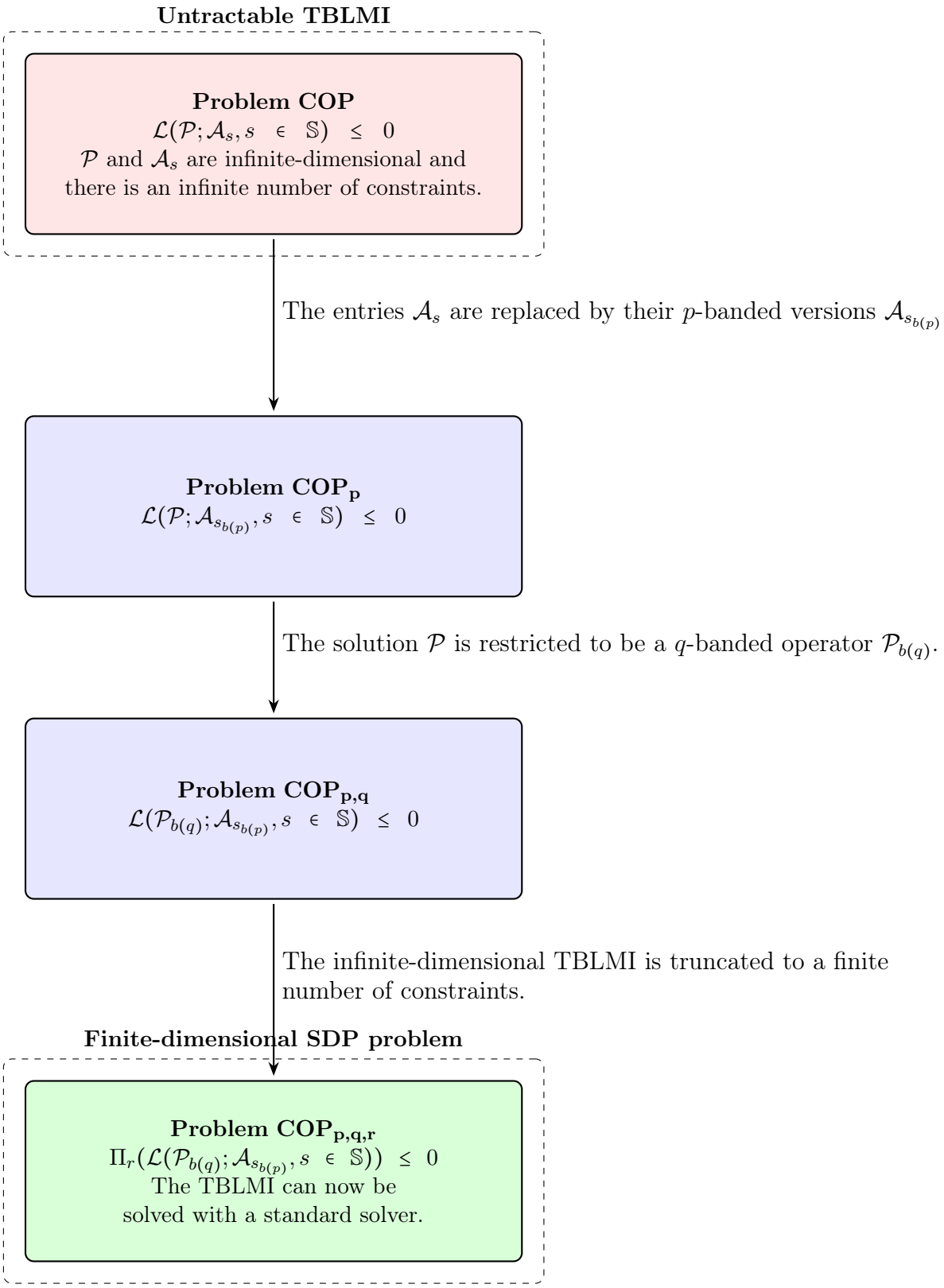

Figure 3.2: Steps of the approximation scheme for solving infinite-dimensional TBLMIs.

Proof 16 *Let us show that the following three limits hold:*

$$\lim_{p\to+\infty} \|\hat{\mathcal{P}}_p - \hat{\mathcal{P}}\|_{\ell^2} = 0, \quad \lim_{q\to+\infty} \|\hat{\mathcal{P}}_{p,q} - \hat{\mathcal{P}}_p\|_{\ell^2} = 0, \ p > 0$$
$$\textit{and} \lim_{r\to+\infty} \|\hat{\mathcal{P}}_{p,q,r} - \hat{\mathcal{P}}_{p,q}\|_{\ell^2} = 0, p, q > 0.$$

The first limit is a direct consequence of the continuity of the optimal solution with respect to the entries $\mathcal{A}_s$, $s \in \mathbb{S}$ and 1) in Theorem 13.

To prove that the solution of the fully-banded problem converges to the p-banded problem solution, we first establish that the values of the objective function constitute a monotone and bounded sequence. Indeed, for a given p, as for any q, $\hat{\mathcal{P}}_{p,q}$ is admissible for both $\mathbf{COP_{p,q+1}}$ *and* $\mathbf{COP_p}$*, it follows necessarily that*

$$tr_0(\hat{\mathcal{P}}_{p,q}) \geq tr_0(\hat{\mathcal{P}}_{p,q+1}) \geq \cdots \geq tr_0(\hat{\mathcal{P}}_p) > 0. \tag{3.25}$$

On the other hand, from 1) in Theorem 13, it is clear that there exists q_0 such that for any $q > q_0$ the q−banded operator $\hat{\mathcal{P}}_{p_{b(q)}}$ of $\hat{\mathcal{P}}_p$ is positive definite. Thus, $\hat{\mathcal{P}}_{p_{b(q)}}$ is obviously admissible for $\mathbf{COP_{p,q}}$*. It follows that:*

$$tr_0(\hat{\mathcal{P}}_{p_{b(q)}}) \geq tr_0(\hat{\mathcal{P}}_{p,q}) \geq tr_0(\hat{\mathcal{P}}_p). \tag{3.26}$$

As the Fourier series associated to $\hat{\mathcal{P}}_p$ converges uniformly (see Theorem 9), Theorem 13 implies $\|\hat{\mathcal{P}}_{p_{b(q)}} - \hat{\mathcal{P}}_p\|_{\ell^2} \to 0$ when $q \to +\infty$. Taking the limit w.r.t. q in (3.26) *leads to:*

$$\lim_{q\to+\infty} tr_0(\hat{\mathcal{P}}_{p,q}) = tr_0(\hat{\mathcal{P}}_p). \tag{3.27}$$

Now, let us show that we also have: $\lim_{q\to+\infty} \hat{\mathcal{P}}_{p,q} = \hat{\mathcal{P}}_p$ on ℓ^2. As $\hat{\mathcal{P}}_{p,q}$ is TB, Hermitian, positive definite and bounded on ℓ^2, there exists a bounded operator on ℓ^2, $\mathcal{Z}_{p,q}$ such that the following decomposition holds:

$$\hat{\mathcal{P}}_{p,q} = \mathcal{Z}^*_{p,q}\mathcal{Z}_{p,q} \textit{ for any } p, q.$$

Moreover as $\mathcal{Z}_{p,q}$ is a constant matrix function, it belongs trivially in H (see Def. 1) and there exists a representative $Z_{p,q} \in L^\infty([0\ T])$ (see Theorem 2) such that $\mathcal{Z}_{p,q} = \mathcal{T}(Z_{p,q})$. Using similar arguments, $\hat{\mathcal{P}}_p = \mathcal{Z}^*_p\mathcal{Z}_p$ with $\mathcal{Z}_p = \mathcal{T}(Z_p)$ and $Z_p \in L^\infty([0\ T])$. Therefore, Def. 2 implies:

$$tr_0(\hat{\mathcal{P}}_{p,q}) = tr_0(\mathcal{Z}^*_{p,q}\mathcal{Z}_{p,q}) = < Z_{p,q}, Z_{p,q} >$$

and from (3.27)*, it can be concluded that*

$$\lim_{q\to+\infty} < Z_{p,q}, Z_{p,q} > = < Z_p, Z_p > . \tag{3.28}$$

Moreover as the sequence $Z_{p,q}$ indexed by q is bounded (see (3.25)*), there exists a subsequence that converges weakly on L^∞ and Eq.* (3.28) *implies that it also converges strongly and necessarily to Z_p by uniqueness of solution. Finally, the uniqueness of the solution implies that the whole sequence converges to Z_p. It follows that $\lim_{q\to+\infty} \hat{\mathcal{P}}_{p,q} = \hat{\mathcal{P}}_p = \mathcal{Z}^*_p\mathcal{Z}_p$ on ℓ^2.*

Finally to prove the third limit: for any r and following similar steps as the proof of Theorem 12, as $\hat{\mathcal{P}}_{p,q}$ is admissible for Problem $\mathbf{COP_{p,q,r}}$ *and $\hat{\mathcal{P}}_{p,q,r+1}$ is admissible for Problem* $\mathbf{COP_{p,q,r}}$ *, it follows that:*

$$tr_0(\hat{\mathcal{P}}_{p,q,r}) \leq tr_0(\hat{\mathcal{P}}_{p,q,r+1}) \leq \cdots \leq tr_0(\hat{\mathcal{P}}_{p,q}) \tag{3.29}$$

which proves that the sequence $tr_0(\hat{\mathcal{P}}_{p,q,r})$ *indexed by* r *is an increasing and bounded real sequence, and thus a converging sequence. Moreover, for any* r*, as there exists* $\hat{\mathcal{Z}}_{p,q,r}$ *s.t.* $\hat{\mathcal{P}}_{p,q,r} := \hat{\mathcal{Z}}^*_{p,q,r}\hat{\mathcal{Z}}_{p,q,r}$*, Eq.* (3.13) *and* (3.29) *imply*

$$\|\hat{\mathcal{Z}}_{p,q,r}\|_{\ell^2} \leq \sqrt{n}\|\hat{\mathcal{Z}}_{p,q}\|_{\ell^2}$$

and it follows that the sequence $\|\hat{\mathcal{P}}_{p,q,r}\|_{\ell^2} = \|\hat{\mathcal{Z}}_{p,q,r}\|^2_{\ell^2}$ *indexed by* r *is necessarily bounded. Therefore, for any* r*, the phasors of* $\hat{\mathcal{P}}_{p,q,r}$ *are bounded on* ℓ^2 *and belong to a finite dimensional subspace of* ℓ^2 *(thanks to the constraints* $P_{ij,k} = 0$ *for* $|k| > q$*). By compactness, there exists a subsequence that converges on this finite subspace of* ℓ^2 *and the uniqueness of the solution implies that the whole sequence converges necessarily to* $\hat{\mathcal{P}}_{p,q}$*.*
The final result follows since $\forall \epsilon > 0$*,* $\exists p_0$*,* $\forall p > p_0$*,* $\exists q_0(p)$*,* $\forall q > q_0$*,* $\exists r_0(p,q)$ *such that:*

- $\|\hat{\mathcal{P}}_p - \hat{\mathcal{P}}\|_{\ell^2} \leq \frac{\epsilon}{3}$
- $\|\hat{\mathcal{P}}_{p,q} - \hat{\mathcal{P}}_p\|_{\ell^2} \leq \frac{\epsilon}{3}$
- $\forall r > r_0$*,* $\|\hat{\mathcal{P}}_{p,q,r} - \hat{\mathcal{P}}_{p,q}\|_{\ell^2} \leq \frac{\epsilon}{3}$*,*

and thus it follows that

$$\begin{aligned}\|\hat{\mathcal{P}}_{p,q,r} - \hat{\mathcal{P}}\|_{\ell^2} &\leq \|\hat{\mathcal{P}}_{p,q,r} - \hat{\mathcal{P}}_{p,q}\|_{\ell^2} + \|\hat{\mathcal{P}}_{p,q} - \hat{\mathcal{P}}_p\|_{\ell^2} + \|\hat{\mathcal{P}}_p - \hat{\mathcal{P}}\|_{\ell^2} \\ &\leq \epsilon.\end{aligned}$$

The proof ends invoking Theorem 2. ■

Remark 2 (A regularization strategy) *The proof of Theorem 14 requires that the Fourier series of the entries of the TBLMI* $A_s, s \in \mathbb{S}$ *converge uniformly. Therefore, the case where Assumption 3 does not hold should be carefully examined. We exploit the regularization scheme proposed in Chapter 2 to deal with non-smooth functions. According to Theorem 3, there always exists a regularized system whose matrix entries satisfy Assumption 3, and such that its trajectories are arbitrarily close to the true system trajectories on any compact time interval. The theoretical guarantees provided in Theorem 14 remain valid for regularized matrices* $A_{s,\varepsilon}$*,* $s \in \mathbb{S}$ *in* (3.4) *since the latter belong to* C^∞*. Therefore, the TBLMI design methods and the results presented in this section can be applied by replacing* A_s*,* $s \in \mathbb{S}$ *in* (3.4) *with their regularized counterparts* $A_{s,\varepsilon}$*. This applicability is ensured by the continuous dependence of system trajectories on the regularization parameter* ε*.*

In conclusion, the infinite-dimensional solution can be approximated as closely as desired by solving $\mathbf{COP_{p,q,r}}$ for sufficiently large values of the parameters p, q and r. Although this result is theoretical rather than constructive, it is practical. As demonstrated in the next section, it is sufficient to increase p, q, r until the approximated solution converges. A simple approach is to set the band size for the unknowns and LMI inputs to $p = r$, $q = r$, then increment the truncation order r until no significant improvement is observed in the solution of $\mathbf{COP_{p,q,r}}$.

3.3 Illustrative examples

In this section, we use several illustrative examples to assess the validity of the harmonic framework for solving PDLMIs. Because the theoretical solution is exactly known in these cases, the solution of the truncated problem $\mathbf{COP_{p,q,r}}$ can be directly compared with the true solution. In Subsection 3.3.1, a Riccati inequality is solved for different values of p, q and r, which helps to understand the role of each parameter of the truncation and their effect on the complexity of the problem. As for Subsection 3.3.2, it highlights the effect of regularizing the TBLMI entries when Assumption 3 is not satisfied. The examples show that the regularization strategy that was presented in Chapter 2 can be implemented to solve complex optimization problems.

3.3.1 Validation on a periodic differential Riccati inequality with a known solution

To validate the TBLMI method for solving PDLMIs, we use a benchmark problem from [37] where the analytical solution is provided. The PDLMI is defined as:

$$\forall t \in [0,T], \dot{P}(t) + A(t)'P(t) + P(t)A(t) - P(t)B(t)R(t)^{-1}B(t)'P(t) + Q(t) \geq 0 \tag{3.30}$$

with $P(t) = P(t)'$. From the following matrices: $A_c = \begin{pmatrix} 4 & 3 \\ -4.5 & -3.5 \end{pmatrix}, B_c = \begin{pmatrix} 1 \\ -1 \end{pmatrix}, R_c = 1, Q_c = \begin{pmatrix} 10 & 6 \\ 6 & 4 \end{pmatrix}$, a periodic operator $S(t) = \frac{1}{1.5+\cos(\omega t)} \begin{pmatrix} \cos(\omega t) & \sin(\omega t) \\ -\sin(\omega t) & \cos(\omega t) \end{pmatrix}$, and the solution of the algebraic Riccati equation $A_c'H_c + H_cA_c - H_cB_cR_c^{-1}B_c'H_c + Q_c = 0$, the periodic entries of (3.30) are given by:

$$\begin{aligned} A(t) &= S(t)^{-1}(A_cS(t) - \dot{S}(t)) \\ B(t) &= S(t)^{-1}B_c \\ Q(t) &= S(t)'Q_cS(t) \\ R(t) &= R_c \end{aligned}$$

Then the maximal solution of (3.30) is equal to $P(t) = S(t)'H_cS(t)$.

The harmonic counterpart of the PDLMI in [37] can be written as the following TBLMI:

$$\begin{aligned} &\max_{\mathcal{P}=\mathcal{P}^*} \ tr_0(\mathcal{P}) \\ &\begin{pmatrix} (\mathcal{A}-\mathcal{N})^*\mathcal{P} + \mathcal{P}(\mathcal{A}-\mathcal{N}) + \mathcal{Q} & \mathcal{P}\mathcal{B} \\ * & \mathcal{R} \end{pmatrix} \geq 0 \end{aligned} \tag{3.31}$$

This corresponds to an optimal harmonic LQR control problem, which will be studied in more detail in the next chapter on robust control. To solve this infinite-dimensional TBLMI, we must truncate it with the operator Π_r. The bands on the entries and the solution are given respectively by p and q. Given the products that appear in the TBLMI and formula (3.19), we require $r \geq \frac{1}{2}(\min(p,q)-1)$.

The error between the true solution and its estimation can be defined as the essential supremum $\|P - \hat{P}_{p,q,r}\|_{L^\infty}$. Since the periodic solution of (3.30) is known exactly, it is possible to evaluate the precision of the harmonic approach for different choices of p, q and r. To understand the influence of each variable on the solution, we conduct three experiments in which we keep two variables fixed to sufficiently large values while increasing the last one. The results are

p	5	10	15	20	25	30
Time (s)	1.5	1.6	2.5	2.7	2.5	2.5
$\|P - \hat{P}\|_{L^\infty}$	0.4	2 e-3	1.14e-05	1.06e-05	1.06e-05	1.11e-05

Table 3.1: Computation time and error according to the number of Fourier coefficients p of the LMI entries ($q = 30, r = 15$)

q	10	15	20	25	30
Time (s)	4.1	5.6	8.8	10	10.5
$\|P - \hat{P}\|_{L^\infty}$	4.2	0.06	8e-04	1.1e-05	1.0e-07

Table 3.2: Computation time and error according to the number of Fourier coefficients q of the solution ($p = 30, r = 25$)

presented in Table 3.1, Table 3.2 and Table 3.3. In general, larger values of q and r are associated with a larger computational complexity, which implies that a trade-off should be found between the precision and complexity of the method.

Table 3.1 shows the impact of p, the number of Fourier coefficients of the entries that are retained for resolution of the TBLMI. Here, the entries of the TBLMI correspond to the functions A, B, Q and R. While B and R are perfectly represented by a finite number of Fourier coefficients, A and Q display an infinite degree because of the factor $\frac{1}{1.5+\cos(\omega t)}$, but respect Assumption 3. As soon as $p \geq 15$, the error $\|P - \hat{P}\|_{L^\infty}$ has an order of magnitude of 10^{-5}, which confirms that the TBLMI approach returns satisfactory results even if higher-order phasors of the entries are neglected. At some point, increasing p does not lead to significant improvement, which means that this value should be chosen carefully to guarantee convergence to a sufficiently precise solution in a limited time. However, increasing p does not seem to lead to a dramatic increase in computation time, as opposed to q and r. The reason for this is that the number of unknowns and constraints does not increase when p becomes larger.

Table 3.2 illustrates the effect of q, namely the number of Fourier coefficients of the solution. A larger value of q allows an improvement in the precision of the solution, as it increases the size of the space in which admissible solutions can be found. Since the number of unknowns, and therefore the computation time necessary to find a q-banded solution increases with q, we could be satisfied with a reduced number of Fourier coefficients, provided the error in the determined solution is below a certain threshold.

Last but not least, Table 3.3 represents the effect of the truncation order of the LMI, denoted as r. As stated before, the constraint $r \geq \frac{1}{2}(\min(p, q) - 1)$ is necessary for the TBLMI to possess a solution, which is why we only provide results for $r \geq 15$. Generally, increasing r leads to a

r	15	20	25	30
Time (s)	2.4	4	9.9	9.3
$\|P - \hat{P}\|_{L^\infty}$	1.1e-05	1.8e-07	1.0e-07	1.7e-07

Table 3.3: Computation time and error according to the truncation order r of the LMI ($p = 30, q = 30$)

more precise solution, but from $r = 20$, all solutions are associated with an error of the same order of magnitude. Therefore, it might not always be useful to increase r if it does not lead to significant improvement in the precision of the solution.

In conclusion, we showed that the TBLMI method successfully approximates the true solution of the associated PDLMI as long as p, q and r are adequately chosen. Moreover, a satisfactory solution can be achieved even with moderate values of p, q and r, avoiding excessive computational cost.

3.3.2 Validation of a regularization approach on a periodic differential Lyapunov equation

We now present an example in which the periodic entries $A_s, s \in \mathbb{S}$ of the TBLMI violate Assumption 3. A rigorous analysis requires a regularized version $A_{s,\varepsilon}$ of each non-regular entry to ensure consistency of the numerical scheme that solves the TBLMI problem. However, it is observed that the numerical results for this example remain valid even without explicitly applying the regularization.

Consider for simplicity the 1-periodic scalar function defined by:

$$A(t) = \begin{cases} 2, & \text{if } 0 \le t < \frac{1}{2} \\ 0, & \text{if } \frac{1}{2} \le t < 1 \end{cases}$$

Due to its discontinuous nature, this function exhibits an infinite degree. In fact, its Fourier series is given by $A(t) = 1 + \frac{4}{\pi}\sum_{k=0}^{\infty} \frac{1}{2k+1}\sin(\omega(2k+1)t)$ where $\omega = 2\pi$. Our aim is to find a banded solution of a Lyapunov harmonic equation of the form $(\mathcal{A}-\mathcal{N})^*\mathcal{P}+\mathcal{P}(\mathcal{A}-\mathcal{N}) = -\mathcal{Q}$. The equivalent periodic differential equation is given by $\dot{P}(t) + A(t)'P(t) + P(t)A(t) = -Q(t)$ *a.e.*. Since the function A only takes two different values over a period, $P(t) = \sin(\omega t)$ solves the PDLMI if

$$Q(t) = \begin{cases} -\omega\cos(\omega t) - 4\sin(\omega t), & \text{if } 0 \le t < \frac{1}{2} \\ -\omega\cos(\omega t), & \text{if } \frac{1}{2} \le t < 1 \end{cases}$$

Q is continuous but its derivative is not, which means that Q exhibits an infinite number of Fourier coefficients. While the entries $\mathcal{A}$ and $\mathcal{Q}$ of the TBLMI are characterized by an infinite degree, P only has one nonzero Fourier coefficient.

To observe the effect of regularization of the entries of a TBLMI on its solution, we proceed as follows. For $\varepsilon \in \{0.001, 0.01, 0.05, 0.1, 0.2\}$, we plot the regularized functions A_ε and Q_ε on Figures 3.3 and 3.4 respectively. The larger the regularization parameter, the smoother the associated function, but the less it resembles the original function.

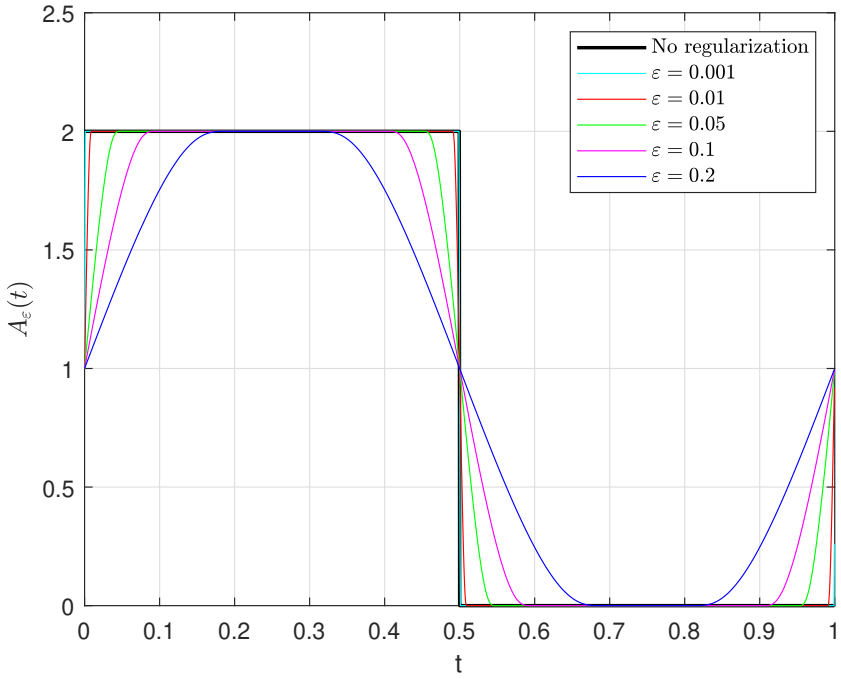

Figure 3.3: Comparison of $A(t)$ and its regularized version $A_\varepsilon(t)$ for $\varepsilon \in \{0.001, 0.01, 0.05, 0.1, 0.2\}$

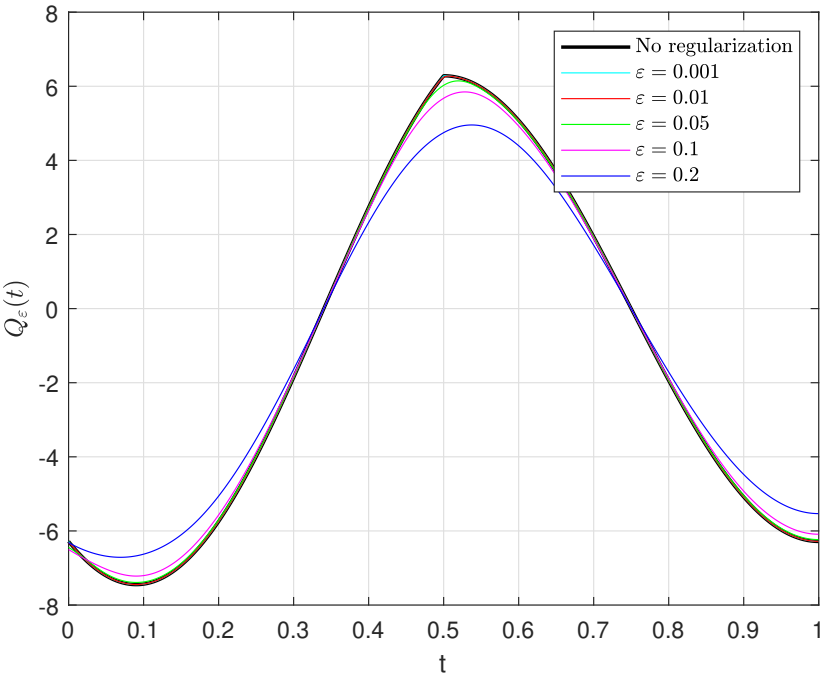

Figure 3.4: Comparison of $Q(t)$ and its regularized version $Q_\varepsilon(t)$ for $\varepsilon \in \{0.001, 0.01, 0.05, 0.1, 0.2\}$

ε	$\|P-\hat{P}\|_{L^\infty}$
0.001	0.002
0.01	0.002
0.05	0.020
0.1	0.077
0.2	0.281

Table 3.4: Comparison of $\|P-\hat{P}\|_{L^\infty}$ for different values of ε

For $p = q = r = 10$, we solve the truncated and regularized optimization problem

$$\Pi_r((\mathcal{A}_{\varepsilon_{b(p)}} - \mathcal{N})^* \mathcal{P}_{b(q)} + \mathcal{P}_{b(q)}(\mathcal{A}_{\varepsilon_{b(p)}} - \mathcal{N})) = \Pi_r(\mathcal{Q}_{\varepsilon_{b(p)}}).$$

Since the true solution $P(t)$ is known, we can compare it with the solution of the truncated TBLMI by means of the essential supremum $\|P-\hat{P}\|_{L^\infty}$. The results can be found in Table 3.4.

We can observe that the smaller the regularization parameter, the better the precision of the solution. This can be explained by the fact that when $\varepsilon \to 0$, the regularized entries converge to the entries almost everywhere if the latter belong to $L^\infty([0,T])$. It is clear that when the regularization parameter becomes too large, the error increases, probably because the regularized entries are too different from the true functions in that case. Therefore, a satisfactory solution should be found by adjusting the regularization parameter.

In summary, after truncation of the TBLMI entries to a finite order p, the entries $A_{\varepsilon_{b(p)}}$ and $A_{b(p)}$ become nearly indistinguishable for sufficiently small ε. The role of regularization is analogous to that of a low-pass filter in that it suppresses high-frequency components that would otherwise lie beyond the truncation threshold. Consequently, in practical implementations, one can directly use the truncated matrix $A_{b(p)}$ without regularization, while theoretical regularization remains essential to guarantee convergence in the infinite-dimensional setting.

3.4 Conclusion

In this chapter, we have presented a novel resolution method for Periodic Differential LMIs. By exploiting the equivalence between PDLMIs and Toeplitz Block LMIs, the solution of a PDLMI can be deduced from the solution of an algebraic LMI. This allows to avoid the numerical issues typically associated with differential equations, such as differentiation, discretization, or the complexity associated with larger periods. However, difficulties arise due to the infinite dimension of TBLMIs. Leveraging their inherent Toeplitz structure, we have established a systematic and consistent methodology to solve these semidefinite optimization problems with precision, achieving solutions that are arbitrarily close to the ideal outcome. Our approach is built upon the formulation of well-defined finite-dimensional truncated problems, which serve as the foundation for this method. A regularization approach ensures that the method is also applicable on non-smooth LMI entries. The main limitation of our method is that the complexity of the method becomes very large if the band on the solution or the truncation order of the TBLMI are overestimated.

4

A TBLMI Framework for Harmonic Robust Control

Contents

4.1 Framework for harmonic robust control 58
4.1.1 Harmonic transfer and transition functions 58
4.1.2 Harmonic H_2 and H_∞ norms 60
4.2 Harmonic H_2 and H_∞ optimal control 63
4.2.1 Harmonic H_2 optimal control 64
4.2.2 Harmonic H_∞ optimal control 66
4.2.3 Reconstruction of the periodic feedback gain 67
4.3 Illustrative examples 68
4.3.1 H_2 harmonic control-LQR case 69
4.3.2 H_∞ harmonic control 72
4.4 Conclusion 74

Introduction

In this chapter, we present a TBLMI formulation for the H_2 and H_∞ problems associated with harmonic LTI systems. A review of robust control methods for periodic systems was given in Section 1.4 of Chapter 1. The difficulty of solving these control problems in the time domain justifies the introduction of equivalent harmonic control problems to be solved. The truncation method introduced in Chapter 3 allows to find an approximate solution for infinite-dimensional robust control problems. The chapter is structured as follows. In Section 4.1, a framework for harmonic robust control is provided. This framework encompasses the definition of harmonic transition and transfer functions, the H_2 and H_∞ norms in the harmonic domain, and their interpretation in the time domain. In particular, defining the harmonic H_2 norm is not a straightforward task, primarily because the Frobenius norm is not trace-class. We then formulate harmonic robust control problems in terms of infinite-dimensional convex optimization problems involving TBLMI constraints in Section 4.2. Such TBLMIs become numerically tractable with the truncation approach presented in the previous chapter. We apply the proposed procedure to design harmonic H_2 and H_∞ optimal state feedbacks in Section 4.3, which proves the success of the TBLMI framework for robust control.

4.1 Framework for harmonic robust control

In this section, we adapt several notions associated with robust control to harmonic systems. Since the latter are infinite-dimensional, precautions must be taken for the H_2 and H_∞ norms to be well defined.

4.1.1 Harmonic transfer and transition functions

Consider a signal $X \in L^2(\mathbb{R}^+, \ell^2(\mathbb{C}^n))$ with its induced norm

$$\|X\|_{L^2}^2 := \int_0^{+\infty} \|X(t)\|_{\ell^2}^2 dt$$

and its Laplace transform:

$$\hat{X}(s) := \int_0^{+\infty} X(t) e^{-st} dt.$$

The associated H_2 induced norm [67] is given by

$$\|\hat{X}\|_{H_2} := \left(\frac{1}{2\pi} \int_{-\infty}^{+\infty} \|\hat{X}(\mathrm{j}\omega)\|_{\ell^2}^2 d\omega \right)^{\frac{1}{2}}.$$

By Paley Wiener theorem, we have : $\|\hat{X}\|_{H_2} = \|X\|_{L^2}$.

The transfer function that can be defined for harmonic systems is very similar to its finite-dimensional LTI counterpart.

To this aim, consider $T-$periodic functions $A(\cdot)$, $B(\cdot)$ and $C(\cdot)$ of class L^∞ and let the LTP system:

$$\begin{aligned} \dot{x}(t) &= A(t)x(t) + B(t)u(t) \\ y(t) &= C(t)x(t) \end{aligned} \tag{4.1}$$

and its LTI harmonic version:

$$\begin{aligned} \dot{X}(t) &= (\mathcal{A} - \mathcal{N})X(t) + \mathcal{B}U(t), \\ Y(t) &= \mathcal{C}X(t) \end{aligned} \tag{4.2}$$

where $X := \mathcal{F}(x)$, $U := \mathcal{F}(u)$, $\mathcal{A} = \mathcal{T}(A)$, $\mathcal{B} = \mathcal{T}(B)$ and $\mathcal{N} := Id_n \otimes diag(\mathrm{j}\omega k,\ k \in \mathbb{Z})$. In this chapter, we work with a Toeplitz Block (TB) representation, which is better suited to control but all results could be reformulated in a Block Toeplitz (BT) framework.

Definition 9 *[32] For harmonic system* (4.2)*, the harmonic transfer function between input* $\hat{U}(s)$ *and output* $\hat{Y}(s)$ *is given by:*

$$\hat{\mathcal{G}}(s) := \mathcal{C}(s\mathcal{I} - (\mathcal{A} - \mathcal{N}))^{-1}\mathcal{B} \tag{4.3}$$

and is the Laplace transform of

$$\mathcal{G}(t) := \mathcal{C}e^{(\mathcal{A}-\mathcal{N})t}\mathcal{B}. \tag{4.4}$$

As shown in [63, 68], the spectrum denoted as σ of the operator $(\mathcal{A} - \mathcal{N})$ in (4.2) exclusively comprises eigenvalues forming an unbounded, discrete set that relies solely on a finite number of complex values λ_i, $i = 1, \cdots, n$:

$$\sigma := \{\lambda_i + \mathrm{j}\omega k, k \in \mathbb{Z}, i = 1, \cdots, n\}.$$

For the sake of clarity and simplicity in our exposition, we make the assumption that $(\mathcal{A}-\mathcal{N})$ is non-defective. Under this assumption, the following eigenvalue decomposition holds, as described in [14]:

$$(\mathcal{A}-\mathcal{N})\mathcal{V} = \mathcal{V}(\Lambda \otimes \mathcal{I} - \mathcal{N}) \tag{4.5}$$

with $\Lambda = diag(\lambda_i, i = 1, \cdots, n)$ and where $\mathcal{V}$ is a constant, invertible TB and bounded operator on ℓ^2. As demonstrated in [14], $V = \mathcal{T}^{-1}(\mathcal{V})$ defines a periodic change-of-basis that transforms the periodic system $\dot{x} = A(t)x$ into a time-invariant diagonal system $\dot{z} = \Lambda z$, where $z(t) = V^{-1}(t)x(t)$. In other words, V is a Floquet factorization that reduces A to a diagonal and time-invariant form.

Notice that if $(\mathcal{A}-\mathcal{N})$ is defective, the diagonal matrix Λ can be substituted with a Jordan canonical form denoted as J (as outlined in [14]).

The following property will be particularly useful later, as it clarifies the effect of a time shift on the computation of a phasor vector.

Property 1 *For any real number δ, if $z(t) := x(t-\delta)$ a.e where $x \in L^2_{loc}$ is a vector function then*

$$Z(t) := e^{-\mathcal{N}\delta}X(t-\delta)$$

where $Z := \mathcal{F}(z)$, $X := \mathcal{F}(x)$ and where $\mathcal{N} = Id_n \otimes diag(j\omega k,\ k \in \mathbb{Z})$. Moreover, if $M(t) := G(t-\delta)$ a.e. where $G \in L^\infty_{loc}$ is a matrix function, then

$$\mathcal{M}(t) := e^{-\mathcal{N}\delta}\mathcal{G}(t-\delta)e^{\mathcal{N}\delta}$$

where $\mathcal{M} := \mathcal{T}(M)$ and $\mathcal{G} := \mathcal{T}(G)$.

Proof 17 *A simple change of variables allows to show that for any k, $Z_k(t) = e^{-j\omega k\delta}X_k(t-\delta)$ from which we can deduce the results of this property.* ■

In the following theorem, a relationship is established between the representative of $\mathcal{V}$ in (4.5) and the state transition function associated with the LTP system.

Theorem 15 *For any time instant t, the exponential of the harmonic state operator in (4.2), denoted as $e^{(\mathcal{A}-\mathcal{N})t}$, is a bounded operator on ℓ^2 and it is not TB. Furthermore, the state transition function associated with the LTP system (4.1) for the time interval between t_0 and t, namely the function such that $x(t) = \Phi(t,t_0)x(t_0)$, is expressed as follows:*

$$\Phi(t,t_0) := V(t)e^{\Lambda(t-t_0)}V^{-1}(t_0) \tag{4.6}$$

where the matrix function V is a T-periodic, invertible, and absolutely continuous function, defined as $V := \mathcal{T}^{-1}(\mathcal{V})$, where $\mathcal{V}$ is given by (4.5). Furthermore, for any (t,t_0):

$$\Phi(t,t_0) = \Phi(t+T,t_0+T). \tag{4.7}$$

Proof 18 *For any t, we have:*

$$\|e^{(\Lambda\otimes\mathcal{I}-\mathcal{N})t}\|_{\ell^2} := \sup_{\|X\|_{\ell^2}=1} \|e^{(\Lambda\otimes\mathcal{I}-\mathcal{N})t}X\|_{\ell^2} = \bar{\sigma}(t) < +\infty$$

where $\bar{\sigma}(t) := \max_{i=1,\cdots,n} e^{2Re(\lambda_i)t}$. Here, we use the fact that $e^{-\mathcal{N}^*t}e^{-\mathcal{N}t} = \mathcal{I}$ which implies $e^{(\Lambda\otimes\mathcal{I}-\mathcal{N})^*t}e^{(\Lambda\otimes\mathcal{I}-\mathcal{N})t} = e^{((\Lambda^*+\Lambda)\otimes\mathcal{I})t}$. Using (4.5), we have that $e^{(\mathcal{A}-\mathcal{N})t}$ is bounded on ℓ^2 for every t. Moreover, $e^{(\mathcal{A}-\mathcal{N})t}$ is obviously not TB due to the non Toeplitz diagonal term $\mathcal{N}$. In

addition, the free response of (4.1) *between time* t_0 *and* t *from an initial condition* $x(t_0)$ *is given by* $x(t) = \Phi(t, t_0)x(t_0)$ *and its associated harmonic free response is given by:*

$$\begin{aligned} X(t) &= e^{(\mathcal{A}-\mathcal{N})(t-t_0)}X(t_0) \\ &= \mathcal{V}e^{(\Lambda\otimes\mathcal{I})(t-t_0)}e^{-\mathcal{N}(t-t_0)}\mathcal{V}^{-1}X(t_0). \end{aligned}$$

As $\mathcal{V}^{-1}X(t_0) = \mathcal{V}^{-1}e^{\mathcal{N}(t-t_0)}e^{-\mathcal{N}(t-t_0)}X(t_0)$*, using Property 1 and rules* (1.4) *and* (1.5) *leads to:*

$$\begin{aligned} \Phi(t, t_0)x(t_0) &= \mathcal{F}^{-1}(e^{(\mathcal{A}-\mathcal{N})(t-t_0)}X(t_0)) \\ &= V(t)e^{\Lambda(t-t_0)}V^{-1}(t_0)x(t_0) \end{aligned}$$

for any $x(t_0)$*. The last result is established noticing that the absolute continuity of* V *is proved in [14].* ■

It is essential to emphasize that $\mathcal{T}(\Phi(t, t_0)) = e^{\mathcal{A}(t-t_0)}$ and should not be confused with the harmonic transition function $e^{(\mathcal{A}-\mathcal{N})(t-t_0)}$.

4.1.2 Harmonic H_2 and H_∞ norms

Definitions of the H_2 and H_∞ norms for periodic systems have already been given in the time domain in [55]. However, defining the H_2 norm in the harmonic framework is not a straightforward task, primarily because the Frobenius norm of $\hat{\mathcal{G}}(\mathrm{j}\omega)$, given by (4.3),

$$\|\hat{\mathcal{G}}(\mathrm{j}\omega)\|_F^2 := tr(\hat{\mathcal{G}}(\mathrm{j}\omega)^*\hat{\mathcal{G}}(\mathrm{j}\omega))$$

is not trace-class [66]. To address this challenge, let us first introduce the following result, which shows that the operator $\mathcal{G}(t)^*\mathcal{G}(t)$ is bounded.

Theorem 16 *For any time instant* t*,*

$$\mathcal{M}(t) := \mathcal{G}(t)^*\mathcal{G}(t) \tag{4.8}$$

where $\mathcal{G}(t) := \mathcal{C}e^{(\mathcal{A}-\mathcal{N})t}\mathcal{B}$*, is a hermitian and non-negative, TB and bounded operator on* ℓ^2*. Moreover,* $M := \mathcal{T}^{-1}(\mathcal{M})$ *exists and is given at time* τ *by:*

$$M_t(\tau) := G(\tau, t)'G(\tau, t) \tag{4.9}$$

where $G(\tau, t) := C(\tau + t)\Phi(\tau + t, \tau)B(\tau)$ *and satisfies*

$$G(\tau + T, t) = G(\tau, t). \tag{4.10}$$

Proof 19 *Hermitian and non-negativity properties are readily evident for* $\mathcal{M}(t)$*. Using the decomposition* (4.5)*, we have:*

$$e^{(\mathcal{A}-\mathcal{N})^*t}\mathcal{C}^*\mathcal{C}e^{(\mathcal{A}-\mathcal{N})t} = \mathcal{V}^{-1*}e^{(\Lambda\otimes\mathcal{I})^*t}e^{-\mathcal{N}^*t}\mathcal{H}e^{-\mathcal{N}t}e^{(\Lambda\otimes\mathcal{I})t}\mathcal{V}^{-1} \tag{4.11}$$

where $\mathcal{H} = \mathcal{V}^*\mathcal{C}^*\mathcal{C}\mathcal{V}$*. Thus, as* $e^{-\mathcal{N}^*t}\mathcal{H}e^{-\mathcal{N}t} = e^{\mathcal{N}t}\mathcal{H}e^{-\mathcal{N}t}$*, Property 1 implies that* $e^{-\mathcal{N}^*t}\mathcal{H}e^{-\mathcal{N}t}$ *is obviously a TB operator since it is equal to* $\mathcal{T}(L)$ *where*

$$L(\tau) := H(\tau + t) \tag{4.12}$$

for almost all τ with $H \coloneqq \mathcal{T}^{-1}(\mathcal{H})$. It follows that $\mathcal{M}(t)$ is a product of TB operators and thus a TB operator (see (1.5)).

Finally as $e^{(\mathcal{A}-\mathcal{N})t}$ is also bounded on ℓ^2 for every t (its maximal singular value is $e^{\sigma t}$ where $\sigma \coloneqq \max_i 2Re(\lambda_i)$), $\mathcal{M}(t)$ is also a bounded operator on ℓ^2. For the last assertion, using Property 1, we see that (4.11) is the Toeplitz transformation of $Z(\tau)$ where $Z(\tau) \coloneqq V'^{-1}(\tau)e^{\Lambda^* t}L(\tau)e^{\Lambda t}V^{-1}(\tau)$ with L defined by (4.12). As $H(\tau) \coloneqq V'(\tau)C'(\tau)C(\tau)V(\tau)$, it follows, using (4.6), that $Z(\tau)$ can be rewritten as:

$$Z(\tau) \coloneqq \Phi'(\tau+t,\tau)C'(\tau+t)C(\tau+t)\Phi(\tau+t,\tau).$$

Consequently, multiplying $Z(\tau)$ on the left by $B'(\tau)$ and on the right by $B(\tau)$, we get the final result (thanks to (1.5)). Finally, the relation $G(\tau+T,t) = G(\tau,t)$ follows directly from the periodicity of B and C, together with equation (4.7). ■

Given the assumption that $(\mathcal{A}-\mathcal{N})$ is Hurwitz, we define the following induced operator-norm for $\mathcal{G}(t) \coloneqq \mathcal{C}e^{(\mathcal{A}-\mathcal{N})t}\mathcal{B}$:

$$\|\mathcal{G}\|_{L^2} \coloneqq \left(\int_0^{+\infty} tr_0(\mathcal{G}^*(t)\mathcal{G}(t))dt\right)^{\frac{1}{2}} \tag{4.13}$$

where tr_0 is given in Definition 5 for TB and bounded operators on ℓ^2. Consequently, as $tr_0(\mathcal{G}^*(t)\mathcal{G}(t))$ is finite for every t and is clearly in L^2, the harmonic H_2 norm can now be defined.

Definition 10 *The H_2 operator norm of the harmonic transfer function $\hat{\mathcal{G}}(s)$ is defined by*

$$\|\hat{\mathcal{G}}\|_{H_2} \coloneqq \left(\frac{1}{2\pi}\int_{-\infty}^{+\infty} tr_0(\hat{\mathcal{G}}(j\omega)^*\hat{\mathcal{G}}(j\omega))d\omega\right)^{\frac{1}{2}}. \tag{4.14}$$

The next theorem states that the L^2 norm of the sliding average Frobenius norm of $G(\tau,t)$ over a window of length T is equal to the H_2 operator norm of its associated harmonic transfer function.

Theorem 17 *Let $\hat{\mathcal{G}}$, $\mathcal{G}$, and G be defined in (4.3), (4.4), and (4.9), respectively. Then the following norm equivalences hold:*

$$\|G\|_{L^2} = \|\mathcal{G}\|_{L^2} = \|\hat{\mathcal{G}}\|_{H_2} \tag{4.15}$$

where $\|\mathcal{G}\|_{L^2}$ and $\|\hat{\mathcal{G}}\|_{H_2}$ are defined in (4.13) and (4.14), respectively, while

$$\|G\|_{L^2} \coloneqq \left(\int_0^{+\infty} \|G(\cdot,t)\|_F^2 dt\right)^{\frac{1}{2}} = \left(\frac{1}{T}\int_0^T \|G(\tau,\cdot)\|_F^2 d\tau\right)^{\frac{1}{2}} \tag{4.16}$$

with

$$\|G(\tau,\cdot)\|_F^2 \coloneqq \sum_{i=1}^{p}\sum_{j=1}^{m}\int_0^{+\infty}\|G_{ij}(\tau,t)\|^2 dt.$$

Proof 20 *The first equality in (4.15) follows by Theorems 10 and 16 and noticing that*

$$\begin{aligned}\|G\|_{L^2} &\coloneqq \left(\int_0^{+\infty}\frac{1}{T}\int_{t-T}^{t} tr(G(\tau,t)'G(\tau,t))d\tau dt\right)^{\frac{1}{2}}\\ &= \left(\int_0^{+\infty} tr_0(\mathcal{G}^*(t)\mathcal{G}(t))dt\right)^{\frac{1}{2}} = \|\mathcal{G}\|_{L^2}.\end{aligned}$$

The second equality is due to Paley-Wiener Theorem. Finally, to prove (4.16)*, we use the property* $G(\tau+T,t)=G(\tau,t)$ *given in Theorem 16. Hence, it follows that*

$$\begin{aligned}\|G\|_{L^2} &:= \left(\int_0^{+\infty}\|G(\cdot,t)\|_F^2 dt\right)^{\frac{1}{2}} \\ &= \left(\int_0^{+\infty}\frac{1}{T}\int_{t-T}^{t} tr(G(\tau,t)'G(\tau,t))d\tau dt\right)^{\frac{1}{2}} \\ &= \left(\int_0^{+\infty}\frac{1}{T}\int_{0}^{T} tr(G(\tau,t)'G(\tau,t))d\tau dt\right)^{\frac{1}{2}} \\ &= \left(\frac{1}{T}\int_0^{T}\|G(\tau,\cdot)\|_F^2 d\tau\right)^{\frac{1}{2}}.\end{aligned} \tag{4.17}$$

■

It is worth noting that the expression above recovers the H_2 norm up to the multiplicative factor $\frac{1}{\sqrt{T}}$, as defined in [55, 56], namely

$$\left(\int_0^{T}\|G(\tau,\cdot)\|_F^2 d\tau\right)^{\frac{1}{2}}. \tag{4.18}$$

The H_∞ norm can now be defined in the harmonic context.

Definition 11 *The* H_∞ *operator norm of the harmonic transfer function* $\hat{\mathcal{G}}(s)$ *is defined by:*

$$\|\hat{\mathcal{G}}\|_{H_\infty} := ess\sup\bar{\sigma}(\hat{\mathcal{G}}(j\omega)) \tag{4.19}$$

where $\bar{\sigma}$ *refers to the maximal singular value.*

The next theorem states that the H_∞ operator norm of the harmonic transfer function defines a bound for the L^2 norm of the sliding quadratic average of the output y over a window of length T.

Theorem 18 *The following relations hold true:*

$$\|\hat{\mathcal{G}}\|_{H_\infty} := \sup_{\|\hat{U}\|_{L^2}=1}\|\hat{\mathcal{G}}\hat{U}\|_{L^2} \tag{4.20}$$

$$= \sup_{\|U\|_{L^2}=1}\|\mathcal{G}*U\|_{L^2} \tag{4.21}$$

$$\geq \sup_{\|U\|_{L^2\cap H}=1}\|\mathcal{G}*U\|_{L^2} \tag{4.22}$$

$$= \sup_{\|u\|_{L^2}=1}\left(\int_0^{\infty}\|y\|^2_{L^2([t-T\ t])}dt\right)^{\frac{1}{2}} \tag{4.23}$$

where $*$ *denotes the convolution product and* $y(t) := C(t)\int_0^t \Phi(t,s)B(s)u(s)ds$.

Proof 21 *Relations* (4.20)-(4.22) *are obvious. To prove* (4.23)*, for any* $U\in L^2\cap H$ *then* $u := \mathcal{F}^{-1}(U)$ *exists since* $U\in H$ *and it follows as a direct consequence of Theorem 4 in [5] that* $Y := \mathcal{G}*U$ *belongs to* H*. Thus,* $y := \mathcal{F}^{-1}(Y)$ *exists and satisfies*

$$y(t) := \int_0^t C(t)\Phi(t,s)B(s)u(s)ds$$

where $\Phi(t,s)$ denotes the transition matrix associated to (1.7).

Moreover, invoking Parseval's Theorem, we have for any t,

$$\|y\|_{L^2([t-T\ t])} := \Big(\frac{1}{T}\int_{t-T}^{t}|y(\tau)|^2 d\tau\Big)^{\frac{1}{2}} = \|Y(t)\|_{\ell^2}.$$

It follows that the L^2 norm of the sliding quadratic average of y over a window of length T defined as

$$\|y\|_{L^2} := \Big(\int_0^\infty \|y\|^2_{L^2([t-T\ t])} dt\Big)^{\frac{1}{2}}$$

fulfils the relation:

$$\|y\|_{L^2} = \Big(\int_0^\infty \|Y(t)\|^2_{\ell^2} dt\Big)^{\frac{1}{2}} := \|Y\|_{L^2}. \tag{4.24}$$

As it is assumed that $Y := \mathcal{G} * U$, taking the supremum on U in Eq. (4.22) *leads to Eq.* (4.23) *thanks to the equality* (4.24). ∎

Having introduced the harmonic H_2 and H_∞ norms, our aim in the sequel is to demonstrate how the TBLMI framework introduced in Chapter 3 allows to tackle infinite-dimensional robust control problems associated with the harmonic system.

4.2 Harmonic H_2 and H_∞ optimal control

With the H_2 and H_∞ norms in place, the corresponding optimal control problems can be formulated as TBLMIs and solved using the consistent truncation operator introduced in the previous chapter. The periodic feedback gain is then recovered in the time domain from the harmonic operator. We also address the case of non-smooth system functions.

Consider a LTP system with control input u, exogenous input w, controlled output z and measured output y given by

$$\begin{aligned}\dot{x}(t) &= A(t)x(t) + B(t)u(t) + B_w(t)w(t)\\ z(t) &= C_z(t)x(t) + D_{zw}(t)w(t) + D_{zu}(t)u(t)\\ y(t) &= C_y(t)x(t) + D_{yw}(t)w(t) + D_{yu}(t)u(t)\end{aligned} \tag{4.25}$$

where all inputs belong to $L^2(\mathbb{R}^+)$ and all matrices are assumed to belong to $L^\infty([0\ T])$ and satisfy Assumption 3. For each of these matrices, the associated infinite dimensional TB matrix function is obtained using (1.10). This allows to write the harmonic LTI representation as follows:

$$\begin{aligned}\dot{X}(t) &= (\mathcal{A}-\mathcal{N})X(t) + \mathcal{B}U(t) + \mathcal{B}_w W(t)\\ Z(t) &= \mathcal{C}_z X(t) + \mathcal{D}_{zw}W(t) + \mathcal{D}_{zu}U(t)\\ Y(t) &= \mathcal{C}_y X(t) + \mathcal{D}_{yw}W(t) + \mathcal{D}_{yu}U(t).\end{aligned} \tag{4.26}$$

From this perspective, it is clear that any robust optimal control problem formulated for finite-dimensional LTI systems can be naturally extended to its infinite-dimensional harmonic counterpart. In this chapter, we focus on the full-state feedback H_2 and H_∞ problems, with

$$\mathcal{C}_y = \mathcal{I}, \quad \mathcal{D}_{zw} = \mathcal{D}_{yw} = \mathcal{D}_{yu} = 0.$$

4.2.1 Harmonic H_2 optimal control

Consider the full state feedback H_2 periodic optimal control problem, which consists in determining a control law $u = K(t)x$, where $K(.)$ is a T-periodic control gain to be designed so that the H_2 norm of the transfer function between w and z is minimized. According to [55, 56] and especially (Theorem 2.2, p. 331), the optimal solution is

$$K(t) = -(D'_{zu}(t)D_{zu}(t))^{-1}(B'(t)P(t) + D'_{zu}(t)C_z(t))$$

where $P(t)$ is the unique stabilizing periodic positive semi-definite solution of the periodic Riccati equation

$$\begin{aligned}\dot{P}(t)+&A'(t)P(t) + P(t)A(t) + C'_z(t)C_z(t)\\ &- (B(t)'P(t) + D'_{zu}(t)C_z(t))'(D'_{zu}(t)D_{zu}(t))^{-1}(B(t)'P(t) + D'_{zu}(t)C_z(t)) = 0\end{aligned}$$

For this result to hold, the following assumptions are required: the pair $(A(\cdot), B(\cdot))$ is stabilizable, $D_{zu}(t)$ is full column rank for each t and the periodic system (A, B, C_z, D_{zu}) does not have invariant zeros on the imaginary axis.

It can be readily shown that the harmonic algebraic Riccati equation is given by

$$(\mathcal{A}-\mathcal{N})^*\mathcal{P} + \mathcal{P}(\mathcal{A}-\mathcal{N}) + \mathcal{C}_z^*\mathcal{C}_z - (\mathcal{B}^*\mathcal{P} + \mathcal{D}_{zu}^*\mathcal{C}_z)^*(\mathcal{D}_{zu}^*\mathcal{D}_{zu})^{-1}(\mathcal{B}^*\mathcal{P} + \mathcal{D}_{zu}^*\mathcal{C}_z) = 0$$

where $\mathcal{P}$ is the unique hermitian positive semi definite operator bounded on ℓ^2 and the optimal gain reads

$$\mathcal{K} = -(\mathcal{D}_{zu}^*\mathcal{D}_{zu})^{-1}(\mathcal{B}^*\mathcal{P} + \mathcal{D}_{zu}^*\mathcal{C}_z).$$

An equivalent TBLMI-based optimization problem [69] is given by

$$\begin{aligned}&\max_{\mathcal{P}}\ tr_0(\mathcal{P})\\ &\mathcal{P}^* = \mathcal{P} \succeq 0\\ &\begin{bmatrix} \mathcal{P}(\mathcal{A}-\mathcal{N}) + (\mathcal{A}-\mathcal{N})^*\mathcal{P} + \mathcal{C}_z^*\mathcal{C}_z & \mathcal{B}^*\mathcal{P} + \mathcal{D}_{zu}^*\mathcal{C}_z \\ (\mathcal{B}^*\mathcal{P} + \mathcal{D}_{zu}^*\mathcal{C}_z)^* & \mathcal{D}_{zu}^*\mathcal{D}_{zu} \end{bmatrix} \succeq 0\end{aligned} \tag{4.27}$$

whose time domain formulation is the PDLMI-based optimization problem

$$\begin{aligned}&\max_{P}\ tr_0(P) := \frac{1}{T}\int_0^T tr(P)dt\\ &P^* = P \succeq 0\\ &\begin{bmatrix} \dot{P} + PA + A'P + C'_zC_z & B'P + D'_{zu}C_z \\ (B'P + D'_{zu}C_z)' & D'_{zu}D_{zu} \end{bmatrix} \succeq 0\end{aligned} \tag{4.28}$$

We also recall from Theorem 9 that the solution of a TBLMI ensures that $\mathcal{P}$ is bounded on ℓ^2, and that $P = \mathcal{T}^{-1}(\mathcal{P})$ is a periodic, absolutely continuous function whose Fourier series converges uniformly. Moreover, since $\mathcal{P} = \mathcal{P}^* \succ 0$, for all t, $P(t) = P(t)' \succ 0$ and $P(t)^{-1}$ is well defined.

In fact, any LMI-based optimization problem that can be used to solve an H_2 optimization problem for a finite-dimensional LTI system admits a natural harmonic counterpart. Indeed, formulating the corresponding TBLMI-based optimization problems requires no additional difficulty, since the same arguments as in the finite-dimensional LTI case apply, provided that

1. the state matrix $A(t)$ is replaced by $\mathcal{A}-\mathcal{N}$,

2. all entries in the harmonic domain are bounded on ℓ^2, and
3. the trace operator is replaced by the average trace operator tr_0.

For example, consider the controllability Grammian

$$\mathcal{P} = \int_0^\infty e^{(\mathcal{A}-\mathcal{N}+\mathcal{B}\mathcal{K})t}\mathcal{B}_w\mathcal{B}_w^* e^{(\mathcal{A}-\mathcal{N}+\mathcal{B}\mathcal{K})^* t}dt,$$

which satisfies the Lyapunov equation

$$(\mathcal{A}-\mathcal{N}+\mathcal{B}\mathcal{K})\mathcal{P} + \mathcal{P}(\mathcal{A}-\mathcal{N}+\mathcal{B}\mathcal{K})^* + \mathcal{B}_\omega\mathcal{B}_\omega^* = 0.$$

The H_2 norm of the transfer function between W and Z is given by

$$\|\hat{\mathcal{G}}(s)\|_{H_2} = tr_0((\mathcal{C}_z + \mathcal{D}_{zu}\mathcal{K})\mathcal{P}(\mathcal{C}_z + \mathcal{D}_{zu}\mathcal{K})^*)$$

and the H_2 problem, in the harmonic framework, can be stated as follows: there exists $\mathcal{K}$ such that $\|\hat{\mathcal{G}}(s)\|_{H_2} < \gamma$ if

$$\begin{aligned} &tr_0((\mathcal{C}_z + \mathcal{D}_{zu}\mathcal{K})\mathcal{P}(\mathcal{C}_z + \mathcal{D}_{zu}\mathcal{K})^*) < \gamma \\ &(\mathcal{A}-\mathcal{N}+\mathcal{B}\mathcal{K})\mathcal{P} + \mathcal{P}(\mathcal{A}-\mathcal{N}+\mathcal{B}\mathcal{K})^* + \mathcal{B}_\omega\mathcal{B}_\omega^* < 0 \end{aligned}$$

By applying standard arguments (the Schur complement and a classical change of variables), the optimal solution that minimizes γ can be formulated as the following convex optimization problem

$$\begin{aligned} &\min_{\mathcal{P},\mathcal{S},\mathcal{Z}} \quad tr_0(\mathcal{Z}) \\ &\mathcal{P}^* = \mathcal{P} > 0 \\ &\begin{bmatrix} \mathcal{Z} & \mathcal{C}_z\mathcal{P} + \mathcal{D}_{zu}\mathcal{S} \\ \mathcal{P}\mathcal{C}_z^* + \mathcal{S}^*\mathcal{D}_{zu}^* & \mathcal{P} \end{bmatrix} \geq 0 \\ &(\mathcal{A}-\mathcal{N})\mathcal{P} + \mathcal{P}(\mathcal{A}-\mathcal{N})^* + \mathcal{B}\mathcal{S} + \mathcal{S}^*\mathcal{B}^* + \mathcal{B}_w\mathcal{B}_w^* \quad < 0. \end{aligned} \tag{4.29}$$

The optimal gain is given by $\mathcal{K} = \mathcal{S}\mathcal{P}^{-1}$ where $\mathcal{P}$, $\mathcal{S}$ and $\mathcal{Z}$ are TB and bounded operators on ℓ^2. Using Theorem 8 together with the identity

$$\mathrm{tr}_0(\mathcal{Z}) = \frac{1}{T}\int_0^T \mathrm{tr}(Z(t))\,dt, \quad \text{with } Z = \mathcal{F}^{-1}(\mathcal{Z}) \text{ (see Def. 5)},$$

the time-domain counterpart of the harmonic H_2 optimization problem (4.29) can be expressed as the following periodic differential convex optimization problem:

$$\min_{P,S,Z} \frac{1}{T}\int_0^T tr(Z(t))dt \tag{4.30}$$

$$\begin{aligned} &P = P' > 0 \\ &\begin{bmatrix} Z & C_zP + D_{zu}S \\ PC_z' + S'D_{zu}' & P \end{bmatrix} \geq 0 \\ &\dot{P} + AP + PA' + BS + S'B' + B_wB_w' < 0 \end{aligned} \tag{4.31}$$

where P, S, and Z are periodic unknowns belonging to $L^\infty([0,T])$. The corresponding optimal gain is then given by $K = SP^{-1}$.

4.2.2 Harmonic H_∞ optimal control

Our objective is to determine a periodic full-state feedback gain K such that the closed-loop system is stable and the H_∞-norm of the transfer function from w to z remains below a prescribed threshold γ. Before presenting the results for the system in (4.26), we first introduce the Bounded Real Lemma in an infinite-dimensional setting, specifically adapted to the harmonic framework. This formulation generalizes the classical finite-dimensional result to accommodate operators acting on infinite-dimensional Hilbert spaces.

Theorem 19 *Consider the system $\dot{X} = (\mathcal{A}-\mathcal{N})X + \mathcal{B}W$ and $Z = \mathcal{C}X$ with $\mathcal{A}$, $\mathcal{B}$ and $\mathcal{C}$ bounded on ℓ^2. If the pair $(\mathcal{A}-\mathcal{N},\mathcal{B})$ is exponentially stabilizable, then the following three statements are equivalent*

(i) $(\mathcal{A}-\mathcal{N})$ is Hurwitz and
$$\|\mathcal{C}(s\mathcal{I}-(\mathcal{A}-\mathcal{N}))^{-1}\mathcal{B}\|_\infty < \gamma$$

(ii) The following algebraic Riccati equation has a hermitian, positive semi-definite solution $\mathcal{P}$ bounded on ℓ^2 such that $\mathcal{A}-\mathcal{N}+\gamma^{-2}\mathcal{B}\mathcal{B}^*\mathcal{P}$ is Hurwitz
$$(\mathcal{A}-\mathcal{N})^*\mathcal{P} + \mathcal{P}(\mathcal{A}-\mathcal{N}) + \gamma^{-2}\mathcal{P}\mathcal{B}\mathcal{B}^*\mathcal{P} + \mathcal{C}^*\mathcal{C} = 0$$

(iii) There exists a $\tilde{\mathcal{P}}$ bounded on ℓ^2, hermitian, positive semi-definite solution to the following Riccati inequality for some real μ
$$(\mathcal{A}-\mathcal{N})^*\tilde{\mathcal{P}} + \tilde{\mathcal{P}}(\mathcal{A}-\mathcal{N}) + \gamma^{-2}\tilde{\mathcal{P}}\mathcal{B}\mathcal{B}^*\tilde{\mathcal{P}} + \mathcal{C}^*\mathcal{C} + \mu^2\mathcal{I} < 0.$$

Proof 22 *This is a direct translation of Theorem 1.1 in [70] to our harmonic setting for which $(\mathcal{A}-\mathcal{N})$ plays the rule of the infinitesimal generator of the C^0 semi-group $T(t) = e^{(\mathcal{A}-\mathcal{N})t}$ on ℓ^2-Hilbert space.*

Theorem 20 *Consider the system in (4.26) with $\mathcal{C}_y = \mathcal{I}$, $\mathcal{D}_{zw} = \mathcal{D}_{yw} = \mathcal{D}_{yu} = 0$ and let $\gamma > 0$ and $(\mathcal{Q},\mathcal{Y})$ solution of the TBLMI*

$$\begin{aligned} &\mathcal{Q} = \mathcal{Q}^* > 0 \\ &\begin{bmatrix} (\mathcal{A}-\mathcal{N})\mathcal{Q} + \mathcal{Q}(\mathcal{A}-\mathcal{N})^* + \mathcal{B}\mathcal{Y} + \mathcal{Y}^*\mathcal{B}^* & \mathcal{B}_w & (\mathcal{C}_z\mathcal{Q} + \mathcal{D}_{zu}\mathcal{Y})^* \\ \mathcal{B}_w^* & -\gamma^2\mathcal{I} & 0 \\ \mathcal{C}_z\mathcal{Q} + \mathcal{D}_{zu}\mathcal{Y} & 0 & -\mathcal{I} \end{bmatrix} < 0. \end{aligned} \tag{4.32}$$

Then, the state feedback $U = \mathcal{K}X$ with $\mathcal{K} = \mathcal{Y}\mathcal{Q}^{-1}$ ensures that the transfer function $\hat{\mathcal{G}}_{zw}$ from w to z satisfies $\|\hat{\mathcal{G}}_{zw}\|_\infty < \gamma$, and that the resulting closed-loop system is asymptotically stable.

Proof 23 *It is standard to show that, if $(\mathcal{Q},\mathcal{Y})$ is a solution of the TBLMI (4.32), then by applying the change of variables $\mathcal{Y}\mathcal{Q}^{-1} = \mathcal{K}$, $\mathcal{Q}^{-1} = \mathcal{P}$ and performing a congruence transformation with $\mathrm{diag}(\mathcal{P},\mathcal{I},\mathcal{I})$, one obtains the following equivalent inequality*

$$\begin{bmatrix} (\mathcal{A}_{cl}-\mathcal{N})^*\mathcal{P} + \mathcal{P}(\mathcal{A}_{cl}-\mathcal{N}) & \mathcal{P}\mathcal{B}_w & \mathcal{C}_{cl}^* \\ \mathcal{B}_w^*\mathcal{P} & -\gamma^2\mathcal{I} & 0 \\ \mathcal{C}_{cl} & 0 & -I \end{bmatrix} < 0$$

where $\mathcal{P} = \mathcal{P}^* \succ 0$ *and* $\mathcal{A}_{cl} = \mathcal{A} + \mathcal{B}\mathcal{K}$, $\mathcal{C}_{cl} = \mathcal{C}_z + \mathcal{D}_{zu}\mathcal{K}$. *By applying the Schur complement, the above expression can be rewritten as the following Riccati inequality*

$$(\mathcal{A}_{cl} - \mathcal{N})^*\mathcal{P} + \mathcal{P}(\mathcal{A}_{cl} - \mathcal{N}) + \gamma^{-2}\mathcal{P}\mathcal{B}_w\mathcal{B}_w^*\mathcal{P} + \mathcal{C}_{cl}^*\mathcal{C}_{cl} \prec 0. \tag{4.33}$$

According to the Bounded Real Lemma, this implies that the closed-loop system is asymptotically stable and that the corresponding transfer matrix from W *to* Z *has an* H_∞ *norm strictly less than* γ.

With these results, it is straightforward to formulate the optimal harmonic H_∞ optimization problem as the following convex optimization problem

$$\begin{aligned} &\min_{\mathcal{P},\mathcal{S},\gamma} \gamma \\ &\mathcal{P}^* = \mathcal{P} \succ 0 \\ &\begin{bmatrix} (\mathcal{A} - \mathcal{N})\mathcal{P} + \mathcal{P}(\mathcal{A} - \mathcal{N})^* + \mathcal{B}\mathcal{S} + \mathcal{S}^*\mathcal{B}^* & \star & \star \\ \mathcal{B}_w^* & -\gamma^2\mathcal{I} & \star \\ \mathcal{C}_z\mathcal{P} + \mathcal{D}_{zu}\mathcal{S} & 0 & -\mathcal{I} \end{bmatrix} \prec 0. \end{aligned} \tag{4.34}$$

where $\mathcal{P}$ and $\mathcal{S}$ are TB and bounded operators on ℓ^2. The solution to the state-feedback harmonic H_∞ optimal control problem is given by $U = \mathcal{K}X$, where $\mathcal{K} := \mathcal{S}\mathcal{P}^{-1}$. Moreover, the time-domain counterpart of the H_∞ optimization problem (4.34) is the following PDLMI based convex optimization problem

$$\min_{P,S,\gamma} \gamma \tag{4.35}$$

$$P = P' \succ 0 \tag{4.36}$$

$$\begin{bmatrix} \dot{P} + AP + PA' + BS + S'B' & \star & \star \\ B_w' & -\gamma^2 I & \star \\ C_zP + D_{zu}S & 0 & -I \end{bmatrix} \prec 0$$

where P and S are T-periodic matrix functions belonging to $L^\infty([0,T])$.

4.2.3 Reconstruction of the periodic feedback gain

The connection between robust harmonic H_2 and H_∞ problems and TBLMI is now clearly established. Even if the associated TBLMI are infinite-dimensional, they can be solved with the method developed in Chapter 3. The main idea of the current chapter is illustrated on Fig. 4.1: instead of solving a PDLMI to find the solution of the robust periodic control problem in the time-domain, the equivalent TBLMI is solved. Let $\mathbf{COP}_{\mathbf{p},\mathbf{q},\mathbf{r}}$ be the r-truncated, fully banded convex optimization problem associated with each TBLMI. If the infinite-dimensional TBLMI possesses a solution, for high enough values of p, q and r, an approximation of the former can be determined.

For harmonic control design, Theorem 1 in the preliminaries of this thesis in Chapter 1 has a fundamental consequence: a control U in the harmonic domain must be designed so that it belongs to the space H (see Def. 1). This ensures that its time domain counterpart u exists. To design a state feedback $U := \mathcal{K}X$ with a constant gain operator $\mathcal{K}$, it is proven that $\mathcal{K}$ must be a

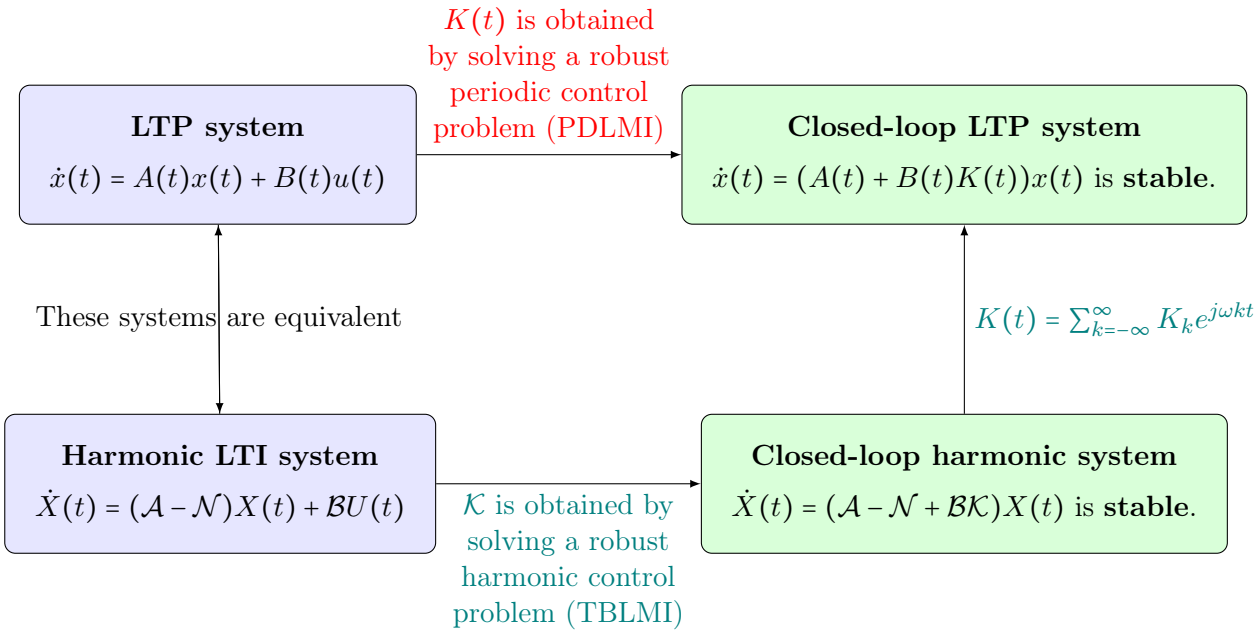

Figure 4.1: The robust periodic control problem is solved with our TBLMI framework instead of solving PDLMIs.

Toeplitz block operator [5]. Hence, u is determined by $u := Kx$ where the time-domain gain can be reconstructed from the phasors in $\mathcal{K}$ with formula (1.9):

$$K(t) = \sum_{k=-\infty}^{\infty} K_k e^{j\omega kt} \tag{4.37}$$

Moreover, to ensure controlled boundedness in the control signal u, it is imperative that $\mathcal{K}$ represents a bounded operator on ℓ^2. This condition, in accordance with Theorem 2 in the preliminaries on harmonic modeling in Chapter 1, implies that $K \in L^\infty$. Obviously, not all Fourier coefficients of K can be determined by solving $\mathbf{COP}_{\mathbf{p},\mathbf{q},\mathbf{r}}$ since the unknowns are $q-$banded. However, K is usually sufficiently regular to be described by a finite number of Fourier coefficients.

In general, a matrix inversion must be performed to obtain $\mathcal{K}$, as seen in the formula $\mathcal{K} = \mathcal{S}\mathcal{P}^{-1}$. To avoid the numerical issues associated with inverting a truncated Toeplitz matrix, it is preferable to convert $\mathcal{S}$ and $\mathcal{P}$ into their time domain formulation with (1.9), then compute $K(t) = S(t)P(t)^{-1}$. Indeed, $P(t)$ is finite-dimensional as opposed to $\mathcal{P}$, which makes its inversion numerically tractable.

The effectiveness of the TBLMI approach for solving robust harmonic control problems, even when Assumption 3 is not satisfied, is demonstrated in Section 4.3.

4.3 Illustrative examples

In this section, we illustrate the successful resolution of robust control problems with a TBLMI approach on a system that does not respect Assumption 3 and without applying regularization.

In Subsection 4.3.1, we solve an H_2 optimal control problem. In particular, we show that the feedback obtained with the proposed approach overlaps with the results of two other methods, which confirms the validity of the harmonic framework for solving robust control problems. The space and time complexity of our method is presented. In Subsection 4.3.2, the H_∞ control problem is solved. In both cases, we show that tracking of a T-periodic trajectory can be achieved with the obtained feedback gain.

We consider the example given in [14] that was identified in Chapter 2:

$$\dot{x} = \begin{pmatrix} a_{11}(t) & a_{12}(t) \\ a_{21}(t) & a_{22}(t) \end{pmatrix} x + \begin{pmatrix} b_{11}(t) \\ 0 \end{pmatrix} u \tag{4.38}$$

$$\begin{aligned}
a_{11}(t) &:= 1 + \frac{4}{\pi} \sum_{k=0}^{\infty} \frac{1}{2k+1} \sin(\omega(2k+1)t), \\
a_{12}(t) &:= 2 + \frac{16}{\pi^2} \sum_{k=0}^{\infty} \frac{1}{(2k+1)^2} \cos(\omega(2k+1)t), \\
a_{21}(t) &:= -1 + \frac{2}{\pi} \sum_{k=1}^{\infty} \frac{(-1)^k}{k} \sin(\omega k t), \\
a_{22}(t) &:= 1 - 2\sin(\omega t) - 2\sin(3\omega t) + 2\cos(3\omega t) + 2\cos(5\omega t), \\
b_{11}(t) &:= 1 + 2\cos(2\omega t) + 4\sin(3\omega t) \text{ with } \omega = 2\pi.
\end{aligned}$$

Note that a_{11}, a_{12} and a_{21} are respectively square, triangular and sawtooth signals and include an offset part. The associated TB $\mathcal{A}$ matrix has an infinite number of phasors and is not banded. This system is unstable insofar as its equivalent harmonic LTI system (4.2) is characterized by a spectrum given by the set $\sigma := \{\lambda + \mathrm{j}\omega k, k \in \mathbb{Z}\}$ where $\lambda \in \{1 \pm \mathrm{j}1.64\}$ (see [14]). The function A does not satisfy Assumption 3. Despite that, we will show that solving the TBLMI associated with H_2 and H_∞ problems can provide a stabilizing feedback for the true system even without regularizing the TBLMI entries. Indeed, banding the TBLMI entries naturally regularizes them.

4.3.1 H_2 harmonic control-LQR case

Comparison of several approaches for solving PDLMI

We consider the LQR problem whose solution can be obtained by solving the associated infinite dimensional convex optimization problem [69]:

$$\begin{aligned}
&\mathbf{LMI_1}: \max_{\mathcal{P}=\mathcal{P}^*>0} tr_0(\mathcal{P}), \quad \text{s.t.} \\
&\begin{pmatrix} (\mathcal{A}-\mathcal{N})^*\mathcal{P} + \mathcal{P}(\mathcal{A}-\mathcal{N}) + \mathcal{Q} & \mathcal{P}\mathcal{B} \\ \mathcal{B}^*\mathcal{P} & \mathcal{R} \end{pmatrix} \succeq 0
\end{aligned} \tag{4.39}$$

where the trace operator is defined by (3.12) and $\mathcal{Q}$ and $\mathcal{R}$ are the harmonic LQR weighting matrices. The matrix gain is given by $\mathcal{K} := \mathcal{R}^{-1}\mathcal{B}^*\mathcal{P}$ where $\mathcal{P}$ is a TB matrix of infinite dimension and a bounded operator on ℓ^2; see [5] for more details. We have opted for the following choices for TB weighting matrices $\mathcal{Q}$ and $\mathcal{R}$: $\mathcal{Q} := \mathcal{T}(diag([1\ 10^4]))$ and $\mathcal{R} := \mathcal{T}(Id_m)$. These values are determined through trial and error to achieve a fast response. Similar to the classical LQR problem, the purpose of these quantities is to penalize the components of the control and the state. In our context, the focus is on their phasors. As the harmonic versions of the diagonal and constant weighting matrix functions are Toeplitz block diagonal operators, all the phasors of a given component of x or u are penalized with the same weight.

To demonstrate the effectiveness of the proposed LMI formulation, we compare the results with two existing numerical methods. First, we employ the Periodic System Toolbox to solve the equivalent time-domain Periodic Differential Riccati Equation (PDRE) [36, 71]. Then, we use the Kleinman-like algorithm presented in [14] to directly solve the Harmonic Algebraic Riccati Equation (HARE) by considering the first 40 harmonics. Next, we impose the required TB structure on the unknown matrices and solve Problem $\mathbf{COP_{p,q,r}}$ associated with equations (4.39) where $p = q = r = 40$. Notably, the time-periodic gain matrix functions K obtained from all three methods exhibit perfect alignment, as shown in Fig. 4.2.

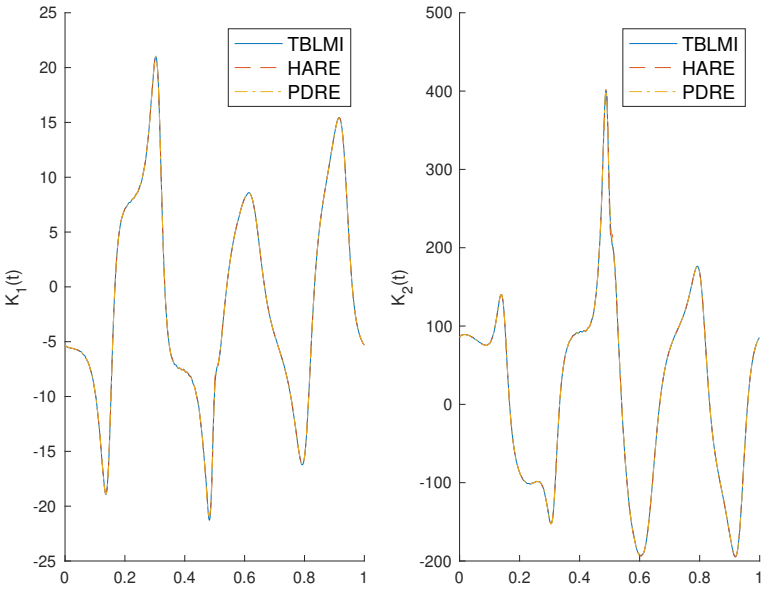

Figure 4.2: Numerical comparisons for Periodic Gain K by solving PDRE, HARE and TBLMI associated to the LQ problem

Space and time complexity

For comparison purposes, we also consider an equivalent formulation which consists in solving the following infinite-dimensional convex optimization problem [72]:

$$\mathbf{LMI_2}: \min_{\mathcal{S}=\mathcal{S}^*\succ 0,\mathcal{W}} tr_0(\mathcal{W}), \text{ s.t.} \tag{4.40}$$
$$\begin{pmatrix} (\mathcal{A}-\mathcal{N})\mathcal{S}+\mathcal{S}(\mathcal{A}-\mathcal{N})^*-\mathcal{B}\mathcal{Y}-\mathcal{Y}^*\mathcal{B}^* & \star & \star \\ \mathcal{R}^{\frac{1}{2}}\mathcal{Y} & -\mathcal{I} & \star \\ \mathcal{Q}^{\frac{1}{2}}\mathcal{S} & 0 & -\mathcal{I} \end{pmatrix} \preceq 0$$
$$\begin{pmatrix} \mathcal{W} & \mathcal{I} \\ \mathcal{I} & \mathcal{S} \end{pmatrix} \succ 0$$

With this formulation, the matrix gain is given by $\mathcal{K} := \mathcal{Y}\mathcal{S}^{-1}$. Finally, the LQR problem can also be solved through a harmonic H_2 problem formulation provided by (4.29) with $\mathcal{C}_z := [\mathcal{Q}^{\frac{1}{2}}; 0]$,

$\mathcal{C}_y := \mathcal{I}$, $\mathcal{D}_{zu} := [0; \mathcal{R}^{\frac{1}{2}}]$ and $\mathcal{D}_{zw} = \mathcal{D}_{yw} = \mathcal{D}_{yu} := 0$. In the sequel, we refer to this problem as **LMI** H_2. Imposing as required a TB structure to the unknown matrices, we solve Problem

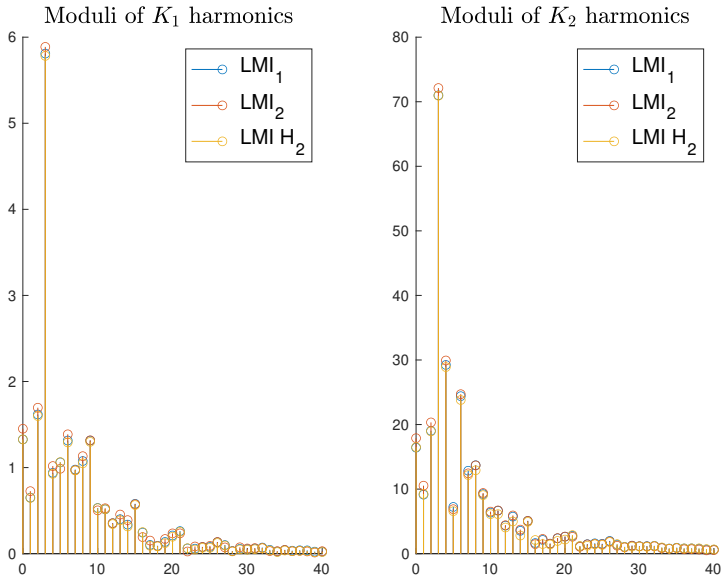

Figure 4.3: Moduli of harmonics of $K = [K_1, K_2]$ for Problem $\mathbf{COP_{p,q,r}}$ associated to (4.39), (4.40) and (4.29) with $r = 40$, $p = 2r$ and $q = r$.

$\mathbf{COP_{p,q,r}}$ associated with problems $\mathbf{LMI}_1$ (4.39), $\mathbf{LMI}_2$ (4.40), and **LMI** H_2 (4.29). Specifically, the truncation order is fixed to $r = 40$, the band size of the entries is fixed to $p = 2r$, and finally the band size of the unknowns is fixed to $q = r$.

With these choices and taking advantage of the TB structure, if $n = 2$ denotes the dimension of the state and $m = 1$ the dimension of the control, the number of scalar unknowns are respectively $\frac{n(n+1)}{2}(2q+1) = 245$, $(n(n+1)+nm)(2q+1) = 405$ and $(nm + \frac{n(n+1)}{2} + \frac{nm(nm+1)}{2})(2q+1) = 648$ for problems (4.39), (4.40) and (4.29). The computation times required to obtain solutions for these three problems are as follows: $T_{comp} = 15.1s$, $64.8s$ and $44.2s$ respectively. In summary, the number of unknowns increases linearly with respect to the number of harmonics q to be taken into account.

For this substantial truncation order of $r = 40$, Fig. 4.3 displays the magnitudes of the phasors within $\mathcal{K} = [\mathcal{K}_1, \mathcal{K}_2]$. As evident from the plot, the solutions of these three problems align closely, demonstrating a high degree of accuracy and consistency between these three formulations.

Regarding the computation times for solving (4.39) with different truncation orders $r = 10, 20, 30$, we have the following respective times: $T_{comp} = 0.56s, 2.3s, 7.6s$. Meanwhile, when dealing with the H_2 problem formulation (4.29), we obtain the following times: $T_{comp} = 1.1s, 4.8s, 15.3s$ for the same values of r. To illustrate the convergence of our scheme with the order of truncation, we visualize in Fig. 4.4 and Fig. 4.5 the $T-$periodic gain matrix $K(t)$ over a period T for increasing values of $r = 10, 20, 30$. Notably, the results obtained for both optimization problems exhibit substantial similarity for $r = 20, 30$. However, it is worth mentioning that for $r = 10$, the solution obtained by solving (4.29) lacks accuracy and can be discarded.

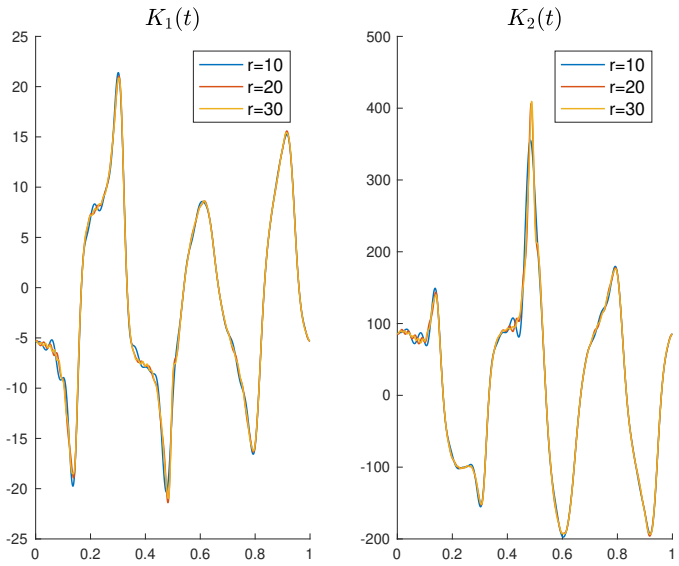

Figure 4.4: T-periodic gain $K(t)$ over a period $T = 1$ for Problem (4.39)

.

Tracking of a T-periodic trajectory

Any pair $(x_{ref}(t), u_{ref}(t))$ defining a $T-$periodic trajectory of the system (4.38) corresponds to an equilibrium for its associated harmonic system. Namely, $(X_{ref}, U_{ref}) := \mathcal{F}(x_{ref}(t), u_{ref}(t))$ satisfies the harmonic equilibrium equation

$$0 = (\mathcal{A} - \mathcal{N})X_{ref} + \mathcal{B}U_{ref}. \tag{4.41}$$

The control law given by:

$$u(t) := u_{ref}(t) - K(t)(x(t) - x_{ref}(t))$$

where $K(t)$ is the $T-$periodic gain matrix defined as $K(t) := \sum_{k=-n_k}^{n_k} K_k e^{j\omega kt}$ (with n_k representing the degree of the numerically obtained TB matrix $\mathcal{K}$), effectively stabilizes the unstable LTP system (4.38) both globally and asymptotically on its reference trajectory x_{ref}, thanks to the equivalence provided by Theorem 4 in [5].

To illustrate this, we visualize the closed-loop response for three $T-$periodic reference trajectories (x_{ref}, u_{ref}) in Fig. 4.6. We begin with $(x_{ref}(t), u_{ref}(t)) := (0, 0)$ for $t < 2$. Subsequently, for $2 \leq t < 4$, we set $u_{ref}(t) := 4\cos(2\pi t)$ and solve (4.41) to determine x_{ref}. For $t \geq 4$, we introduce a desired steady state X_d defined as $\mathcal{F}^{-1}(X_d)(t) := (\frac{1}{4}\cos(2\pi t), 0)$ and seek the nearest harmonic equilibrium. This involves solving the minimization problem $\min_{U_{ref}} |X_d - X_{ref}|^2$ subject to (4.41). It is evident from Fig. 4.6 that the provided state feedback enables tracking of any $T-$periodic trajectory associated with any equilibrium of (4.41).

4.3.2 H_∞ harmonic control

Now, let us consider solving the H_∞ optimal full-state feedback problem. In the context of H_∞ constraints, our objective is to minimize the maximum singular value of the harmonic transfer

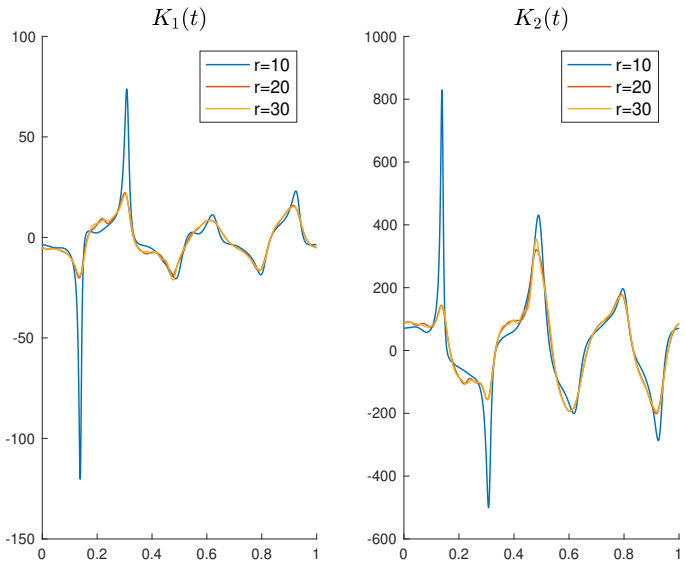

Figure 4.5: T-periodic gain $K(t)$ over a period $T = 1$ for Problem (4.29)

function between the input vector W and the output vector $Z := (\mathcal{Q}^{\frac{1}{2}}X, \mathcal{R}^{\frac{1}{2}}U)$. To achieve this, we set $\mathcal{B}_w := \mathcal{B}$, $\mathcal{C}_z := \begin{pmatrix} \mathcal{I} & 0 \\ 0 & 10^2\mathcal{I} \\ 0 & 0 \end{pmatrix}$, $\mathcal{D}_{zw} := 0$ and $\mathcal{D}_{zu} := (0, 0, \mathcal{I})^T$.

Similar to the previous case, we solve Problem $\mathbf{COP_{p,q,r}}$ associated with (4.34), but this time we choose $r = 10, 20, 30$, with $p = \frac{r}{2}$ and $q = r$. It is worth noting that in this configuration, we have intentionally set p to be much smaller than in the previous example. This adjustment ensures that we obtain a practical solution even for smaller values of r. Fig. 4.7 and 4.8 depict the computed magnitudes of gain-phasors and the computed values of $K(t)$ over a period T, respectively for increasing values of r.

Finally, for the same reference trajectories, Fig. 4.9 presents the closed-loop response. It is evident that the solution obtained for $r = 10$ does not accurately track the reference trajectories. This discrepancy is primarily attributed to the fact that not enough phasors have been taken into account in the approximation of $\mathcal{A}$ by $\mathcal{A}_{b(p)}$ with $p = 5$.
Even though H_∞ optimal control aims to minimize the worst-case scenario, represented here as:

$$\sup_{\|W\|_{\ell^2}=1} \|Z\|_{L^2} = \sup_{\|W\|_{\ell^2}=1} \Big(\int_0^{+\infty} X^*\mathcal{Q}X + U^*\mathcal{R}U\,dt \Big)^{\frac{1}{2}},$$

the obtained gain is approximately the same as the one obtained for the LQR control problem. This similarity suggests that the LQR control meets our H_∞ criterion effectively. This observation can be rationalized as follows: as detailed in [73], the optimal solution to the H_∞ problem for $\mathcal{C}_y := \mathcal{I}$, $\mathcal{D}_{yu} = \mathcal{D}_{yw} = \mathcal{D}_{zw} := 0$ and $\mathcal{C}_z := \mathcal{H}$, $\mathcal{D}_{zu} := \mathcal{I}$ satisfies the Riccati equation:

$$(\mathcal{A} - \mathcal{N})^*\mathcal{P} + \mathcal{P}(\mathcal{A} - \mathcal{N}) - \mathcal{P}(\mathcal{B}\mathcal{B}^* - \frac{1}{\gamma^2}\mathcal{B}_w\mathcal{B}_w^*)\mathcal{P} + \mathcal{H}^*\mathcal{H} = 0.$$

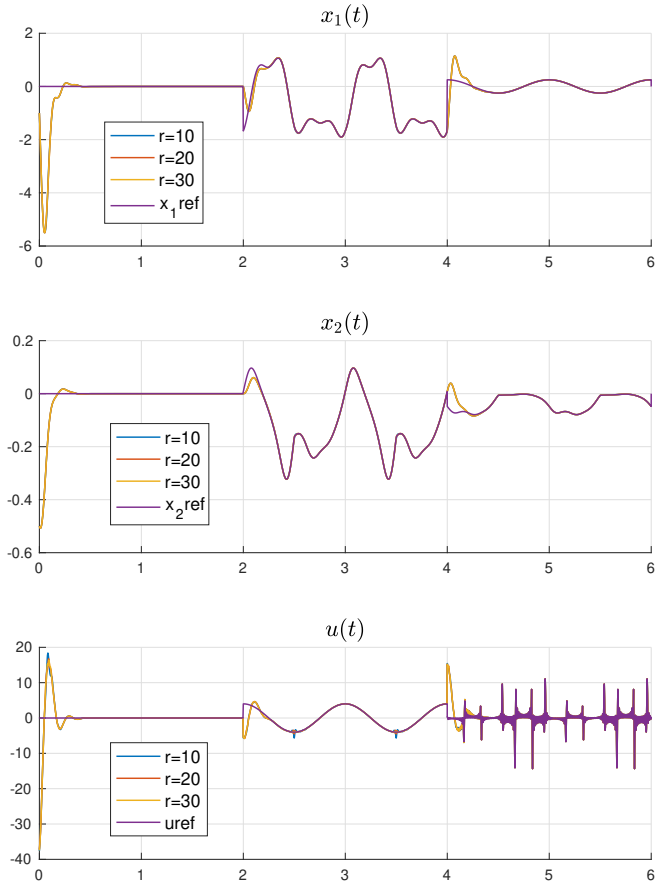

Figure 4.6: Closed-loop response with harmonic LQ control achieved by solving (4.39) for $r = 10, 20, 30$.

In our case, as $\mathcal{H} := \mathcal{Q}^{\frac{1}{2}}$ and $\mathcal{B}_w := \mathcal{B}$, we get:

$$(\mathcal{A} - \mathcal{N})^*\mathcal{P} + \mathcal{P}(\mathcal{A} - \mathcal{N}) - (1 - \frac{1}{\gamma^2})\mathcal{P}\mathcal{B}\mathcal{B}^*\mathcal{P} + \mathcal{Q} = 0.$$

Given that the obtained optimal value for γ is approximately $\gamma \approx 574$, $1 - \frac{1}{\gamma^2} \approx 1$ and we can conclude, drawing on the continuity of the Riccati solution with respect to its parameters, that the H_∞ solution closely aligns with the LQR solution, given that we have set $\mathcal{R} := \mathcal{I}$.

4.4 Conclusion

In this chapter, we have introduced a TBLMI-based framework for harmonic robust control design. This novel framework enables the formulation of robust control problems for harmonic systems as semidefinite optimization problems, akin to those encountered in classical LTI systems. Given that harmonic systems are infinite dimensional, some notions related to robust control are

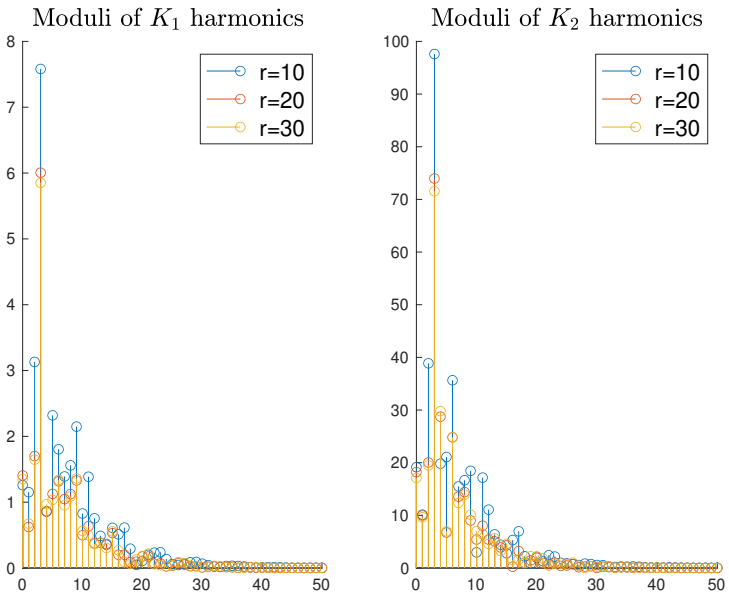

Figure 4.7: Moduli of gain-phasors $K = [K_1, K_2]$(Harmonic H_∞)

redefined in the context of harmonic systems. The associated optimization problems are solved numerically with the consistent truncation method proposed in Chapter 3. The equivalence between LTP and harmonic systems means that any harmonic controller obtained by solving a harmonic robust problem can be converted into the time-domain solution of the equivalent periodic robust control problem. Illustrations are provided for both H_2 and H_∞ harmonic robust control problems.

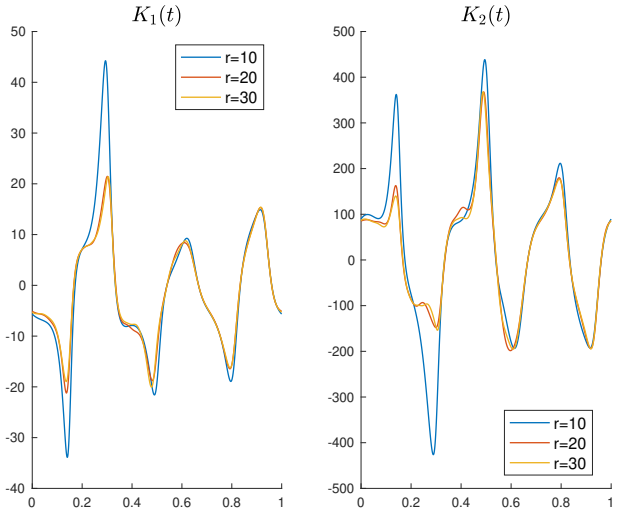

Figure 4.8: T-periodic gain $K(t)$ over a period $T = 1$(Harmonic H_∞)

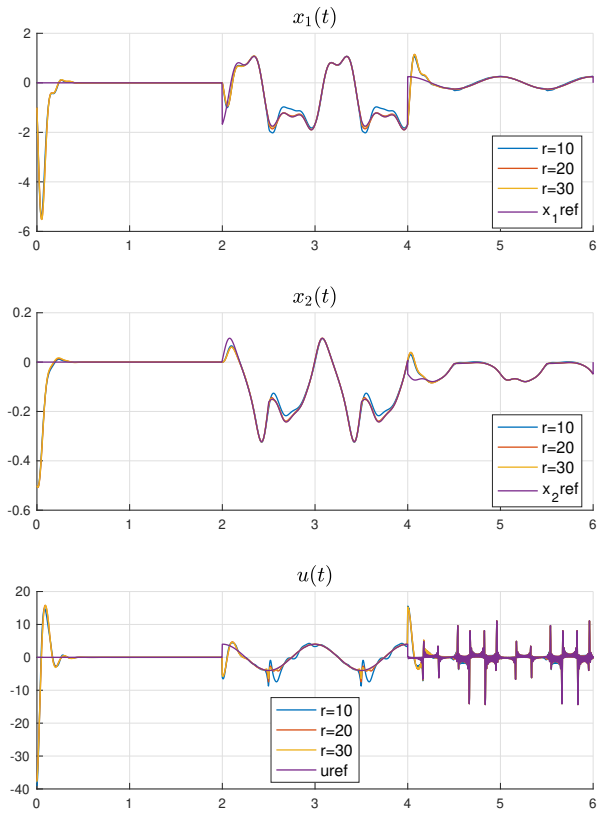

Figure 4.9: Closed loop response with optimal harmonic H_∞ control for $r = 10, 20, 30$

Conclusion and perspectives

Summary of the contributions

This thesis proposes a harmonic framework for identification and control of continuous-time linear time-periodic (LTP) systems. The identification and control of LTP systems is a valuable area of research given that these systems have many industrial applications, including in wind turbines, satellites, and power electronics. However, the time-varying nature of LTP systems makes their study more challenging than linear time-invariant (LTI) systems. Harmonic modeling is an interesting alternative to time-domain representations for studying LTP systems. Indeed, the periodic nature of the latter can be exploited to derive an equivalent LTI representation. This model is called a harmonic model because it describes the interactions between the harmonics of the system. However, the harmonic model is infinite-dimensional. Therefore, in this thesis, we developed identification and control methods in the harmonic framework that rigorously deal with the problems resulting from this infinite dimension.

Most existing methods for LTP system identification require strong hypotheses such as stability of the open-loop system, reaching steady state or choosing input signals that exhibit a specific form. Moreover, many methods apply to discrete-time systems despite continuous-time systems having a direct physical interpretation. This led us to introduce an identification method for continuous-time LTP systems, which does not assume system stability and can exploit input/state data from transient dynamics. We exploited the Toeplitz structure and time-invariant nature of harmonic models to reformulate the problem of identifying an LTP model to that of computing the phasors that characterize the state and input matrices of the equivalent harmonic system. Since the harmonic model displays a theoretically infinite dimension, the identification problem must be simplified to become numerically tractable. Most notably, the derivative of the harmonic state variable exhibits a special form, which leads to a redundancy of information in its components. This implies that the identification problem can be restricted to the central band of the harmonic system corresponding to the 0-th phasor $\dot{X}_0$ and that the state derivative $\dot{x}$ is not required to be estimated at any point of the method. Under regularity assumptions on the LTP system matrices, a finite-dimensional linear least-squares problem can be solved to determine the non-negligible phasors that describe the system. Convergence of the solution of this finite-dimensional problem to the solution of the original infinite-dimensional identification problem is then proven to be achieved up to an arbitrarily small error. The proposed method was shown to be efficient even when the data used in the least-squares algorithm are affected by noise.

The literature review on resolution of Periodic Differential LMIs (PDLMIs) and Toeplitz Block LMIs (TBLMIs) has revealed that solving such LMIs is a challenging problem and requires limiting assumptions such as discretization, approximation, or availability of a Floquet decomposition of the system. We proved that these LMIs are equivalent since PDLMIs can be

transformed into TBLMIs in the harmonic domain. While the algebraic structure of the latter allows to circumvent the previous numerical issues and assumptions, the infinite dimension of these TBLMIs must be dealt with carefully. We exploited the Toeplitz structure of these LMIs to provide a novel approach to solve these semidefinite optimization problems with provable convergence guarantees. The method relies on a truncation operator that takes into account the fact that $(\mathcal{AB})_r \neq \mathcal{A}_r\mathcal{B}_r$, namely the truncation of the product of two infinite-dimensional Toeplitz matrices is not equal to the product of the truncations of both factors. Each product that appears in the TBLMI is truncated with this truncation operator, leading to a finite-dimensional problem. This well-posed truncation is necessary for the method to be consistent, with the solution of the truncated problem converging to the true solution. Similarly to the identification framework, regularity assumptions are theoretically necessary to provide convergence guarantees. However, even if the TBLMI entries are not smooth enough, a regularization approach can be applied on them to achieve practical convergence. The truncation method proposed in our work allows to transform the problem of solving infinite-dimensional TBLMIs into a numerically tractable problem. In particular, only a finite number of phasors are retained in the entries of the TBLMI, and the constraints are truncated to become finite dimensional. In addition, we look for Toeplitz block solutions that are banded. Once the solution of a TBLMI has been estimated, the solution of its equivalent PDLMI can be deduced from the Fourier coefficients of the former.

Since PDLMIs are prevalent in analysis and control problems of LTP systems, being able to solve them indirectly is a crucial result. Following the introduction of this novel method for solving PDLMIs through a harmonic formulation, periodic control problems can be mapped to the harmonic domain to benefit from an LTI framework. There, solving harmonic H_2 and H_∞ robust control problems involves the resolution of infinite-dimensional semidefinite optimization problems. The resulting TBLMIs can be made numerically tractable through the previously introduced truncation method. Moreover, the resulting harmonic feedback gain $\mathcal{K}$ is equivalent to a periodic feedback gain $K(t)$ in the time domain. This equivalence allows to formulate control problem for LTP systems as LTI robust control problems, for which classical LTI methods apply. Many analysis and control problems for LTP systems can be formulated as TBLMIs, which highlights the relevance of a numerically tractable resolution approach. In this thesis, the effectiveness of the harmonic approach is demonstrated on LQR, H_2 and H_∞ problems. The examples presented emphasized the importance of selecting sufficiently high truncation orders when solving TBLMIs. Indeed, if the order of truncation is too low, it can happen that the solution to the truncated optimization problem cannot reach the control objectives due to a lack of precision. However, the larger the truncation order, the greater the numerical complexity associated with the resolution of TBLMIs. Therefore, a balance must be struck between the precision of the solution and computational complexity to achieve satisfactory control performance.

To conclude, the main contributions of this thesis are the following:

- A harmonic identification method for LTP systems.
- A consistent truncation method for solving infinite-dimensional TBLMIs.
- A harmonic approach for the resolution of robust control problems for LTP systems.

Perspectives

While this thesis has advanced the theoretical and practical foundations for the identification and control of LTP systems, it also opens several new avenues for exploration. The transition from complex problems in the time domain to harmonic-domain formulations provides a fertile ground for future research, ranging from fundamental theory to industrial applications.

Identification

The least-squares identification problem defined in Chapter 2 allows the phasors of the true system to be recovered exactly when the data are unaffected by noise. While we conducted an empirical study on the effects of noise on the harmonic identification method, a promising area for future research would be a theoretical analysis of noise. The model uncertainty due to noise could be derived from the data and knowledge of noise characteristics associated with industrial processes. A limiting assumption of the identification framework that was proposed in this thesis is the requirement for state data in order to formulate the least-squares problem for identification. In many practical scenarios, the state is not directly measured. Consequently, a natural extension of this work is the development of input/output identification schemes within the harmonic framework. For instance, the concept of observability could be exploited to reconstruct the harmonic state signal from output data. Indeed, it is well-known that observers for LTP systems can be determined from the solution of a PDLMI similar to the one that appears in control problems, due to the duality between the two notions. Furthermore, while Chapter 2 only considered the case of a constant period T, many physical systems are characterized by a slowly varying period. For instance, this is the case for variable-speed wind turbines. Therefore, extending the current least-squares formulation to accommodate a time-varying fundamental frequency would significantly broaden its applicability. The identification method could also be extended to more general classes of periodic systems, not necessarily linear. Finally, validating these methods against experimental data remains to be done.

Control

Undoubtedly, the scope of the harmonic control framework proposed in Chapter 4 can be extended so that its full potential is reached. Future work should focus on structured uncertainty and designing optimal controllers for periodic systems subject to polytopic or norm-bounded perturbations. A particularly promising direction is the adaptation of classical loop-shaping methods to the harmonic domain. A certain form could be imposed on the phasors of the feedback so that desired performance specifications are satisfied. Additionnally, applications that require solving PDLMIs such as output feedback design or control of time-delay periodic systems could be solved with this framework. PDLMIs concern a wide range of analysis and synthesis problems for periodic systems. Computation time is not a drawback as demonstrated by the numerical results that have been obtained using Matlab and a standard computer. The main limitation appears to be the assumption that the time period T is constant. Adaptive harmonic control laws could be considered for systems with time-varying periods $T(t)$, with applications in power systems and drives.

Model reduction

The trade-off between model accuracy and computational burden is a recurring theme in harmonic analysis. In Chapter 2, the degree of the system, namely the order of the last non-vanishing

phasor, was assumed to be known a priori. A valuable research objective would be the development of data-driven order-selection criteria to determine the minimum number of Fourier coefficients required for a given control objective. If a model of the LTP system is known, it could also be advantageous to approximate this model so that the complexity associated with the TBLMIs that arise in control problems is reduced without sacrificing closed-loop stability. For instance, a system with a theoretically infinite degree or high degree could be well-approximated by a system characterized by a lower number of Fourier coefficients. For control purposes, a bound on the truncation error due to neglecting higher-order phasors could be computed as long as the system matrices are regular enough. The neglected higher-order harmonics would therefore be considered as unmodeled dynamics, allowing for the design of robust controllers that specifically target these known model uncertainties.

A

Systems identified in Chapter 2

A.1 Example 2.3.1: a system with a finite degree

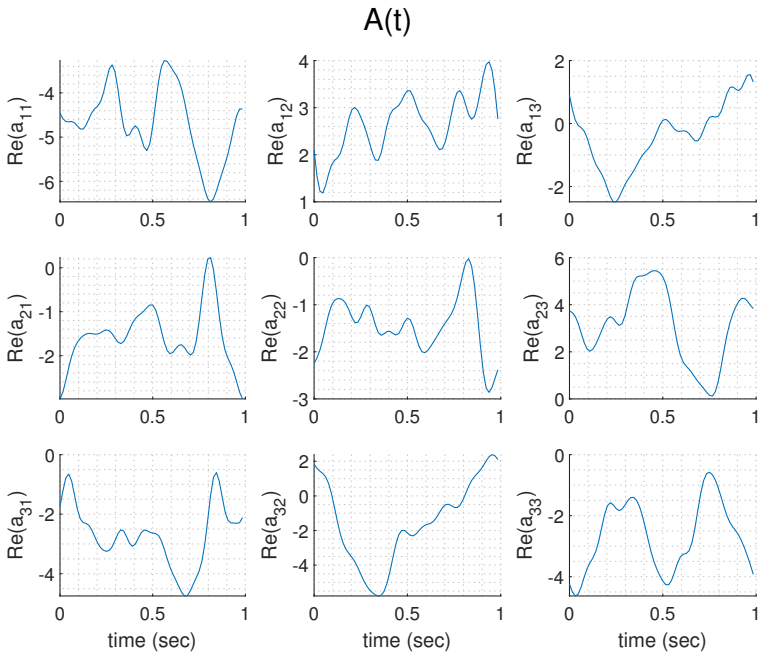

Figure A.1: $A(t)$ in Example 2.3.1

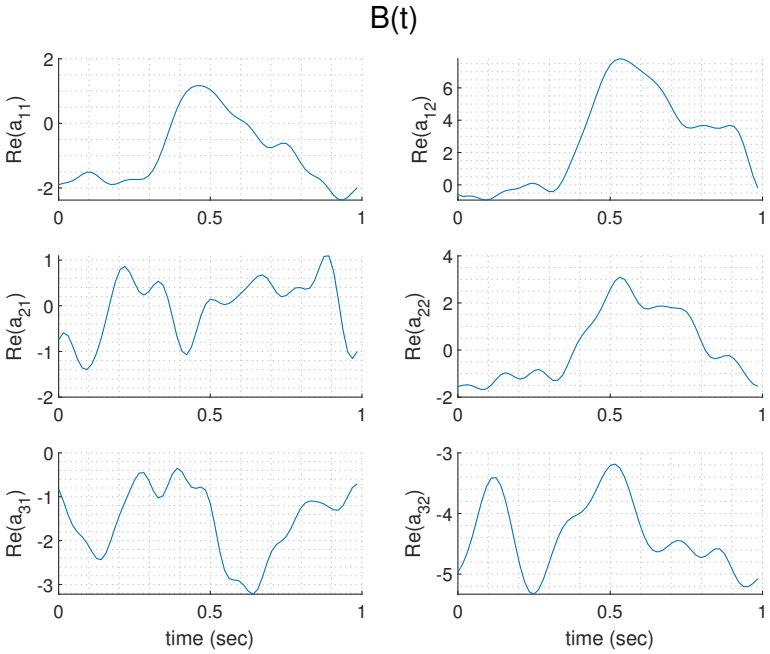

Figure A.2: $B(t)$ in Example 2.3.1

A.2 Example 2.3.2: a system with an infinite degree

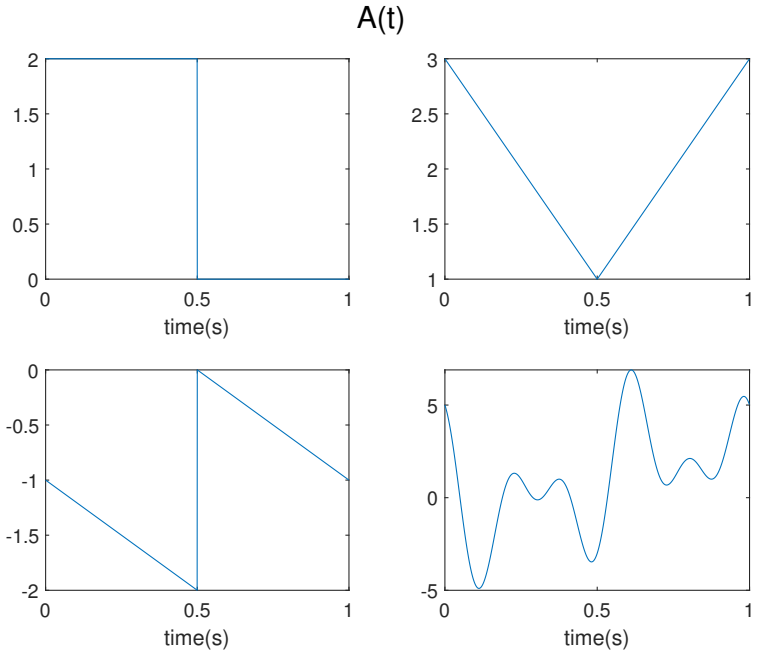

Figure A.3: $A(t)$ in Example 2.3.2

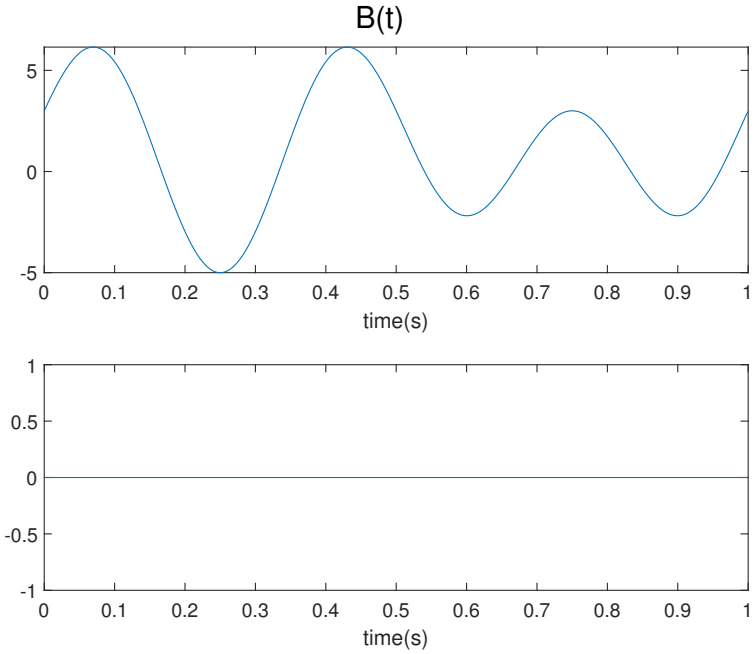

Figure A.4: $B(t)$ in Example 2.3.2

A.3 Example 2.3.3: a wind turbine

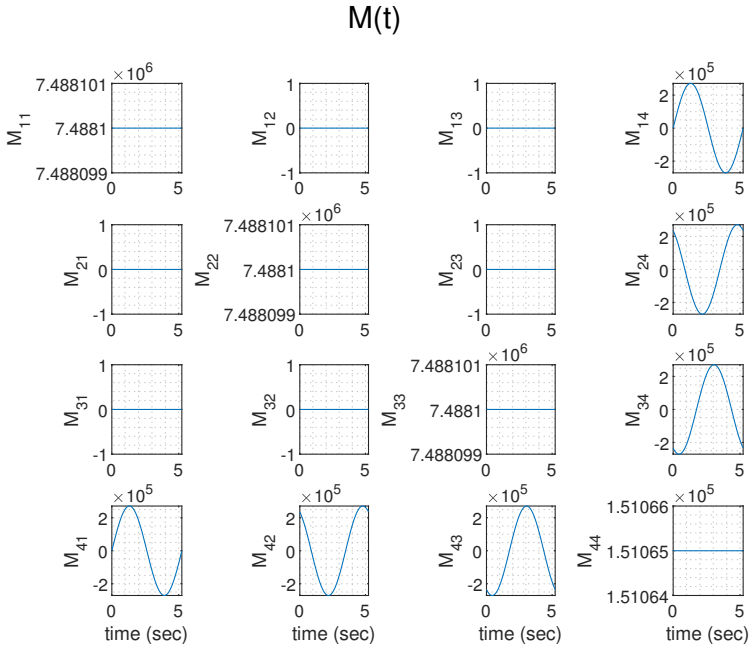

Figure A.5: $M(t)$ in Example 2.3.3

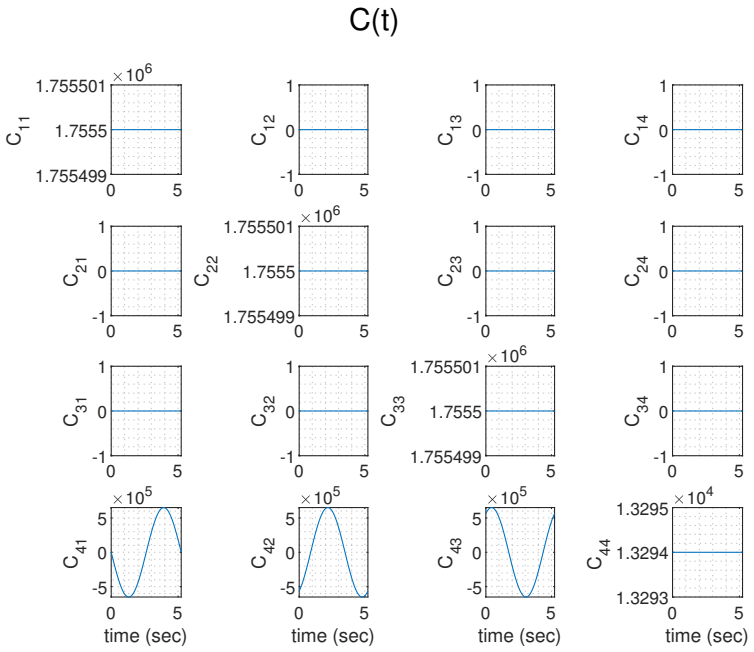

Figure A.6: $C(t)$ in Example 2.3.3

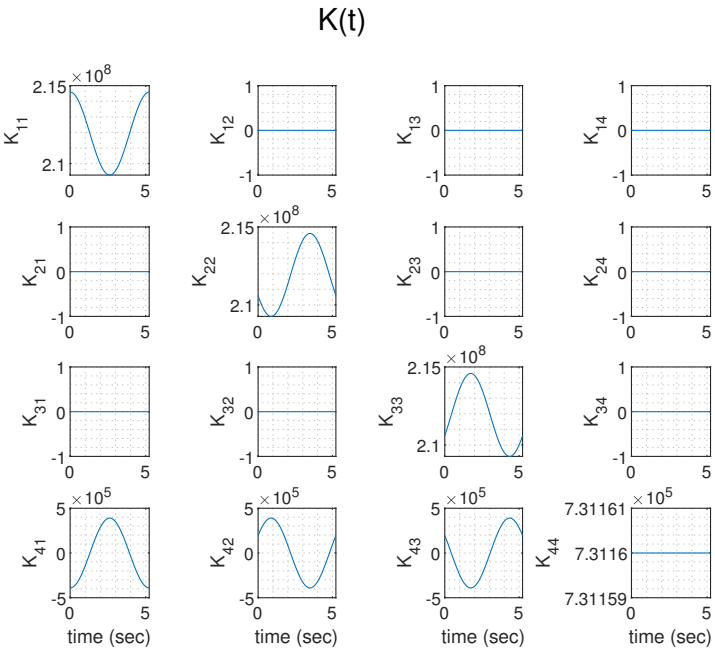

Figure A.7: $K(t)$ in Example 2.3.3

B

Résumé détaillé en français

De nombreux phénomènes physiques et biologiques présentent une nature périodique [1,4]. C'est le cas notamment des vibrations mécaniques des moteurs automobiles et des oscillations des circuits électriques [2, 3]. Puisque la périodicité est une caractéristique omniprésente dans de nombreux domaines de l'ingénierie et des sciences, il est essentiel de comprendre, analyser et contrôler ces comportements périodiques dans le but de garantir la stabilité de tels systèmes et d'optimiser leurs performances. Parmi les applications possibles, on peut citer le contrôle des hélicoptères en vol horizontal, la réduction de l'usure des éoliennes et le positionnement par satellites.

Bien que de nombreux systèmes physiques soient intrinsèquement non linéaires, il est possible de les approcher par des systèmes linéaires périodiques (LTP) en les linéarisant le long d'une trajectoire périodique [3]. Les systèmes LTP constituent une sous-classe des systèmes linéaires variant dans le temps, avec la particularité que leurs paramètres évoluent de manière périodique. De ce fait, ils sont plus complexes que les systèmes linéaires invariants dans le temps (LTI), mais leur structure périodique permet d'exploiter la théorie de Floquet pour analyser leurs propriétés. Cependant, bien que la théorie de Floquet apporte des informations sur la stabilité des systèmes périodiques, elle n'est pas constructive pour la synthèse de lois de commande.

La modélisation harmonique est une alternative fréquentielle à la théorie de Floquet pour l'étude des propriétés des systèmes LTP. La décomposition de Fourier glissante (SFD) permet de transformer un système LTP en un système LTI équivalent, appelé système harmonique. Ce dernier décrit le comportement des harmoniques des signaux qui caractérisent le système au cours du temps. Les harmoniques sont omniprésents dans les réseaux électriques, les télécommunications, les systèmes mécaniques et les dispositifs électroniques. Le modèle harmonique permet d'analyser les interactions entre les harmoniques des signaux étudiés. Comprendre ces interactions est crucial pour obtenir des performances et une robustesse satisfaisantes dans les applications de commande.

Cette thèse repose sur l'hypothèse que de nombreux problèmes complexes dans le domaine temporel, tels que l'identification et la commande robuste des systèmes LTP, ainsi que la résolution des inégalités matricielles linéaires (LMIs) différentielles périodiques, peuvent être transformés en problèmes équivalents dans le domaine harmonique. En effet, le système LTP peut être remplacé par un système invariant dans le temps, ce qui permet de contourner les difficultés posées par un modèle variant dans le temps. Cependant, le système LTI harmonique résultant est de dimension infinie, ce qui implique qu'une étape intermédiaire est nécessaire pour

traiter rigoureusement cette dimension infinie. Cette thèse adapte les méthodes traditionnelles d'identification et de commande robuste des systèmes LTI au cadre harmonique en proposant des approches de troncature et d'approximation pour résoudre des problèmes de dimension infinie.

B.1 Préliminaires sur la modélisation harmonique

La modélisation harmonique repose sur la transformation d'un signal temporel $x \in L^2_{loc}(\mathbb{R}, \mathbb{C}^n)$ par la décomposition de Fourier glissante (SFD) sur une fenêtre de longueur T. Le k-ième phaseur $X_k(t) \in \mathbb{C}^n$ est défini par :

$$X_k(t) := \frac{1}{T} \int_{t-T}^{t} x(\tau) e^{-j\omega k\tau} d\tau \tag{B.1}$$

où $\omega = \frac{2\pi}{T}$. La SFD de x est alors donnée par $X := \mathcal{F}(x) = (\cdots, X_{-1}, X_0, X_1, \cdots)$, qui contient une infinité de phaseurs. Pour une fonction T-périodique matricielle A, on définit la transformation Toeplitz comme la matrice Toeplitz par blocs (se dit *Block Toeplitz* en anglais donc on l'abrège par BT) suivante:

$$\mathcal{A} := \mathcal{T}(A) = \begin{bmatrix} \ddots & & \vdots & & \iddots \\ & A_0 & A_{-1} & A_{-2} & \\ \cdots & A_1 & A_0 & A_{-1} & \cdots \\ & A_2 & A_1 & A_0 & \\ \iddots & & \vdots & & \ddots \end{bmatrix}, \tag{B.2}$$

où $(A_k)_{k\in\mathbb{Z}}$ sont les phaseurs de A. Comme A est périodique, ses phaseurs sont constants et correspondent à des coefficients de Fourier.

Un système LTP est décrit par une équation d'état de la forme

$$\dot{x}(t) = A(t)x(t) + B(t)u(t), \tag{B.3}$$

où A et B sont des fonctions T-périodiques. L'application de la SFD permet de transformer ce type de systèmes en le système LTI harmonique suivant:

$$\dot{X}(t) = (\mathcal{A} - \mathcal{N})X(t) + \mathcal{B}U(t) \tag{B.4}$$

où $\mathcal{A} := \mathcal{T}(A)$, $\mathcal{B} := \mathcal{T}(B)$ et $\mathcal{N} := diag(\mathrm{j}\omega k \otimes Id_n,\ k \in \mathbb{Z})$ est une matrice diagonale issue du calcul de $\mathcal{F}(\dot{x})$. Comme il y a une infinité de phaseurs qui apparaissent avec la SFD, ce système est de dimension infinie.

La formulation BT est adoptée dans ce manuscrit pour tout ce qui concerne l'identification car elle permet de regrouper les phaseurs de même ordre. En revanche, pour le contrôle, il semble plus naturel de considérer des matrices à blocs Toeplitz (se dit *Toeplitz Block* en anglais donc on l'abrège par TB) afin de conserver une structure proche du domaine temporel. En effet, si $x = (x_1, \cdots, x_n)$, alors définir sa SFD comme $X := \mathcal{F}(x) = \big(\mathcal{F}(x_1), \cdots, \mathcal{F}(x_n)\big)$ permet de conserver le même ordre dans le domaine harmonique. Il est possible de passer d'une représentation à l'autre avec une transformation appropriée.

B.2 Identification des systèmes LTP

Les méthodes d'identification pour les systèmes LTP consistent en général à identifier un ou plusieurs systèmes LTI à partir desquels un modèle du système LTP associé peut être déduit. Ces méthodes s'appliquent principalement aux systèmes discrets. Par exemple, une approche appelée *lifting* consiste à concaténer des trajectoires du système LTP discret sur une période afin d'obtenir un système LTI équivalent de dimension plus élevée mais finie [17, 18]. Cette approche est souvent accompagnée d'une méthode d'identification des sous-espaces [18, 21–24]. Dans le cas des systèmes continus, le lifting nécessite un échantillonnage [19] et mène à d'autant plus de systèmes LTI que la fréquence d'échantillonnage est élevée. Une approche fréquentielle reposant sur la fonction de transfert harmonique [32] est possible, mais nécessite de faire attention au choix des entrées [34]. Dans [30], les coefficients de Fourier qui caractérisent le système LTP sont identifiés à partir des transformées de Fourier des entrées et états à différentes fréquences. Cependant, cette méthode nécessite que le régime permanent soit atteint, donc que le système soit stable en boucle ouverte.

Dans le chapitre 2, nous présentons une nouvelle méthode d'identification des systèmes LTP à partir de données échantillonnées d'état/entrée. Cette méthode a de nombreux avantages: elle ne nécessite pas de connaître la dérivée de l'état x ou d'atteindre le régime permanent, et elle s'applique aux systèmes instables. Si la période T d'un système LTP du type (B.3) est connue, identifier un modèle revient à déterminer les coefficients de Fourier associés aux fonctions A et B car on a:

$$A(t) = \sum_{k=-\infty}^{\infty} A_k e^{\mathbf{j}\omega kt} \ a.e. \quad B(t) = \sum_{k=-\infty}^{\infty} B_k e^{\mathbf{j}\omega kt} \ a.e. \tag{B.5}$$

Or, ces coefficients de Fourier apparaissent également dans les matrices Toeplitz $\mathcal{A}$ et $\mathcal{B}$ dans le modèle d'état harmonique (B.4). Ainsi, identifier les phaseurs $(A_k)_{k\in\mathbb{Z}}$ et $(B_k)_{k\in\mathbb{Z}}$ qui caractérisent un système LTP revient à identifier le système harmonique équivalent, qui est invariant dans le temps mais de dimension infinie. Nous démontrons que ce problème d'identification de dimension infinie peut être réduit à un problème des moindres carrés de dimension finie. Sous certaines hypothèses de régularité, nous démontrons que la solution du problème tronqué converge vers la solution du problème de dimension infinie avec une erreur arbitrairement petite. Notre méthode d'identification est validée sur plusieurs exemples, qui illustrent notamment sa robustesse face au bruit.

B.3 Résolution des TBLMIs de dimension infinie

Les équations de Riccati et les inégalités matricielles linéaires (LMIs) sont des outils complémentaires pour le contrôle des systèmes. Les LMIs présentent l'avantage d'offrir un cadre plus souple pour résoudre des problèmes de contrôle robuste et d'optimisation multi-objectifs, et leur application est standard pour les systèmes LTI. Cependant, les LMIs à traiter dans le cas des systèmes LTP sont périodiques et différentielles (PDLMIs), ce qui les rend plus difficiles à résoudre. En particulier, puisque ces PDLMIs sont définies sur une période, cela signifie qu'il y a une infinité de contraintes à vérifier. La plupart des méthodes se concentrent sur les équations différentielles périodiques (PDEs) plutôt que sur les LMIs. En effet, la solution d'une PDE s'écrit comme la solution d'une équation différentielle ordinaire (ODE) périodique [38]. Il est courant d'intégrer numériquement cette ODE pour trouver la solution de la PDE associée. Cependant, puisque cette ODE représente un système Hamiltonien, elle est instable et nécessite de prendre

des précautions [36, 38, 40] afin d'éviter que l'erreur d'intégration explose. Seule la méthode présentée dans [37] s'intéresse à la résolution des PDLMIs. L'idée est de remplacer la solution et sa dérivée par leur série de Fourier tronquée, puis de déterminer les coefficients de Fourier qui permettent de satisfaire la PDLMI à certains instants sur une période. Toutefois, la dimension du problème à résoudre augmente avec la fréquence d'échantillonnage. Pour éviter ces problèmes d'intégration et d'échantillonnage, il est possible de transformer les PDEs en équations harmoniques, ce qui permet de passer d'un problème différentiel à un problème algébrique avec une structure Toeplitz. Cependant, les équations harmoniques présentent une dimension infinie. Les méthodes permettant de résoudre ces équations nécessitent des hypothèses contraignantes, telles que la stabilité du système en boucle ouverte et la connaissance d'une factorisation de Floquet [16] ou un gain initial stabilisant [14]. A notre connaissance, il n'existe pas de méthode permettant de traiter le cas des LMIs harmoniques.

Dans le chapitre 3, nous proposons une méthode pour résoudre les LMIs à blocs Toeplitz (TBLMIs) malgré leur dimension infinie. Ces TBLMIs sont le pendant harmonique des LMIs périodiques différentielles (PDLMIs), dont nous avons établi l'intérêt ci-dessus. De fait, résoudre une PDLMI revient à résoudre la TBLMI associée. Cependant, les TBLMIs présentent une dimension infinie, ce qui implique que seule une solution approchée peut être déterminée numériquement. Nous proposons d'utiliser un opérateur de troncature pour transformer les TBLMIs en problèmes d'optimisation convexe de dimension finie. Puisque les opérateurs TB ne sont pas de classe trace pour la trace classique, il est nécessaire d'introduire un opérateur de trace spécifique aux opérateurs TB pour que le critère à optimiser dans ces problèmes ait un sens. La troncature des TBLMIs est dite *consistante* car la solution du problème tronqué converge vers la solution du problème de dimension infinie tant que des hypothèses de régularité sont vérifiées sur les entrées des TBLMIs. Dans le cas contraire, une régularisation des entrées permet tout de même de fournir des garanties de convergence. Nous vérifions sur des exemples que notre méthode de résolution de TBLMIs permet de retrouver les solutions des PDLMIs associées.

B.4 Contrôle harmonique robuste

Le contrôle périodique désigne non seulement la conception de contrôleurs pour les systèmes périodiques, mais aussi pour les systèmes non périodiques soumis à des références ou perturbations périodiques. Dans cette thèse, nous nous intéressons plutôt à la conception de lois de contrôle périodiques pour les systèmes LTP. Le contrôle de tels systèmes est difficile du fait de leur nature variant dans le temps. Pour les systèmes discrets, la méthode de lifting permet d'aborder le contrôle comme s'il s'agissait d'un système LTI de dimension plus élevée [51–54]. Le cas continu est beaucoup plus complexe [36, 40, 55, 56]. Bien qu'il existe une fonction de transfert harmonique pour caractériser les systèmes LTP continus, cette dernière est de dimension infinie, ce qui complique le calcul des normes H_2 et H_∞ [57]. Il est possible de déterminer la norme H_2 à partir de la solution d'une équation de Lyapunov différentielle périodique [55]. La norme H_∞ peut quant à elle être estimée en tronquant les opérateurs qui apparaissent dans la fonction de transfert harmonique [57]. De manière générale, le contrôle robuste des systèmes périodiques est lié à la résolution d'équations différentielles périodiques telles que celles présentées dans le chapitre 3. Le contrôle harmonique est une alternative qui permet d'appliquer les méthodes LTI, mais qui nécessite de résoudre des équations harmoniques de dimension infinie [5, 14, 64]. Cependant, de nombreux problèmes de contrôle robuste peuvent être formulés comme des LMIs.

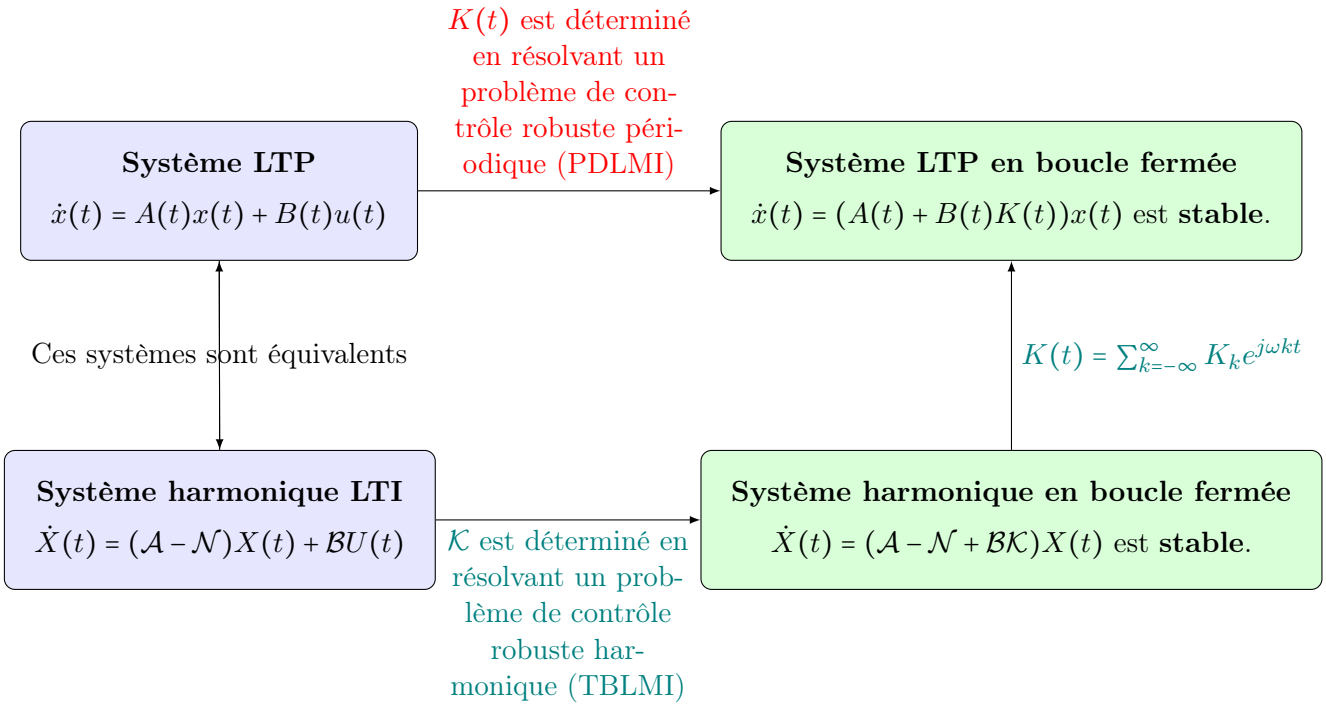

Figure B.1: Les problèmes de contrôle robuste harmonique sont résolus avec notre approche TBLMI au lieu de résoudre des PDLMIs.

Dans le chapitre 4, nous présentons une formulation TBLMI des problèmes H_2 et H_∞ associés aux systèmes harmoniques LTI. Grâce à la méthode de résolution de TBLMIs présentée dans le chapitre 3, il est possible de déterminer une solution approchée des problèmes de contrôle robuste harmonique malgré leur dimension infinie. Pour ce faire, il faut d'abord redéfinir les notions classiques de contrôle robuste (fonction de transfert, normes H_2 et H_∞) dans l'espace harmonique. Les problèmes de contrôle robuste harmonique peuvent ensuite être formulés comme des problèmes d'optimisation convexe impliquant des contraintes TBLMIs. Les gains harmoniques obtenus en résolvant ces problèmes peuvent être convertis en gains périodiques qui satisfont les problèmes de contrôle robuste périodique associés, comme illustré sur le schéma B.1. Nous validons cette approche TBLMI sur plusieurs exemples.

B.5 Perspectives

Les perspectives ouvertes par ce travail sont nombreuses et concernent aussi bien des approches théoriques qu'industrielles. Sur le plan de l'identification, une étude théorique des effets du bruit serait une piste de recherche prometteuse qui pourrait compléter l'analyse empirique menée dans cette thèse. De plus, l'extension à des données d'entrée/sortie (sans mesure d'état) peut être envisagée. En particulier, l'application de notre algorithme d'identification à des données expérimentales issues du fonctionnement d'un système réel reste à faire.

Sur le plan de la commande, l'adaptation des méthodes aux systèmes dont la période varie au cours du temps semble pertinente, étant donné que de nombreux systèmes sont dans ce cas

(par exemple en électronique de puissance et dans certaines configurations des éoliennes). La conception de lois de commande robustes aux perturbations polytopiques ou bornées en norme est une application naturelle des TBLMIs. De manière générale, les concepts du contrôle robuste pour les systèmes LTI devraient pouvoir être étendus aux systèmes harmoniques. En effet, des PDLMIs apparaissent dans de nombreux problèmes d'analyse et de contrôle des systèmes périodiques et peuvent être résolues efficacement avec notre approche TBLMI.

Enfin, on remarque qu'il est souvent nécessaire de trouver un compromis entre la précision d'un modèle et le coût de la résolution des TBLMIs associées. La question de l'approximation des modèles LTP par un modèle contenant un nombre réduit de coefficients de Fourier se pose alors. En considérant les phaseurs négligés comme des incertitudes sur le modèle, il devrait être possible de concevoir des lois de commande robustes à ces incertitudes, avec des garanties de performance malgré l'approximation du système.

B.6 Contributions

Les principales contributions de cette thèse concernent l'identification et le contrôle robuste des systèmes LTP, ainsi que la résolution des TBLMIs. Elles peuvent être résumées de la manière suivante:

1. **Identification des systèmes LTP**
   (a) Développement d'une méthode d'identification des systèmes LTP dans le domaine harmonique à partir de données d'état/entrée du système.
   (b) Etude empirique des effets du bruit (de mesure ou de procédé).
2. **Résolution des TBLMIs**
   (a) Développement d'une méthode de résolution pour les TBLMIs de dimension infinie en exploitant un opérateur de troncature garantissant la convergence de la solution du problème tronqué vers la vraie solution.
   (b) Extension de la méthode précédente au cas des entrées non régulières grâce à un opérateur de régularisation.
3. **Contrôle robuste des systèmes LTP**
   (a) Formulation des problèmes de contrôle robuste des systèmes LTP comme problèmes de contrôle robuste pour les systèmes LTI harmoniques.
   (b) Résolution des problèmes robustes H_2 et H_∞ dans le domaine harmonique au moyen de TBLMIs.

La contribution 1a est issue de [8] et complétée dans ce manuscrit par la contribution 1b. Les contributions 2a, 3a et 3b sont issues de [7] et [9]. La contribution 2b est issue de [74] et est développée dans ce manuscrit, notamment par des exemples illustratifs.

B.7 Publications

Ce travail a donné lieu aux publications suivantes:

Chapitre de livre

1. F. Vernerey, P. Riedinger and J. Daafouz, "Harmonic Modeling and Control," in R. Postoyan, P. Frasca, E. Panteley, L. Zaccarian (dir.), *Hybrid and Networked Dynamical Systems*, Springer, 2024. [6]

Article de revue

1. F. Vernerey, P. Riedinger and J. Daafouz, "A TBLMI Framework for Harmonic Robust Control," in IEEE Transactions on Automatic Control, vol. 70, no. 4, pp. 2537-2551, April 2025. [7]

Articles de conférence

1. F. Vernerey, P. Riedinger, A. Iannelli and J. Daafouz, "A Harmonic Framework for the Identification of Linear Time-Periodic Systems," 2024 American Control Conference (ACC), Toronto, ON, Canada, 2024, pp. 4645-4650. [8]

2. F. Vernerey, P. Riedinger and J. Daafouz, "On Solving Infinite-Dimensional Toeplitz Block LMIs," 2023 62nd IEEE Conference on Decision and Control (CDC), Singapore, Singapore, 2023, pp. 4717-4722. [9]

Bibliography

[1] M. Farkas, *Periodic Motions*, vol. 104 of *Applied Mathematical Sciences*. New York, NY: Springer New York, 1994.

[2] M. S. Allen, "Frequency-Domain Identification of Linear Time-Periodic Systems Using LTI Techniques," *Journal of Computational and Nonlinear Dynamics*, vol. 4, p. 041004, Oct. 2009.

[3] V. Salis, A. Costabeber, S. M. Cox, and P. Zanchetta, "Stability Assessment of Power-Converter-Based AC systems by LTP Theory: Eigenvalue Analysis and Harmonic Impedance Estimation," *IEEE Journal of Emerging and Selected Topics in Power Electronics*, vol. 5, pp. 1513–1525, Dec. 2017.

[4] S. Bittanti and P. Colaneri, *Periodic systems: filtering and control*. Communications and control engineering, London: Springer, 2009.

[5] N. Blin, P. Riedinger, J. Daafouz, L. Grimaud, and P. Feyel, "Necessary and sufficient conditions for harmonic control in continuous time," *IEEE Transactions on Automatic Control*, vol. 67, no. 8, pp. 4013–4028, 2022.

[6] F. Vernerey, P. Riedinger, and J. Daafouz, *Harmonic Modeling and Control*, pp. 301–323. Cham: Springer Nature Switzerland, 2024.

[7] F. Vernerey, P. Riedinger, and J. Daafouz, "A TBLMI Framework for Harmonic Robust Control," *IEEE Transactions on Automatic Control*, vol. 70, no. 4, pp. 2537–2551, 2025.

[8] F. Vernerey, P. Riedinger, A. Iannelli, and J. Daafouz, "A Harmonic Framework for the Identification of Linear Time-Periodic Systems," in *2024 American Control Conference (ACC)*, pp. 4645–4650, 2024.

[9] F. Vernerey, P. Riedinger, and J. Daafouz, "On Solving Infinite-Dimensional Toeplitz Block LMIs," in *2023 62nd IEEE Conference on Decision and Control (CDC)*, pp. 4717–4722, 2023.

[10] L. Ljung, *System Identification: Theory for the User*. Prentice Hall Information and System Sciences Series, Upper Saddle River, NJ: Prentice Hall PTR, 2nd ed., 1999.

[11] J. C. Geromel, "Differential Linear Matrix Inequalities in Sampled-Data Systems Filtering and Control," *Springer*, 2023.

[12] C. Briat, "Stability analysis and stabilization of stochastic linear impulsive, switched and sampled-data systems under dwell-time constraints," *Automatica*, vol. 74, pp. 279–287, 2016.

[13] M. Ariola, G. D. Tommasi, A. Mele, and G. Tartaglione, "On the numerical solution of differential linear matrix inequalities," *J. Optim. Theory Appl.*, vol. 185, pp. 540–553, 2020.

[14] P. Riedinger and J. Daafouz, "Solving infinite-dimensional harmonic Lyapunov and Riccati equations," *IEEE Transactions on Automatic Control*, vol. 68, no. 10, pp. 5938–5953, 2023.

[15] I. Gohberg, S. Goldberg, and M. A. Kaashoek, "Classes of linear operators. vol. II," *Operator Theory: Advances and Applications*, vol. 63, 1993.

[16] J. Zhou, "Derivation and solution of harmonic Riccati equations via contraction mapping theorem," *Transactions of the Society of Instrument and Control Engineers*, vol. 44, no. 2, pp. 156–163, 2008.

[17] J. J. Hench, "A technique for the identification of linear periodic state-space models," *International Journal of Control*, vol. 62, pp. 289–301, Aug. 1995.

[18] I. Markovsky, J. Goos, K. Usevich, and R. Pintelon, "Realization and identification of autonomous linear periodically time-varying systems," *Automatica*, vol. 50, pp. 1632–1640, June 2014.

[19] U. Saetti, J. F. Horn, T. Berger, M. J. S. Lopez, and M. B. Tischler, "Identification of Linear Time-Periodic Systems from Rotorcraft Flight-Test Data," *Journal of Guidance, Control, and Dynamics*, vol. 42, pp. 2288–2296, Oct. 2019.

[20] M. Verhaegen and X. Yu, "A class of subspace model identification algorithms to identify periodically and arbitrarily time-varying systems," *Automatica*, vol. 31, pp. 201–216, Feb. 1995.

[21] K. Liu, "Identification of linear time-varying systems," *Journal of Sound and Vibration*, vol. 206, no. 4, pp. 487–505, 1997.

[22] V. Verdult, M. Lovera, and M. Verhaegen, "Identification of linear parameter-varying state-space models with application to helicopter rotor dynamics," *International Journal of Control*, vol. 77, pp. 1149–1159, Sept. 2004.

[23] I. Uyanik, U. Saranli, M. M. Ankarali, N. J. Cowan, and O. Morgul, "Frequency-Domain Subspace Identification of Linear Time-Periodic (LTP) Systems," *IEEE Transactions on Automatic Control*, vol. 64, pp. 2529–2536, June 2019.

[24] M. Yin, A. Iannelli, and R. S. Smith, "Subspace Identification of Linear Time-Periodic Systems With Periodic Inputs," *IEEE Control Systems Letters*, vol. 5, pp. 145–150, Jan. 2021.

[25] A. Cadoret, E. Denimal, J.-M. Leroy, J.-L. Pfister, and L. Mevel, "Periodic System Approximation for Operational Modal Analysis of Operating Wind Turbine," in *European Workshop on Structural Health Monitoring*, vol. 253, pp. 156–165, Cham: Springer International Publishing, 2023.

[26] A. Jhinaoui, L. Mevel, and J. Morlier, "Subspace Identification for Linear Periodically Time-varying Systems," *IFAC Proceedings Volumes*, vol. 45, pp. 1282–1287, July 2012.

[27] M. S. Allen, M. W. Sracic, S. Chauhan, and M. H. Hansen, "Output-only modal analysis of linear time-periodic systems with application to wind turbine simulation data," *Mechanical Systems and Signal Processing*, vol. 25, no. 4, pp. 1174–1191, 2011.

[28] C. Bottasso and S. Cacciola, "Model-independent periodic stability analysis of wind turbines," *Wind Energy*, vol. 18, pp. 865–887, May 2015.

[29] W. Yin and A. S. Mehr, "Identification of linear periodically time-varying systems using periodic sequences," in *2009 IEEE International Conference on Control Applications*, (St. Petersburg, Russia), pp. 1455–1459, IEEE, July 2009.

[30] İ. Uyanık, U. Saranlı, Ö. Morgül, and M. M. Ankaralı, "Parametric Identification of Hybrid Linear-Time-Periodic Systems," *IFAC-PapersOnLine*, vol. 49, no. 9, pp. 7–12, 2016.

[31] J. Goos and R. Pintelon, "Continuous-time identification of periodically parameter-varying state space models," *Automatica*, vol. 71, pp. 254–263, Sept. 2016.

[32] N. Wereley, *Analysis and Control of Linear Periodically Time Varying Systems*. PhD thesis, 1991.

[33] E. Louarroudi, R. Pintelon, J. Lataire, and G. Vandersteen, "Estimation of nonparametric harmonic transfer functions for linear periodically time-varying systems using periodic excitations," in *2011 IEEE International Instrumentation and Measurement Technology Conference*, pp. 1–6, May 2011.

[34] İ. Uyanık, M. M. Ankaralı, N. J. Cowan, U. Saranlı, and Ö. Morgül, "Identification of a vertical hopping robot model via harmonic transfer functions," *Transactions of the Institute of Measurement and Control*, vol. 38, pp. 501–511, May 2016.

[35] S. J. Shin, C. E. S. Cesnik, and S. R. Hall, "System Identification Technique for Active Helicopter Rotors," *Journal of Intelligent Material Systems and Structures*, vol. 16, pp. 1025–1038, Dec. 2005.

[36] A. Varga, "On solving periodic Riccati equations," *Numerical Linear Algebra with Applications*, vol. 15, pp. 809–835, 2008.

[37] S. V. Gusev, A. S. Shiriaev, and L. B. Freidovich, "SDP-based approximation of stabilising solutions for periodic matrix Riccati differential equations," *International Journal of Control*, vol. 89, pp. 1396–1405, July 2016.

[38] H.-J. Peng, Z.-G. Wu, and W.-X. Zhong, "Fourier expansion based recursive algorithms for periodic Riccati and Lyapunov matrix differential equations," *Journal of Computational and Applied Mathematics*, vol. 235, pp. 3571–3588, Apr. 2011.

[39] A. Varga, "Computational issues for linear periodic systems: Paradigms, algorithms, open problems," *International Journal of Control*, vol. 86, pp. 1227–1239, July 2013.

[40] S. Gusev, S. Johansson, B. Kågström, A. Shiriaev, and A. Varga, "A numerical evaluation of solvers for the periodic Riccati differential equation," *BIT Numerical Mathematics*, vol. 50, no. 2, pp. 301–329, 2010.

[41] B. A. Francis and W. M. Wonham, "The internal model principle of control theory," *Automatica*, vol. 12, no. 5, pp. 457–465, 1976.

[42] S. Hara, Y. Yamamoto, T. Omata, and M. Nakano, "Repetitive control system: a new type servo system for periodic exogenous signals," *IEEE Transactions on Automatic Control*, vol. 33, no. 7, pp. 659–668, 1988.

[43] R. C. H. Lee and M. C. Smith, "Robustness and trade-offs in repetitive control," *Automatica*, vol. 34, pp. 889–896, 1998.

[44] G. Weiss and M. Häfele, "Repetitive control of MIMO systems using H_∞ design," *Automatica*, vol. 35, no. 7, pp. 1185–1199, 1999.

[45] R. Teodorescu, F. Blaabjerg, M. Liserre, and P. C. Loh, "Proportional-resonant controllers and filters for grid-connected voltage-source converters," *IEE Proceedings-Electric Power Applications*, vol. 153, no. 5, pp. 750–762, 2006.

[46] G. Weiss and M. Häfele, "Approximate regulation for nonlinear systems in presence of periodic disturbances," *In 54th IEEE Conference on Decision and Control*, p. 7665–7670, 2015.

[47] D. Astolfi, L. Praly, and L. Marconi, "Harmonic internal models for structurally robust periodic output regulation," *Systems & Control Letters*, vol. 161, p. 105154, 2022.

[48] M. Bodson, A. Sacks, and P. Khosla, "Harmonic generation in adaptive feedforward cancellation schemes," *IEEE Transactions on Automatic control*, vol. 39, no. 9, pp. 1939–1944, 2002.

[49] H. Jiang and B. Zhou, "Optimal control of unknown continuous time linear periodic systems by adaptive dynamic programming with applications to magnetic attitude control," *Optimal Control Applications and Methods*, vol. 44, no. 3, pp. 1341–1355, 2023.

[50] F. Thiele, S. Wisbacher, S. Diaconescu, D. Ossmann, and H. Pfifer, "Periodic LQG Wind Turbine Control with Adaptive Load Reduction," *IFAC-PapersOnLine*, vol. 56, no. 2, pp. 7674–7679, 2023.

[51] B. Bamieh, J. B. Pearson, B. A. Francis, and A. Tannenbaum, "A lifting technique for linear periodic systems with applications to sampled-data control," *Systems & Control Letters*, vol. 17, no. 2, pp. 79–88, 1991.

[52] B. A. Bamieh and J. B. Pearson, "A general framework for linear periodic systems with applications to H_∞/sampled-data control," *IEEE Transactions on Automatic Control*, vol. 37, no. 4, pp. 418–435, 1992.

[53] Y. Yamamoto and P. P. Khargonekar, "Frequency response of sampled-data systems," *IEEE Transactions on Automatic Control*, vol. 41, no. 2, pp. 166–176, 1996.

[54] P. P. Khargonekar and N. Sivashankar, "H_2 optimal control for sampled-data systems," *Systems & Control Letters*, vol. 17, no. 6, pp. 425–436, 1991.

[55] P. Colaneri, "Continuous-time periodic systems in H_2 and H_∞. Part I: Theoretical aspects," *Kybernetika*, vol. 36, no. 2, pp. 211–242, 2000.

[56] P. Colaneri, "Continuous-time periodic systems in H_2 and H_∞. Part II: State feedback problems," *Kybernetika*, vol. 36, no. 3, pp. 329–350, 2000.

[57] J. Zhou and T. Hagiwara, "H_2 and H_∞ norm computations of linear continuous-time periodic systems via the skew analysis of frequency response operators," *Automatica*, vol. 38, no. 8, pp. 1381–1387, 2002.

[58] B. Pang and Z.-P. Jiang, "Adaptive Optimal Control of Linear Periodic Systems: An Off-Policy Value Iteration Approach," *IEEE Transactions on Automatic Control*, vol. 66, pp. 888–894, Feb. 2021.

[59] B. Pang, Z.-P. Jiang, and I. Mareels, "Reinforcement learning for adaptive optimal control of continuous-time linear periodic systems," *Automatica*, vol. 118, p. 109035, Aug. 2020.

[60] X. Li, H. Jiang, and B. Zhou, "Bias-policy iteration based optimal control for unknown continuous-time linear periodic systems," *Systems & Control Letters*, vol. 189, p. 105819, July 2024.

[61] S. R. Sanders, J. M. Noworolski, X. Z. Liu, and G. C. Verghese, "Generalized averaging method for power conversion circuits," *IEEE Transactions on Power Electronics*, vol. 6, no. 2, pp. 251–259, 1991.

[62] J. Zhou and T. Hagiwara, "Stability analysis of continuous-time periodic systems via the harmonic analysis," in *Proceedings of the 2001 American Control Conference*, pp. 535–540 vol.1, 2001.

[63] J. Zhou, T. Hagiwara, and M. Araki, "Spectral characteristics and eigenvalues computation of the harmonic state operators in continuous-time periodic systems," *Systems & Control Letters*, vol. 53, no. 2, pp. 141–155, 2004.

[64] P. Riedinger and J. Daafouz, "Harmonic pole placement," in *2022 IEEE 61st Conference on Decision and Control (CDC)*, pp. 5505–5510, 2022.

[65] H. J. Van Waarde, C. De Persis, M. K. Camlibel, and P. Tesi, "Willems' fundamental lemma for state-space systems and its extension to multiple datasets," *IEEE Control Systems Letters*, vol. 4, no. 3, pp. 602–607, 2020.

[66] J. B. Conway, *A Course in Operator Theory*. American Mathematical Society, 2000.

[67] K. Zhou and J. Doyle, *Essentials of Robust Control*. Prentice Hall, 1998.

[68] R. M. Beam and R. F. Warming, "The asymptotic spectra of banded toeplitz and quasi-toeplitz matrices," *SIAM Journal on Scientific Computing*, vol. 14, no. 4, pp. 971–1006, 1993.

[69] J. Willems, "Least squares stationary optimal control and the algebraic Riccati equation," *IEEE Transactions on Automatic Control*, vol. 16, no. 6, pp. 621–634, 1971.

[70] R. F. Curtain, "The strict bounded real lemma in infinite dimensions," *Systems & Control Letters*, vol. 20, no. 2, pp. 113–116, 1993.

[71] A. Varga, "A periodic systems toolbox for matlab," *IFAC Proceedings Volumes*, vol. 38, no. 1, pp. 450–455, 2005. 16th IFAC World Congress.

[72] S. Boyd, L. El Ghaoui, E. Feron, and V. Balakrishnan, *Linear matrix inequalities in system and control theory*. SIAM, 1994.

[73] A. Bensoussan and P. Bernhard, "On the standard problem of H_∞-optimal control for infinite-dimensional systems," *Identification and Control in Systems Governed by Partial Differential Equations*, vol. 68, p. 117, 1993.

[74] F. Vernerey, P. Riedinger, and J. Daafouz, "Erratum to "A TBLMI Framework for Harmonic Robust Control"," *IEEE Transactions on Automatic Control*, vol. 71, no. 3, pp. 2120–2121, 2026.

[75] M. M. Ankarali and N. J. Cowan, "System identification of rhythmic hybrid dynamical systems via discrete time harmonic transfer functions," in *53rd IEEE Conference on Decision and Control*, pp. 1017–1022, Dec. 2014.

[76] J. Coulson, H. J. van Waarde, J. Lygeros, and F. Dörfler, "A Quantitative Notion of Persistency of Excitation and the Robust Fundamental Lemma," *IEEE Control Systems Letters*, vol. 7, pp. 1243–1248, 2023.

[77] H. Garnier, "Direct continuous-time approaches to system identification. Overview and benefits for practical applications," *European Journal of Control*, vol. 24, pp. 50–62, July 2015.

[78] H. Garnier and L. Wang, eds., *Identification of Continuous-Time Models from Sampled Data*. Advances in Industrial Control, London: Springer, 2008.

[79] I. Gohberg, S. Goldberg, and M. Kaashoek, *Classes of Linear Operators*. Operator Theory: Advances and Applications, Birkhäuser Basel, 2013.

[80] K. S. Narendra and K. Esfandiari, "Adaptive identification and control of linear periodic systems using second-level adaptation," *International Journal of Adaptive Control and Signal Processing*, vol. 33, no. 6, pp. 956–971, 2019.

[81] A. A. Stoorvogel, "Stabilizing solutions of the H_∞ algebraic Riccati equation," *Linear Algebra and its Applications*, vol. 240, pp. 153–172, 1996.

[82] J. Zhou, "Harmonic Lyapunov equations in continuous-time periodic systems: solutions and properties," *IET Control Theory & Applications*, vol. 1, no. 4, pp. 946–954, 2007.

[83] D. Astolfi, S. Marx, and N. van de Wouw, "Repetitive control design based on forwarding for nonlinear minimum-phase systems," *Automatica*, vol. 129, p. 109671, 2021.

[84] P. Bolzern and P. Colaneri, "The periodic Lyapunov equation," *SIAM Journal on Matrix Analysis and Applications*, vol. 9, no. 4, pp. 499–512, 1988.